DISSERTATIONES
CHIMICAE
UNIVERSITATIS
TARTUENSIS
244

SHRIKANT SHIVAJI PAWADE

Metrological aspects of sampling and water/moisture determination on the example of lignin

DISSERTATIONES CHIMICAE UNIVERSITAS TARTUENSIS
244

DISSERTATIONES CHIMICAE UNIVERSITAS TARTUENSIS
244

SHRIKANT SHIVAJI PAWADE

Metrological aspects of sampling and water/moisture determination on the example of lignin

UNIVERSITY OF TARTU
Press
1632

Institute of Chemistry, Faculty of Science and Technology, University of Tartu, Estonia

Dissertation is accepted for the commencement of the degree of *Doctor Philosophiae* in Chemistry on April 8, 2026, by the Council of Institute of Chemistry, Faculty of Science and Technology, University of Tartu.

Supervisors: Prof. Ivo Leito (PhD)
Institute of Chemistry, University of Tartu, Estonia

Associate Prof. Koit Herodes (PhD)
Institute of Chemistry, University of Tartu, Estonia

Dr. Lauri Toom (PhD)
Institute of Chemistry, University of Tartu, Estonia

Opponents: Dr. Stephanie Bell (PhD)
National Physical Laboratory (NPL), UK

Prof. Riina Aav (PhD)
Tallinn University of Technology (TalTech), Estonia.

Commencement: June 9, 2026, at 15.15, Auditorium 1020, Ravila 14a, (Chemicum), Tartu, and Microsoft Teams (online).

Publication of this dissertation is granted by University of Tartu, Estonia.

This work has been partially supported by the ASTRA project PER ASPERA Graduate School of Functional Materials and Technologies, funded by the European Regional Development Fund under a project at the University of Tartu, Estonia.

ISSN 1406-0299 (print) ISSN 2806-2159 (pdf)
ISBN 978-9908-57-213-0 (print) ISBN 978-9908-57-214-7 (pdf)

University of Tartu Press
www.tyk.ee

TABLE OF CONTENTS

LIST OF ORIGINAL PUBLICATIONS

I. **S. S. Pawade**, L. Toom, K. Herodes, and I. Leito, "Accuracy of Quantitative NMR Analysis: A Case Study of Lignin," *Journal of Chemical Metrology* 17, no. 1 (January/June 2023): 114–127, https://doi.org/10.25135/jcm.88.2304.2753

II. **S. S. Pawade**, L. Toom, K. Herodes, and I. Leito, "Evaluating Sampling Uncertainty in the Quantitative ^{1}H Nuclear Magnetic Resonance Analysis of Lignin." *BioResources* 20, no. 1 (January 27, 2025): 2234–42. https://doi.org/10.15376/biores.20.1.2234-2242

III. **S. S. Pawade**, M. Vilbaste, A. Siiman, L. Toom, K. Herodes, I. Leito, A quantitative approach to determine water and moisture content of different types of lignin using attenuated total reflectance Fourier transform infrared spectroscopy combined with partial least squares regression, Biofuels, Bioproducts & Biorefining 20 (2026) 919–930. https://doi.org/10.1002/bbb.70124

IV. M. Vilbaste, **S. S. Pawade**, I. Leito, Optimisation of temperature for accurate water content determination in plant-derived materials using vaporisation–coulometric Karl Fischer titration, *Journal of Chemical Metrology* (2025) 114–127. https://doi.org/10.25135/jcm.126.2511.3730

Author's contribution

Paper I. Lead author in preparing the manuscript. Conducted the literature analysis and wrote the initial draft. Contributed to discussions and critical revision.

Paper II. Lead author in writing the manuscript. The main person responsible for performing the experiments and data treatment.

Paper III. Lead author in writing the manuscript. The main person responsible for performing the experiments and data treatment.

Paper IV. Contributed substantially to the writing of the manuscript and performed a major part of the lignin experiments and data treatment.

ABBREVIATIONS

^{13}C NMR	Carbon-13 nuclear magnetic resonance
2D NMR	Two-dimensional nuclear magnetic resonance
^{31}P NMR	Phosphorus-31 nuclear magnetic resonance
ANOVA	Analysis of variance
APCI-MS	Atmospheric pressure chemical ionisation mass spectrometry
APPI-MS	Atmospheric pressure photoionisation mass spectrometry
ATR	Attenuated total reflectance
BBO	Broadband observe
C-KFT	Coulometric Karl Fischer titration
COMAR	Code d'Indexation des Matériaux de Référence
CP/MAS	Cross-polarisation/magic angle spinning
DAL	Dealkaline lignin
DRFC	Derivatisation followed by reductive cleavage
DVS	Dynamic vapour sorption
ESI-MS	Electrospray ionisation mass spectrometry
FTIR	Fourier transform infrared spectroscopy
G unit	guaiacyl /(*E*)-4-hydroxy-3-methoxycinnamyl alcohol
GC–MS	Gas chromatography-mass spectrometry
H unit	*p*-hydroxyphenyl/ 4-(3-hydroxy-1-propenyl)phenol
HMBC	Heteronuclear multiple bond correlation
HPLC	High-performance liquid chromatography
HRMS	High-resolution mass spectrometry
HSQC	Heteronuclear single quantum coherence
KL	Kraft lignin
LC-MS	Liquid chromatography–mass spectrometry
MALDI-MS	Matrix-assisted laser desorption/ionisation mass spectrometry
MSC	Multiplicative scattering correction
MWL	Milled wood lignin
NIR	Near-infrared spectroscopy
NMR	Nuclear magnetic resonance
OÜ	A private limited company
PLS	Partial least squares
PLS-R	Partial least squares regression
ppm	Parts per million
qNMR	Quantitative nuclear magnetic resonance
R^2	Squared coefficient of correlation
RMS	Root mean square
RMSECV	Root mean square error of cross-validation
RMSEP	Root mean square error of prediction
RSD	Relative standard deviation

RSD_{Meas}	Relative standard deviation arising from measurement variability
RSD_{sampling}	Relative standard deviation arising from sampling variability
RSD_{Total}	Total relative standard deviation
S unit	Syringyl / (*E*)-4-hydroxy-3,5-dimethoxycinnamyl alcohol
SNV	Standard normal variate
T_{opt}	The optimal analysis temperature
TGA	Thermogravimetric analysis
TMS	Tetramethylsilane
UV-Vis	Ultraviolet–visible spectroscopy
vap-C-KFT	vaporisation-based coulometric Karl Fischer titration
W_{moisture}	Moisture content
δ	Chemical shift (NMR)
$\delta C_{\mathrm{model}}$	Correction due to mismatch between model and experimental data
$\delta C_{\mathrm{sampl}}$	Correction due to repeated sampling

1 INTRODUCTION

Lignin is an amorphous, cross-linked complex natural polymer in plant cell walls that binds cellulose and hemicellulose fibres [1,2]. Lignin provides structural support, pathogen resistance, water impermeability and vascular integrity [3]. Previously, industrially produced lignin was considered a waste product or a low-value by-product of paper and pulp industries, primarily used as a fuel source in pulping process boilers for energy generation [4]. Lignin, constituting 30% of Earth's organic carbon, i.e., more than 3×10^{11} metric tons, is the second most abundant source of biomass after cellulose [5–7]. Due to lignin's abundance in biomass, it has the potential to serve as a suitable replacement for a significant amount of aromatic petrochemicals [8].

Lignin exhibits significant heterogeneity that varies depending on plant species, extraction methods, and processing methods. Therefore, precise characterisation in terms of molecular weight, functional groups (e.g., phenolic hydroxyl and methoxy groups), moisture content, and thermal stability is essential for its utilisation in polymers, biofuels, and other value-added chemicals [9–12].

In natural products, water content is critical for determining stability, quality, shelf-life, and efficacy. Lignin in particular exhibits inherent hygroscopic behaviour due to the presence of numerous hydrophilic groups [13]. The moisture content of lignin varies widely with changes in the manufacturing process and surrounding environmental conditions, especially changes in temperature and humidity [14]. Therefore, accurate measurement of lignin's water and/or moisture content is necessary for the efficient utilisation of lignin across industries, including chemical production, biofuels, and bioplastics. To increase efficiency and productivity, moisture/water determination methods should be rapid, inexpensive, and minimally labour-intensive. These criteria can be met by Fourier transform infrared (FTIR) spectroscopy, a widely used analytical technique.

Instrumental analysis techniques play critical roles in quantitative and qualitative analysis of lignin. In the solution phase, spectroscopic techniques such as ^{1}H NMR, ^{13}C NMR, ^{31}P NMR [8,15–19], two-dimensional (2D) NMR, high-resolution mass spectrometry (HRMS), atmospheric pressure chemical ionisation mass spectrometry (APCI-MS), matrix-assisted laser desorption/ionisation–mass spectrometry (MALDI-MS), electrospray ionisation–mass spectrometry (ESI-MS), atmospheric pressure photoionisation mass spectrometry (APPI-MS), high-performance liquid chromatography (HPLC) [20] and ultraviolet–visible (UV–Vis) spectroscopy are predominantly used to assess lignin's hydroxyl and monolignol content [15,21,22]. In contrast, solid-state characterisation of lignin involves a variety of methods: FTIR spectroscopy [23], thermogravimetric analysis (TGA), Raman spectroscopy, gas chromatography–mass spectrometry (GC-MS) and pyrolysis–GC-MS [21,24]. Solid-state characterisation is generally simpler in terms of sample preparation; however, it can lead to significant variability in results due to factors such as the method used to isolate the lignin from its source, water content, and the molecular weight of the lignin [21]. Attenuated total

reflectance (ATR) FTIR combined with partial least squares regression (PLS-R) can be employed to determine the water and moisture content of lignin. Although various analytical methods exist for this purpose, each has its own advantages and limitations [13,25,26]. Nuclear magnetic resonance (NMR) measurements have attracted growing interest as a reliable technique for analysing and characterising lignin [8,16–19,27]. NMR proves to be an effective analytical tool for quantifying complex organic materials, including lignin.

In previous studies, the use of various types of lignin in different measurements and the diversity in providing precision and trueness data have made it difficult to compare the accuracy achieved throughout the procedure. In many published reports, insufficient information was supplied regarding precision, trueness, and measurement uncertainty, and recent reviews highlight inconsistencies in how these factors are reported [15,28,29]. Although lignin is often treated as a relatively homogeneous material in analytical studies, it remains a solid, natural product and, like all such substances, exhibits a certain degree of inherent inhomogeneity, and therefore sampling uncertainty represents an important component of measurement uncertainty [30].

This dissertation aims to:

1. Evaluate the accuracy and uncertainty of quantitative lignin analysis using qNMR, including a critical assessment of how accuracy has been reported in the literature and a quantitative evaluation of sampling uncertainty and its contribution to overall measurement variability (Articles I and II).
2. Develop and optimise reliable methods for the determination of water and moisture content in lignin, using ATR-FTIR combined with a PLS-R-based predictive approach, and to optimise the oven temperature for vaporisation–coulometric Karl Fischer titration (vap-C-KFT) using a “sigmoid curve” approach (Articles III and IV).

2 LITERATURE OVERVIEW

This study utilised various lignin samples, obtained via different processes and from diverse sources. These samples include dealkaline lignin (DAL), two types of Kraft lignin (KL), and different Lignova lignin samples from Fibenol OÜ.

2.1 Lignin

Since ancient times, humans have depended on plants for food, shelter, medicine, energy and various environmental benefits [31]. Plants are primarily composed of cellulose, hemicellulose, and lignin, which serve as the main structural components of the cell wall, providing strength, flexibility, and resistance to degradation. Lignin is a significant constituent of lignocellulosic biomass. Lignin accounts for 15–40% of lignocellulosic biomass, which depends on the source and type of biomass [32–35].

The term *lignin* was first introduced in 1813 by the Swiss botanist A. P. de Candolle [36] and is derived from the Latin word *lignum*, meaning wood [37]. Lignin is a structurally complex, heterogeneous polymer composed of aromatic units with varying compositions depending on plant species, tissue type, and cell wall layer. Lignin is the largest renewable source of aromatic compounds on earth [38]. Lignin is primarily built by interlinking in different ways three distinct phenylpropane units: guaiacyl (G), syringyl (S), and *p*-hydroxyphenyl (H) units, as depicted in Figure 1. These monolignols are connected through various interunit linkages, predominantly β–O–4, α–O–4, β–β, β–5, 5–5 bonds [39,40]. Softwood lignin (e.g., pine and spruce) primarily consists of G units, whereas hardwood lignin (e.g., birch, poplar, eucalyptus) contains both G and S units [41]. In most plants, coniferyl alcohol is the most abundant monomer (50–95%), followed by sinapyl alcohol (5–50%), and *p*-coumaryl alcohol (0–5%) [38].

The structural complexity of lignin, arising from its diverse interunit linkages and irregular polymerisation, makes its depolymerisation into value-added products challenging. The presence of ether and carbon–carbon linkages often require advanced and energy-intensive processes for efficient conversion. In addition, chemical modifications introduced during pulping further hinder the utilisation of lignin as a renewable resource for biofuels and chemicals [38,42–44]. Nevertheless, the wide variety of functional groups in lignin offers significant potential for chemical modification [21].

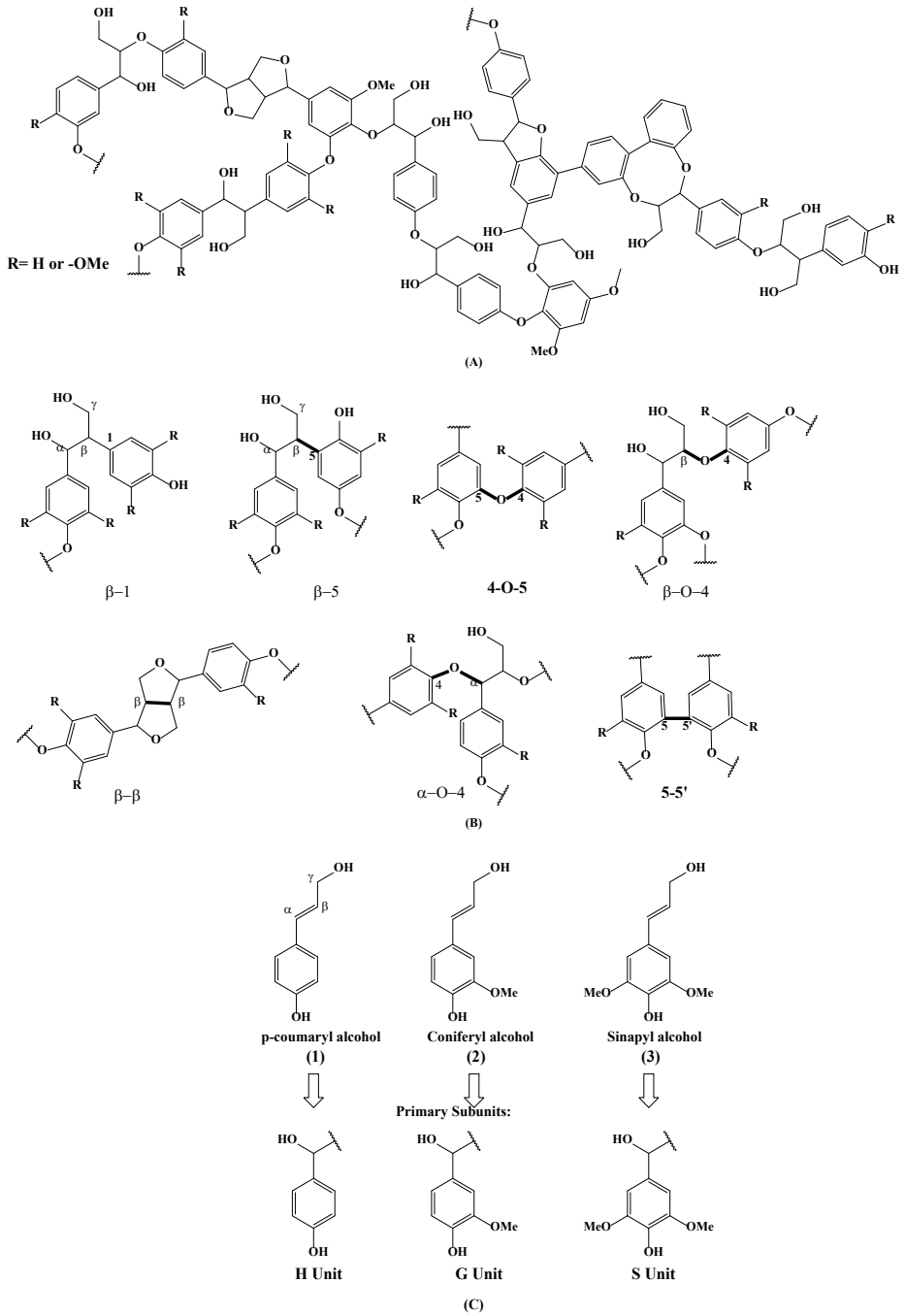

Figure 1. Schematic representation of structural composition of the lignin units: (A) representation of a lignin polymer, (B) the major interunit linkages present in lignin, (C) structure of the major monolignol precursors of lignin: (1) *p*-coumaryl alcohol/*p*-hydroxyphenyl (H) unit, (2) coniferyl alcohol/guaiacyl (G) unit, and (3) sinapyl alcohol/syringyl (S) unit [45–48].

A detailed structural analysis of lignin has been an important issue in wood and pulping chemistry. For years, lignin chemists focused extensively on understanding lignin polymers [1]. Due to its complexity, lignin cannot be fully characterised using a single analytical technique, and different methods may yield varying results. Therefore, a combination of approaches is recommended for a more comprehensive characterisation [49]. Both destructive and non-destructive methods are used to characterise lignin. The most commonly employed destructive methods include thioacidolysis [50,51], nitrobenzene oxidation [52], derivatisation followed by reductive cleavage (DRFC) method [53], and pyrolysis–GC-MS [16]. In contrast, non-destructive methods include spectroscopic methods such as ultraviolet-visible spectroscopy [54], FTIR spectroscopy [55] and NMR techniques [56]. The characterisation techniques used to reveal and understand the chemical structure of lignin include ^{13}C NMR [18,29,57], ^{31}P NMR, 2D NMR [19,27,58,59] and FTIR spectroscopy [13,15,55,60,61]. After over a century of study, many aspects of lignin structure remain unresolved [62].

Lignin can be extracted from softwood, hardwood, and grasses, and its composition varies significantly across different plant sources [63]. The lignin content in wood varies among plant species, and softwood typically contains 27–33% lignin, hardwood 18–25%, and grasses 17–27% [38]. Due to its aromatic, polymeric structure, it is a sustainable alternative to fossil-based resources for the production of valuable chemicals, materials, biofuels, bioplastics, and food flavouring agents [64–66].

2.1.1 Kraft Lignin

The Kraft pulping process, also known as the sulphate process, remains the most widely used chemical pulping method, accounting for approximately 90% of total lignin production capacity due to its efficiency and ability to produce high-quality pulp [4,38]. In this process, cellulose fibres are separated by dissolving the lignin and hemicellulose in a sodium hydroxide solution and sodium sulphide [38]. The Kraft pulping process was first developed in 1879 by the German chemist Carl F. Dahl [4].

In the Kraft pulping process, wood chips are treated with white liquor, a mixture of sodium hydroxide and sodium sulphide, at temperatures between 140–170 °C for approximately 3–4 h [67,68]. This high temperature, highly alkaline environment (pH 13–14) enhances the cleavage of ether bonds such as β–O–4 linkages in lignin, resulting in its dissolution and the formation of phenolic hydroxyl groups, which enhance lignin's solubility. Lignin is subsequently precipitated by acidifying the solution to pH 5–7.5, typically using sulphuric acid [69–71].

2.1.2 Dealkaline Lignin

Dealkaline lignin (DAL), which is derived from the dealkalisation of papermaking black liquor (a dark alkaline by-product generated during wood pulping that contains dissolved lignin), may contain a significant amount of sulphonate

functionality in its salt form, depending on the processing conditions [72]. This functionality arises from the chemical processes involved in dealkalisation and contributes to the distinct chemical properties of DAL, making it different from other lignin types [72]. Commercially, DAL can be further modified through chemical modification processes such as partial desulphonation, oxidation, hydrolysis, and demethylation [73].

DAL has attracted considerable attention due to its potential applications in catalysis, energy production, and advanced materials [74]. The DAL-based catalyst has been utilised in acid-catalysed reactions, where the sulphonate groups can be converted via ion exchange to the $–SO_3H$ group, which acts as the primary acidic site in solid acid catalysts [72].

2.1.3 Lignova Lignin

Lignova™ is a high-purity hydrolysis lignin produced by Estonian biotech company Fibenol OÜ. It is obtained using an extrusion-based fractionation technology that separates lignin, wood sugars, and specialty cellulose from hardwood residues. The resulting lignin can be used for biochemical coatings and adhesive resins, whereas cellulosic sugars can be used for fuel or bulk chemical production [75,76]. Fibenol offers lignin in two grades: Lignova™ Crude, which contains 88–95 % lignin and <6% carbohydrates. Lignova™ Pure consists of 92–96% lignin, with total carbohydrates <2% and minimal impurities. Due to its higher purity, functionality, and reactivity, Lignova™ Pure is well-suited for diverse industrial applications, including adhesives, thermosetting resins, and coatings. Lignova™ Pure shows good solubility in a range of solvents [76].

The process of Lignova™ lignin production starts with a mechanical process in a twin-screw extruder, where biomass or feedstock is treated with a strong acid or exposed to high-temperature or high-pressure conditions. The combination of steam explosion and chemical action disrupts the lignocellulosic structure, promoting the solubilisation of hemicellulose. Simultaneously, mechanical shearing by the screws reduces the particle size to approximately 15–25 μm, facilitating downstream processing. This step separates the biomass into a solid fibrous fraction (containing cellulose and lignin) and a liquid fraction (containing sugars from hemicellulose) [77,78]. Thereafter, enzymatic hydrolysis is applied to the cellulose and lignin-rich solid fraction. Cellulases are used to break down cellulose into fermentable sugars. The remaining residue is crude lignin (Lignova™ Crude). This crude material is further purified by removing cellulosic residues to obtain Lignova™ Pure lignin [76–78], safe for use in demanding applications, such as cosmetic products [79].

2.1.4 Chemical Properties and Thermal Behaviour of Lignin

As discussed in Section 2.1, lignin has a complex, heterogeneous, and highly branched structure containing hydroxyl and methoxy groups capable of forming hydrogen bonds with water. Its amphiphilic nature results in limited solubility

under acidic or neutral conditions, whereas under alkaline conditions, lignin becomes more hydrophilic and readily absorbs water [80]. Under elevated pressure, lignin exhibits increased solubility and stronger interactions with water through both chemical bonding and physical interactions [80].

The thermal behaviour of lignin is highly dependent on temperature and heating duration, because of its structurally complex and heterogeneous composition [81–83]. Thermal treatment induces a series of physical and chemical transformations beginning already at around 100–120 °C, where free and bound water are removed, and lignin undergoes thermal softening as the temperature approaches its glass transition temperature (typically 90–160 °C, depending on lignin origin and moisture content) [84,85]. In this temperature range, the sodium or alkaline form of lignin can also undergo significant changes during dry-oven heating [86]. Continued heating up to approximately 240 °C may cause structural modifications, including changes in molecular weight due to chemical rearrangements and thermal decomposition, together with changes in FTIR absorption near 1730 cm^{-1}, a region typically associated with carbonyl groups such as carboxylic acids and esters [87]. Under inert conditions, heat treatment induces simultaneous condensation and depolymerisation reactions in lignin, resulting in mass loss due to the release of phenolic compounds. These transformations are driven by the cleavage of β–O–4 linkages and structural rearrangements, which modify the structural and thermal behaviour of the lignin macromolecules [71]. At higher temperatures (150–300 °C), lignin begins to lose volatile compounds such as water, carbon dioxide, and low-molecular-weight fragments due to side-chain degradation, while prolonged heating promotes condensation reactions and cleavage of β–O–4 linkages, leading to the formation of low-molecular-weight phenolic compounds such as guaiacol-type phenolic products containing side-chain hydroxymethyl groups [66,70,88]. At elevated temperatures, functionalities such as hydroxyl, methoxy, and carboxyl groups degrade, which makes lignin more hydrophobic in nature [89].

Recent studies have shown that drying can significantly reduce the hydroxyl group content in lignin, indicating that heating alters the chemical structure of lignin with the release of water [71,88]. A possible route for the loss of hydroxyl groups is presented in Eq. (1).

$$–CH_2–CHOH– \rightarrow –CH=CH– + H_2O \quad (1)$$

This reaction suggests that thermal treatment facilitates reactions such as dehydration and condensation, which consume –OH functionalities, contributing to a reduction in hydroxyl group content and increased hydrophobicity of lignin [88,89]. Quantitative studies have shown that hydroxyl group content may decrease by 50–70% upon prolonged heating [88]. Molecular fragments of the –CH_2–CHOH– type are abundant in the lignin structure.

These structural and chemical changes are directly relevant to moisture determination, as oven drying at approximately 105 °C, although widely recognised as a standard method for biomass [90], may not exclusively measure water

content. Instead, the observed mass loss can also include contributions from volatilisation of organic compounds, residual sulphur species, and thermally induced reactions such as dehydration and condensation [90–92]. At excessively high drying temperatures, a significant fraction of the released water may additionally originate from lignin decomposition and cleavage of oxygen-containing functional groups rather than from the removal of pre-existing moisture.

2.2 Applications of Lignin

In recent years, lignin chemistry has advanced significantly due to the growing interest in valorising this abundant yet underused biopolymer. It possesses several properties that make it ideal for polymer application, such as high thermal stability, biodegradability, antioxidant and antimicrobial activity, and widespread availability [21]. Lignin is increasingly recognised as a renewable feedstock for producing high-value materials, solvents, chemicals, chemical reagents, polymers, and energy [93].

2.2.1 Lignin as a Feedstock for Bio-Based Chemicals

Lignin has a carbon content of more than 60% by mass and a high abundance of aromatic units, together with various functional groups and linkages, which makes it an attractive renewable feedstock [94]. It is increasingly regarded as a renewable alternative to fossil-based chemicals. Vanillin is one of the few lignin-derived compounds already produced at a commercial scale [95]. Other monomers and derivatives, such as vanillic acid, vanillic alcohol, and phenolic aldehydes, are being studied for scalable production [21,96]. Research focuses on catalytic depolymerisation techniques, including hydrolysis, pyrolysis, and hydrogenolysis, to break down lignin into valuable chemical intermediates [97]. The depolymerisation into low-molecular-weight bioactive compounds shows promising applications in the food, cosmetics [79], and pharmaceutical industries, as it exhibits antioxidant, antimutagenic, hepatoprotective, and anti-inflammatory properties [2].

2.2.2 Lignin in Polymer and Material Science

Lignin's biodegradability, and antioxidant properties make it an ideal component for bio-based materials. Its applications include rigid and flexible polyurethane foams, phenol-formaldehyde resins and adhesives, coatings, and packaging materials. These materials benefit from lignin's ability to partially or fully substitute petroleum-derived aromatic compounds [21].

2.2.3 Lignin-Based Carbon Materials

Lignin-based carbon biomaterials are recognised for their eco-friendly nature and good thermal conductivity [98,99]. The aromatic backbone of lignin makes it an

excellent precursor for carbon-rich materials, including activated carbon used in filtration and catalysis, carbon fibres for lightweight composites, and electrode components for batteries and supercapacitors. Introducing functional groups such as carboxyl, sulphonic acid group (–SO_3H), amine, and hydroxyl enhances lignin's catalytic and adsorptive properties. For instance, lignin-derived activated carbon with acidic groups can serve as a metal-free catalyst for esterification and dehydration reactions [80,100–102]. Moreover, these materials act as bio-adsorbents for removing heavy metals and organic pollutants, offering a green solution for environmental remediation [80].

2.2.4 Energy and Fuel Applications

While direct lignin valorisation into fuels remains technically challenging due to its resistant structure and energy-intensive processing, progress in catalytic upgrading is enabling its use in biofuel production. In many biorefineries, however, lignin is still primarily used as a combustible energy source, limiting its potential. The advanced biorefinery approach enables the production of sustainable jet fuel by preserving the C9–C15 carbon structure of lignin, making the conversion more efficient [103].

2.3 Nuclear Magnetic Resonance

NMR spectroscopy is one of the most informative techniques for lignin analysis, providing detailed molecular-level information on lignin structure in a non-destructive manner [104]. It is widely used to characterise interunit linkages such as β–O–4, β–5, and β–β linkages, the distribution of aromatic S, G, and H units (S/G/H ratio), the degree of condensation, and the presence of functional groups such as methoxy, carbonyl, and hydroxyl groups [104,105]. Multidimensional and heteronuclear techniques, particularly HSQC and HMBC, further enhance structural elucidation by improving signal assignment and resolving overlapping resonances. Although conventional HSQC experiments are primarily qualitative, they provide valuable information on lignin substructures and functional-group distributions [19,27,106–108].

In addition to structural analysis, quantitative NMR (qNMR) methods are widely applied for compositional analysis of lignin [109,110]. Quantitative NMR has been used for the determination of methoxy groups using ^{1}H and ^{13}C NMR spectroscopy [8,15,29,109]. Phenolic and aliphatic hydroxyl groups are commonly quantified using ^{31}P NMR after phosphitylation, while lignin–carbohydrate linkages, interunit linkages such as β–O–4, β–β, and β–5, and S/G unit ratios are obtained from 2D NMR signal integration [15,17,27,57,109–113].

Among one-dimensional techniques, ^{1}H NMR provides quantitative information on aliphatic, aromatic, and phenolic regions, although signal overlap and peak broadening can limit resolution, particularly in technical lignins [17,114]. ^{1}H NMR can also be used for hydroxyl groups the quantification, typically after

acetylation, although non-acetylation-based methods have also been reported [16,57,115].

^{13}C NMR techniques have been extensively employed for quantitative characterisation of lignin substructures and carbon environments [58,114,116]. They can also be used to identify and quantify hydroxyl functionalities after derivatisation. However, quantitative ^{13}C NMR requires relatively long acquisition times because of the low natural abundance and sensitivity of ^{13}C nuclei, the need for a large number of scans, and sufficiently long relaxation delays to ensure complete relaxation. Although paramagnetic relaxation agents can reduce relaxation times, comparatively large sample amounts are still required to obtain an adequate signal-to-noise ratio [57,117]. In addition, one-dimensional spectra may suffer from signal overlap, which can affect baseline correction, signal integration, and quantitative accuracy [118].

Over the years, extensive work has been done using ^{31}P NMR to quantify aliphatic and aromatic hydroxyl groups in lignin following derivatisation with different phosphorylating agents [8,17]. ^{31}P NMR is higher in sensitivity than many other heteronuclear NMR-active nuclei, such as ^{13}C or ^{15}N, due to 100% abundance in nature, moderately high gyromagnetic ratio, and quick relaxation properties. In addition, the wide chemical shift range in ^{31}P NMR reduces signal overlap [119]. When measuring lignin hydroxyls in a single spectrum, the ^{31}P approach offers a distinct advantage over other NMR techniques. ^{31}P NMR provides qualitative and quantitative data on different types of major hydroxyl groups in a comparatively short acquisition time, even with a small sample amounts [117]. The main limitations arise in the phosphitylation procedure rather than in ^{31}P NMR experiment itself. For accurate measurement, samples should be free of sulphur, contain a sufficiently high concentration of hydroxyl groups, and exhibit minimal contamination from carbohydrates and moisture [17].

2.4 Measurement Uncertainty

Measurement uncertainty describes the range of values around a measured value within which the true value of the measurand is expected to lie with a predefined probability [120,121]. It is a fundamental concept of metrology and scientific research, as it quantitatively characterises the reliability and accuracy of measurement results.

The overall uncertainty of a chemical analysis can be attributed to sampling (or subsampling) uncertainty and to the uncertainty associated with analysing the collected sample (or subsample). Sampling uncertainty arises from the variability introduced when selecting a representative portion of a bulk material. It represents an important contributor to the overall measurement uncertainty in analytical chemistry [30]. Sampling uncertainty is introduced because samples or subsamples taken for characterisation may have a somewhat different composition from the whole batch or bulk materials. This uncertainty becomes more relevant in the chemistry of natural products, such as lignin, due to their inherent heterogeneity

[122]. When the measurement result is presented for the bulk (as opposed to a sample), the uncertainty from the sampling stage is an inherent uncertainty component and only with its inclusion is it possible to obtain an accurate and realistic estimate of total measurement uncertainty, as opposed to relying only on uncertainties derived from laboratory-based analytical procedures [123]. In lignin research, sampling uncertainty has been largely ignored in most quantitative studies.

Accuracy is often considered a qualitative concept, but it can be quantitatively assessed through numerical expression of measurement uncertainty [124]. Deviations from the true value arise from both systematic and random effects, which together influence the measured result and contribute to measurement uncertainty. Both systematic and random effects on the measurement procedure are accounted for by accuracy. Precision, commonly reported as the standard deviation, is used to quantify random influences that contribute to variability. Trueness, often expressed as bias or recovery, reflects systematic deviations from the true value.

In this thesis, measurement uncertainty is evaluated for sampling using qNMR, water content determination with vap-C-KFT, and water/moisture determination using FTIR spectroscopy. The specific details relevant to each application are given in the respective sections.

2.5 Water and Moisture Content Determination

Accurate water and/or moisture determination in materials is essential in production, research, and development, as it directly influences product stability, efficacy, shelf-life, and regulatory compliance. Depending on the sample type, various analytical methods are used to determine moisture or water content [125–127]. Water and moisture are closely related concepts, but they are not identical. Water content refers to the amount of H_2O present in a sample, i.e., the absolute or relative abundance of water molecules, which is often represented as concentration or percentage [125,126]. The KF titration is explicitly employed for water content analysis [128]. In contrast, moisture content includes not only water but also other volatile components that may be lost during drying [91,92], and is commonly measured using gravimetric methods such as freeze-drying or oven-drying [86,88].

In this thesis, the term water content of lignin refers to the water physically and chemically bound to the lignin structure, excluding water formed by the thermal decomposition of lignin. The analytical approaches focus on quantifying water molecules initially present in or associated with the lignin material, rather than water generated during lignin degradation.

When lignin samples are heated at elevated temperatures, some other volatile components may also co-evaporate with water. The presence of volatile organic compounds depends on both the origin and the processing method used for lignin production, including lignin pulping and other methods. Typical volatile components in lignin are solvent residues, low molecular weight phenolic moieties, organic acid residues, sulphur-containing compounds, and degradation products.

Water, together with these co-evaporating volatile compounds, is commonly referred to as moisture in lignin.

2.5.1 Gravimetric Analysis

Gravimetric analysis is one of the oldest analytical techniques, with its origins tracing back to the early days of experimental science [129]. Moisture content can be determined gravimetrically by heating the sample under controlled conditions in oven-drying or thermogravimetric analysis and calculating the mass loss on drying. The accuracy of such determinations can be influenced by factors including oven design, temperature uniformity, airflow, sample size, and exposure time [130]. Gravimetric analysis using oven-drying is reliable for determining moisture content, especially in non-volatile organic materials. This method is inexpensive and is preferred when the sample has high moisture content and is not heat-sensitive. However, the accuracy of the results can be affected by factors such as sample size, sample container, oven temperature variations, and time [131]. To determine the moisture content of lignin, the oven-drying method is employed at the conditions prescribed in standard methods for moisture determination at 105 ± 2 °C for 7 h and 48 h [86].

Lyophilisation, commonly known as freeze-drying, is used to stabilise and preserve materials that are sensitive to moisture, and it is effective for a wide range of products that degrade when exposed to water [132]. In lignin analysis, this method is useful because it avoids the risk of altering its chemical structure at elevated temperatures via condensation reactions between lignin functional groups or decomposition. In addition, freeze-drying helps to avoid the loss of volatile organic matter [86]. Besides its uses in sample preparation, it is a valuable technique for determining moisture content in natural products, polymers, food samples, and pharmaceutical products [133], as it preserves the structural integrity of thermosensitive materials [86].

2.5.2 Karl Fischer Titration

Karl Fischer (KF) titration is a widely recognised analytical technique that utilises volumetric or coulometric titration to determine water in a sample. This technique was developed in 1935 by the German chemist Karl Fischer [128,134]. The method is straightforward, accurate, reliable, robust, rapid, sensitive, applicable to a wide range of sample types, and can be automated. As a result, KF titration has become the standard method of water determination in a wide range of materials. It can determine water content at the ppm level and works with liquid, solid, and gas samples [128,135]. KF titration specifically determines water content, rather than total moisture content (i.e. water together with other volatile components) [136]. This method is versatile because it can accommodate different levels of water content through two distinct process modes. Coulometric Karl Fischer titration (C-KFT) is suitable for trace amounts of water and offers higher precision, whereas volumetric KF titration is typically used for moderate

to high water contents [137,138]. KF titration can measure bound and free water, such as water within crystals or on their surfaces [139].

KF titration uses a redox reaction in which iodine oxidises sulphur dioxide (SO_2) in an alcohol medium, with water being quantitatively consumed. In C-KFT, iodine is produced electrochemically at the anode of the generator electrode. The Karl Fischer reaction proceeds via a two-step reaction mechanism can be represented by Eqs. (2) and (3) [136,140,141].

$$ROH + SO_2 + R'N \rightarrow [R'NH]\cdot SO_3R \tag{2}$$

$$[R'NH]\cdot SO_3R + H_2O + I_2 + 2\,R'N \rightarrow 2\,[R'NH]\cdot I + [R'NH]\cdot SO_4R \tag{3}$$

where ROH represents an alcohol, typically methanol or 2-methoxyethanol, and R'N is a base (typically imidazole).

In C-KFT, iodine required for the reaction is produced electrochemically at the generator electrode according to the following reaction (Eq. 4) [141]:

$$2I^- \rightarrow I_2 + 2e^- \tag{4}$$

The key principle of the KF titration method is that one mole of water reacts stoichiometrically with one mole of iodine (I_2) in the measured sample. The iodine generated at the anode participates in the Karl Fischer reaction (Eq. 3), in which one mole of water is consumed per mole of iodine formed. An indicator electrode detects the titration endpoint once all the water present in the sample has reacted and excess iodine appears in the system [140].

At the cathode of the generator electrode, hydrogen ions are reduced by electron uptake, leading to the generation of hydrogen (Eq. 5):

$$2H^+ + 2e^- \rightarrow H_2\uparrow \tag{5}$$

In C-KFT, water content is quantified from the electric charge required to electrochemically generate iodine, which reacts stoichiometrically with water. This charge, obtained by integrating the current over time until the endpoint, is converted to the corresponding amount of water using Faraday's law of electrolysis (Eq. 6) [140,142].

$$m_{H_2O} = \frac{M_{H_2O}\cdot Q}{z\cdot F} \tag{6}$$

where m_{H_2O} is the mass of water, M_{H_2O} is the molecular weight of water, Q is the measured electric charge, z denotes the number of exchanged electrons (z = 2), and F is the Faraday constant (F = 96485 C/mol). Based on Faraday's law of electrolysis, the mass of water is directly proportional to the total charge passed through the system, determined by integrating the measured current over time. C-

KFT can be regarded as a primary measurement method, as the amount of iodine generated is directly proportional to the measured electric charge. Therefore, metrological traceability can be established through measurements of time and current and no analyte-specific calibration is required [143–145]. The titration endpoint is reached when excess iodine is generated and detected voltametrically once the reaction has consumed all the water in the sample.

KF titration is extensively utilised to determine water content in various samples across the pharmaceutical, food, chemical, and petrochemical industries, as well as in the electronics, paper, polymers, and cosmetics industries, where water content can significantly affect processing results, product behaviour, and performance.

Despite its accuracy, the Karl Fischer technique has some limitations. It is incompatible with real-time water content monitoring and uses potentially hazardous chemicals such as methanol, pyridine or imidazole, iodine, and sulphur dioxide [143].

Direct determination of water content in solid materials can be achieved by coupling KF titration with a vaporisation oven, resulting in the vap-C-KFT method. It is a direct, accurate chemical method used for quantitatively determining water content in samples for which the direct injection method is impractical.

However, during vaporisation, the sample may degrade, yielding water, which leads to overestimation of water content. For example, it was shown that in plant-based materials, the measured water content depends on the chosen KF vaporisation oven temperature [146], which makes it important to select appropriate oven temperatures for a material. In this thesis, optimal temperatures for various sample types are determined. The dependence of experimental water content values on KF oven temperatures is approximated with the “sigmoid-curve” model described in detail in Section 4.3.1.

2.6 Fourier Transform Infrared (FTIR) Spectroscopy

FTIR spectroscopy is one of the most versatile analytical techniques for identifying and characterising materials, as well as quantifying their components [147,148]. This technique determines a sample’s absorption of infrared radiation based on the principle that molecular bonds vibrate at specific frequencies, producing a distinct absorption spectrum which acts as a molecular fingerprint; this information is used to reveal the molecular constituents of the material [60,149]. This absorbance behaviour enables the application of FTIR spectroscopy for quantitative analysis, provided that the Beer–Lambert law is obeyed; that is, the absorbance is proportional to the concentration of the absorbing species under the selected measurement conditions [150,151]. A significant development in FTIR sampling was the introduction of the ATR method, which enables direct sample analysis for solid, liquid and semi-solid samples with

minimal sample preparation and provides reproducible and consistent results [152,153].

FTIR spectroscopy is simple, non-destructive, relatively inexpensive, and rapid [154,155]. It offers several advantages, including good sensitivity, in some cases good selectivity, good accuracy and reproducibility of results [61,156–158]. Its broad applicability makes it a vital tool for identifying and characterising the molecular composition of different substances [159]. Many organic and inorganic compounds containing covalent bonds can absorb electromagnetic radiation at various infrared frequencies, making them IR-active and allowing them to be identified and quantified using FTIR spectroscopy [160].

FTIR spectroscopy has been widely employed in the investigation of lignocellulosic materials [161] to characterise chemical structures and compositions [61,162]. FTIR spectroscopy enables qualitative and quantitative analysis of functional groups, such as hydroxyl, carbonyl, and methoxy groups [61,163], as well as various phenolic and aromatic compounds and related molecular interactions [61,154].

FTIR spectroscopy has been used for water determination in different materials. Water absorbs IR radiation primarily in the O–H stretching vibrational region around 3600–3200 cm^{-1} and the H–O–H bending region near 1655–1640 cm^{-1} [13]. In FTIR spectroscopy, different vibration bands are not specific to particular functional groups, and overlapping of absorption bands therefore often occurs. In the region 3600–3200 cm^{-1}, functional groups such as hydroxyl groups from aromatic and aliphatic compounds, carboxyl groups, and water fall in similar regions. In contrast, the H–O–H bending vibration of water around 1650 cm^{-1} may overlap with e.g. the carbonyl stretching band [13,14,164].

The influence of water on lignin spectra extends beyond the O–H stretching and H–O–H bending regions, as water interacts with lignin through adsorption and hydrogen bonding. The band near 1670 cm^{-1}, which is attributed to C=O stretching vibrations, shows increased intensity with increasing water content, suggesting that carbonyl groups may act as additional water sorption sites. Similarly, bands in the 1200 cm^{-1} region, corresponding to C–C and C–O stretching vibrations, also show increased intensity with increasing water content, reflecting interactions between water molecules and lignin macromolecules [13,14,165]. The presence of water molecules can alter the lignin spectra, in wavenumber regions including C=O, C–O, C–O–C functionalities, due to hydrogen bonding, which changes the local environment of lignin functional groups, shifting their vibrational frequencies [165].

Because of the high probability of overlap between bands of components in infrared spectra of mixtures, the traditional univariate calibration is usually insufficient for quantitative FTIR analysis. Instead, multivariate chemometrics methods, such as PLS-R, are often used with FTIR spectroscopy to enable robust quantitative analysis.

FTIR spectroscopy has been used to quantify water and moisture content in various materials, including natural fibres, cellulose, lubricating oils, and hydrocarbon lubricants [166–168]. Although ATR-FTIR spectroscopy combined with

PLS-R has been widely used in the moisture determination of various biomaterials, based on the available literature, it has not been applied to lignin. There is only one report, to our knowledge, that demonstrates moisture absorption behaviour in lignin at nanogram-scale resolution, employing FTIR with PLS-R, and that report did not use ATR [13]. The authors employed only one reference method, Dynamic Vapour Sorption (DVS), to determine reference values and did not elaborate on the accuracy or limitations of moisture quantification. They developed three calibration models spanning different spectral regions of the FTIR range and discussed the relative advantages and disadvantages of each [13].

2.7 Partial Least Squares Regression

Chemometrics is the application of mathematical and statistical methods to extract relevant chemical information from complex data. Chemometric techniques are widely applied in analytical chemistry to interpret complex multivariate datasets. The term "chemometrics" was first introduced in the 1970s [169,170]. Chemometrics relies on multivariate data, i.e. measurement of multiple variables for each sample, resulting in large, complex datasets. These techniques facilitate the interpretation of such data, supporting improved understanding, classification, quantification of analyte concentrations and prediction of chemical properties [169]. Multivariate calibration enables the use of rapid, inexpensive, and non-destructive analytical techniques, such as FTIR and near-infrared spectroscopy (NIR), to accurately predict chemical properties of complex materials [169,171]. Chemometric models have been widely employed in various fields, including food science [172,173], pharmaceuticals [174], petrochemicals [168], biomass analysis [26,175–177], and polymer characterisation [169,178].

Among multivariate calibration methods, PLS-R is one of the most widely used approaches for modelling relationships between spectral data and corresponding variables of interest (e.g., analyte concentration). PLS-R is applicable to data generated by liquid chromatography–mass spectrometry (LC-MS), GC-MS, NMR, FTIR, and NIR spectroscopy [169].

FTIR spectroscopy combined with PLS-R has become an important tool for lignin characterisation, rapid quantification of lignin content and functional groups, and determination of molecular properties [179,176,180]. PLS-R is particularly effective for extracting information from large sets of complex spectral data, most importantly, with overlapping bands and bands belonging to unknown components. This capability has enabled e.g. the prediction of the lignin, cellulose, and hemicellulose concentrations in lignocellulosic materials [61,171,181, 182]. In wood chemistry, PLS-R has been widely employed to determine lignin content [179], to quantify major wood chemical components (i.e., % of lignin, cellulose and hemicellulose in wood) [175,179], and to predict biomass thermal reactivity, energy content and chemical composition [26]. PLS-R has been applied to the characterisation of lignins, including molecular weight distribution, inter-unit linkage abundance, functional group content, and S/G ratios [177].

FTIR spectroscopy with PLS-R has also been used for the determination of water/moisture in various materials [168,183,184], including lignin [13]. Water has distinct IR absorbance bands, but they overlap with absorbance bands of other functionalities, as explained in Section 2.6, so univariate calibration is not sufficient. The spectral response of water is distributed over several wavenumber regions, each of which is influenced by chemical interactions, including hydrogen bonding [13,14,165]. Multivariate PLS-R calibration approach overcomes the overlap between different absorption bands by using latent variables that have been composed to maximise the covariance between the observed spectral features and water or moisture content, providing greater robustness than single-band approaches, particularly in complex systems such as lignin.

3 EXPERIMENTAL SECTION

3.1 Chemicals and Materials

Two KL (product numbers 471003 and 370959) were purchased from Sigma-Aldrich (Saint Louis, USA), while dealkaline lignin was procured from TCI Chemicals (Tokyo, Japan). Fibenol Lignova was supplied by Fibenol OÜ (Tallinn, Estonia). The dimethyl sulphoxide-d_6 (DMSO-d_6) (99.8%, containing 0.03% tetramethylsilane (TMS)) was acquired from Deutero GmbH (Kastellaun, Germany). The α-D-lactose monohydrate (with a water content of 5.00%) was obtained from Acros Organics (Geel, Belgium). Hydranal Coulomat AG anolyte for C-KFT (methanol-based) was purchased from Honeywell Fluka (Seelze, Germany). Additional non-commercial lignin samples were provided by Dr. Siim Salmar's research group. For the remaining materials see papers I–IV.

3.2 Samples, Sampling and Sample Preparation

3.2.1 Sampling and Sample Preparation for Uncertainty Evaluation (Paper II)

A total of 15 lignin samples were prepared from a 1.0 kg container of KL (471003) by systematic sampling from defined spatial regions of the container. Specifically, five samples were taken from each layer: top, middle, and bottom. For proton nuclear magnetic resonance (^{1}H NMR) analysis, 5.0 mg of each sample was weighed on an analytical balance (Sartorius CPA225D-0CE, Repeatability standard deviation for 0–100 g: 0.02 mg) and dissolved in 0.6 g of deuterated dimethyl sulphoxide (DMSO-d_6) inside an NMR tube. A small amount of sample and low concentration of the solution was deliberately chosen to ensure complete dissolution, to avoid the need for large volumes of solvent and in some cases to address limited sample availability. Weighing a small amount of sample mass did not compromise measurement accuracy, as the study relied on peak area ratios and accurate sample mass was not needed in the calculations.

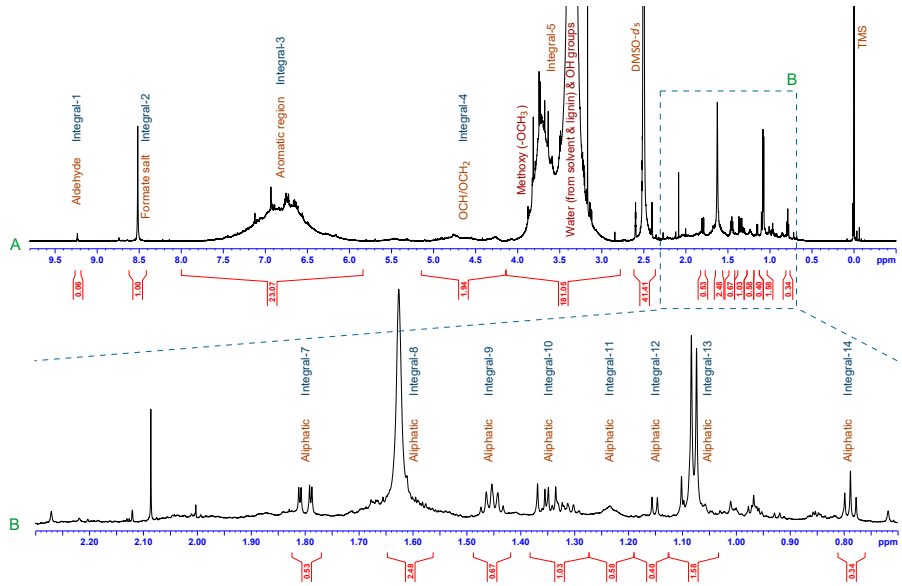

Figure 2. (A) Representative example of an acquired ^{1}H NMR spectrum of a KL (471003) sample dissolved in DMSO-d_6. (B) Detailed view of the aliphatic region ranging from 0.70 to 2.30 ppm.

3.2.2 Preparation of Calibration Samples for Water and Moisture Determination

Commercial lignin samples obtained from different pulping techniques described in Section 3.1 were selected for analysis to ensure robust and externally valid calibration of the predictive model by including a broad spectrum of chemical compositions and moisture profiles. Different subsamples of 60–70 g were either dried or hydrated under controlled conditions to obtain a broad set of calibration samples with a range of moisture levels. Samples with low water content were prepared using a rotary evaporator under reduced pressure. Drying was conducted at 35–40 °C under a reduced pressure of 1–3 mbar for varying durations, ranging from 10 minutes to 4 h, to achieve different levels of water content.

To increase water content, two controlled conditioning approaches were employed. In the first approach, lignin samples were placed inside a desiccator containing a saturated potassium nitrate solution at the bottom. The samples were kept under these conditions at room temperature for 24–72 h, allowing varying amounts of water to be absorbed. In the second approach, samples were placed in a Weiss Umwelttechnik GmbH WK 111-340 climate chamber, where they were exposed to controlled humidity levels between 75% and 95% at a stable temperature of 20 ± 1 °C. The exposure duration varied from 8–72 h, during which lignin samples were homogenised to ensure uniform moisture distribution [III].

3.3 Instrumentation and Methods

3.3.1 Sampling Uncertainty Estimation

Sampling uncertainty was evaluated using ^{1}H NMR spectroscopy by analysing variability in signal intensity ratios across independently prepared subsamples. The measurements were conducted using a Bruker Avance-III 700 MHz NMR spectrometer equipped with a 5 mm BBO (broadband observe) probe. The field strength of the superconducting magnet was 16.4 T. The sample temperature was maintained at 25 °C for all measurements. The NMR spectra were recorded with 81920 data points, a 30° pulse, and a recycle time of 5.91 s (acquisition time 2.9 s and relaxation delay 3.0 s) [19]. Each spectrum was obtained with 2048 scans, preceded by 4 steady-state scans.

Data processing was performed with Bruker TopSpin 3.2 software. The spectra were zero-filled to 262144 points, and an exponential line broadening of 0.1 Hz was applied. Fourier transformation, manual phase correction, and baseline correction were performed using the spline baseline correction method. Two reference peaks were identified for analysis, both sufficiently separated and suitable for reliable baseline correction. The first reference peak, between 8.40–8.65 ppm, was assigned to formate salt in the lignin product, while the second, between 1.56–1.60 ppm, was attributed to aliphatic fragments. These reference signals were used to calculate relative signal intensities of selected lignin structural peaks. All peaks in both the aliphatic and aromatic regions were integrated, and separate data analyses were performed using each of these reference integral peaks. As shown in Figure 2, 11 different signal intensities, listed in Table 1, were used for the quantitative study. To understand the impact of sample preparation on integral variability relative to NMR measurement and integration, only spectral signals and ranges that were fully separated, had moderate signal intensity, and enabled reliable baseline correction were selected for further analysis. Due to the high-intensity signal at 2.80–4.10 ppm, corresponding to combined methoxy and hydroxyl groups, these peaks were excluded, whereas peaks at 9.18–9.20 ppm were excluded because of low intensity.

The NMR tubes were sealed and placed in an ultrasonic bath for 10–15 minutes to promote complete dissolution. All samples were prepared using a consistent protocol over 2–3 days. Each ^{1}H NMR spectrum was recorded in quadruplicate from the same solution, with individual measurements randomised and distributed over more than a week to account for day-to-day instrument variability and to evaluate the intermediate precision of the method, helping to reduce the influence of systematic measurement timing effects and support more reliable results [II]. The variability of these relative signal intensities across subsamples was used as a measure of sampling-related heterogeneity, providing an estimate of the sampling contribution to overall measurement uncertainty.

3.3.2 Determination of Moisture and Water Content Reference Values

Three different methods were employed to determine the reference values of moisture and/or water content in the lignin calibration samples that were subsequently used for calibrating the FTIR method using the PLS-R approach.

3.3.2.1 Oven Drying Method

In the gravimetric oven drying method the reduced weight, attributed to the evaporation of water and possibly other volatile components, is used to calculate the moisture content. The procedure described in the ISO 6350:2024 standard was implemented to determine moisture content in lignin samples [86]. Lignin samples weighing 1.5–4.0 g were weighed on the analytical balance (Sartorius CPA225D-0CE) and then heated in an oven at 105 ± 2 °C for 48 h. The samples were heated for up to 48 hours, and their masses were recorded after 2, 4, 7, 24, and 48 hours of drying. Prior to weighing, samples were allowed to cool in a desiccator to minimise moisture reabsorption.

The mass losses at 7 h and 48 h were used to calculate two different moisture contents using Eq. (7). To evaluate between-day reproducibility, selected experiments were repeated two or three times on different days. For each sample, the mean moisture content was calculated at both 7 h and 48 h drying times.

$$W_{\text{moisture}} = \left(\frac{m_0 - m_1}{m_0}\right) \times 100\% \tag{7}$$

where W_{moisture} represents the moisture content (%), m_0 denotes the mass of the sample before drying (g), and m_1 indicates the mass of the sample after drying (g). Some experiments were conducted twice or thrice to assess repeatability.

3.3.2.2 Freeze-drying (Lyophilisation) Method

The freeze-drying method involved weighing the lignin samples (1.5–3.0 g), pre-cooling to -80 °C for 3–4 h, and freeze-drying in SCIENTZ-10N freeze-dryer (Ningbo Scientz Biotechnology Co., Ltd., Ningbo, Zhejiang, China) at a reduced pressure of 0.06–0.08 mbar for 72 hours [86].

The samples were weighed before and after the process to determine the moisture content using Eq. (7). This method was effective for removing moisture without thermal degradation of lignin. To determine both repeatability and between-day reproducibility, the selected samples were analysed two or three times consecutively to assess repeatability, while measurements were performed on separate days to assess between-day reproducibility. The mean moisture content values were calculated from the replicate determinations.

3.3.2.3 Coulometric Karl Fischer Titration Method

The main measurement parameters in vap-C-KFT comprised oven temperature, carrier gas flow rate, extraction time, drift correction, and endpoint criteria. The carrier gas (dry nitrogen) flow rate was set to 50 mL min^{-1}, and the minimum analysis time (also known as extraction time) was 600 s per sample vial, with the analysis continued until the predefined endpoint criteria were met. Drift correction was applied by determining the water drift rate using a conditioning vial and subtracting the corresponding contribution from the measured water content. The oven temperature was specifically optimised to balance incomplete water release and thermal decomposition effects, with the optimisation methodology discussed in Section 4.3.

The vap-C-KFT measurements were validated using α-D-lactose monohydrate as a reference material (with water content 5.00% by mass) to confirm correct instrument performance and accurate water determination. All the measurements were repeated three times to evaluate the method's repeatability. The standard deviation of the measurement falls within the acceptable range, indicating that measurements show high precision and consistency. The repeatability precision of the process was expressed as a pooled standard deviation, which was 0.08% by mass. Further experimental details can be found in Article III.

3.3.3 Analysis of Lignin with ATR-FTIR Spectroscopy

The ATR-FTIR spectroscopic method was developed to determine both water and moisture content in the lignin samples. ATR-FTIR spectra were recorded on a Bruker Alpha II spectrometer (Ettlingen, Germany). Spectra were recorded in the range 3997–350 cm^{-1} with 4 cm^{-1} resolution and 32 accumulated scans. A single-bounce diamond ATR crystal (2 mm spot diameter) was employed, ensuring consistent contact via a pressure applicator. Before the measurement, all the bulk lignin samples were mixed thoroughly to ensure uniformity and representativeness. Further experimental details can be found in Article III.

The multivariate data analysis was performed using Opus Quant software. All lignin samples were stored in airtight glass containers and thoroughly homogenised by shaking prior to ATR-FTIR analysis. Three replicate measurements with three separate subsamples were performed with each lignin sample on the same day.

The ATR sampling area is not isolated from the atmosphere. In order to evaluate the possible interference from the atmospheric moisture on lignin samples during FTIR measurements, the water content of some samples was determined before and after FTIR measurement using vap-C-KFT. The determined water contents of the lignin samples (before and after FTIR measurement, respectively) were as follows: Lignova 1 (Fibenol): 2.88%, 2.60%; KL (370959): 3.03%, 2.96%; KL (471003): 5.31%, 5.28%; DAL: 11.03%, 9.34%. Except for the DAL sample, the water content variation was minor and within acceptable limits before and after the measurement. The decrease in water content of the DAL sample was

significant. However, as presented in Figure 3, it affected only the surface of the sample pile, not the portion of the sample which is in direct contact with the ATR crystal and the applicator. The change in water content might be due to higher moisture content compared to the other lignin samples. The validity of this assumption is confirmed by the very good agreement of the spectra obtained from replicate measurements of the subsamples of the same lignin sample.

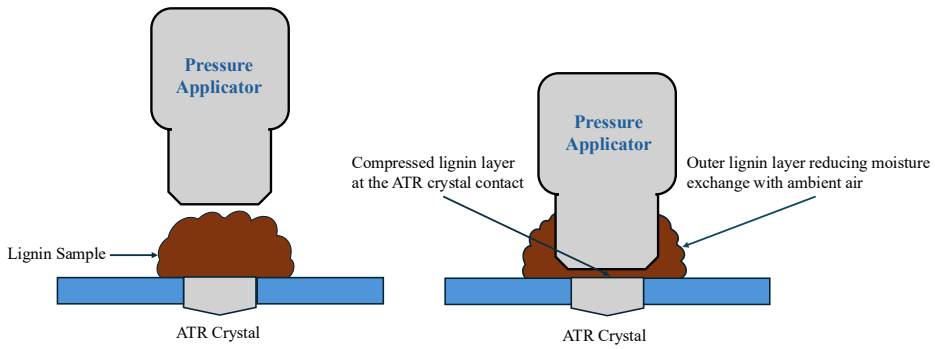

Figure 3. Cross-sectional schematic of the ATR-FTIR pressure applicator setup: (a) pressure applicator before contact with the ATR crystal; (b) pressure applicator after contact with the lignin sample.

3.4 Data Analysis

3.4.1 Statistical Techniques Used for Sampling Uncertainty Evaluation

Sampling errors, baseline irregularities, and partially overlapping peaks in qNMR measurements were identified as the primary sources of uncertainty. Two approaches were used to estimate sampling uncertainty–analysis of variance (ANOVA) and a simplified estimation approach, which is explained in 4.2.1.1.

Pooled standard deviation [185] was used to combine standard deviations from multiple datasets to estimate a more reliable standard deviation, especially when assuming that the variability across the groups is the same. It is employed when the sample size is small, unstable samples for a long period, or it is difficult to make a sufficient number of samples. The pooled standard deviation can be applied when the measurements involve the same analyte/measurand, follow an identical method, and are performed on similar samples and on similar analyte concentrations. Depending on the purpose, it can be employed on samples analysed within a day or over a period of time.

Outlier detection in the collected data was performed using the Dixon Q test [186,187] at a 95% confidence level without applying p-value adjustment. The test was performed separately for each type of integral corresponding to each sample category, that is, the top, middle, and bottom layers of samples, with data

from five replicates pooled together. This procedure resulted in a total of 30 Dixon tests, each involving 20 data points. To assess the normality of the data distribution, all integral values were normalised, and the resulting dataset was pooled into 600 data points. The normality of the distribution was then evaluated through visual comparison with a cumulative normal distribution curve and a linearised normality plot. The detailed analysis process is documented in the Excel file, which is available as Supporting Information of Article II.

The overall variability of the results, as relative standard deviation (RSD_{Total}) (see 4.2.1.1) for each individual intensity ratio, was calculated by determining the relative standard deviation (RSD) from all replicates across the 15 samples. To obtain the variability caused by measurement (RSD_{Meas}) for each signal ratio, a pooled RSD was calculated based on the results of four replicate measurements of the same signal intensity ratio from all 15 samples, following the procedure outlined in ref [185].

3.4.2 Multivariate Data Analysis for Water and Moisture Determination Using ATR-FTIR

A quantitative evaluation of water and moisture content in lignin samples from ATR-FTIR spectra was carried out using PLS-R as implemented in the Bruker Opus Quant software. The calibration models were developed using 30 samples for vap-C-KFT and 27 samples for other methods (4 samples were available in small amounts and were used only for the vap-C-KFT method), with an independent test set of 5 samples. Despite the small number of calibration and test samples, this number of samples is considered adequate for this proof-of-principle study.

Reference values of water content were determined by vap-C-KFT as explained in 3.3.2.3. Reference values of moisture were determined by three methods – air oven-drying (7 h and 48 h) as explained in 3.3.2.1, and freeze-drying, as explained in 3.3.2.2. The models were optimised by minimising root mean square error of cross-validation (RMSECV) by adjusting spectral ranges (within the 3997–350 cm^{-1} range); applying the following preprocessing methods: standard normal variate (SNV) or SNV + the first derivative, Multiplicative scattering correction (MSC), First derivative + MSC and the second derivative; and selecting the optimal number of latent variables. Outlier spectra were detected by software and excluded from the calibration model, ensuring at least two spectra remained for each sample. The models were then re-optimised after removing the outlying spectra. The quality of the final models was evaluated by the root mean square errors of prediction (RMSEP) obtained from the analysis of the test set samples. Further details can be found in Article III.

4 RESULTS AND DISCUSSION

4.1 Accuracy of qNMR for Lignin Quantification

4.1.1 Analysis of Published Data: Insights from Literature Review

A targeted literature review was conducted to identify reports that mainly focused on the accuracy of the qNMR lignin analysis. As highlighted in the literature, qNMR spectroscopy has garnered significant attention and has been extensively employed for the quantitative analysis of various functional groups in different types of lignin, utilising a range of NMR techniques. In contrast to research that just used qNMR to resolve different technical issues, this part of the thesis attempted to evaluate studies specifically focused on assessing the accuracy of lignin qNMR analysis. The selection was narrowed down to 21 most relevant papers out of several hundred potential candidate's [I]. The selection was based on predefined criteria, prioritising studies that explicitly addressed accuracy, validation, or uncertainty in qNMR lignin analysis. These selected studies were categorised into two groups: (i) studies primarily focused on quantifying lignin components through the novel qNMR approach and (ii) studies explicitly addressing the accuracy of qNMR quantification [I].

4.1.2 Sources of Measurement Uncertainty

The selected 21 reports demonstrate multiple variables that contribute to measurement uncertainty in quantifying different structural subunits in lignin using qNMR analysis. The familiar and recognised uncertainty sources in proton NMR include inaccuracies in the integration of the signals, baseline distortions, spectral noise, and overlapping of spectral signals of different structural units, which cause complications in the integration of signals [8,188]. Furthermore, in 2D NMR techniques such as HSQC, more specific contributors to uncertainty have been observed, including variations in coupling constants, resonance offset effects, the effect of proton T_1 relaxation, ^1H and heteronuclear T_2 relaxation, and proton-proton coupling [19]. Beyond these recognised sources, several uncertainty sources have been missed or underappreciated in most reports, yet they are important sources of uncertainty. These are:

(1) Variability due to sampling and subsampling: Although commercially procured lignin is typically considered a relatively homogeneous solid, compositional variation may still arise between subsamples derived from the same bulk sample, particularly if adequate mixing is not performed. Although repetition of measurements is a common practice, many reports provide insufficient data to specify whether these repetitions were from the same or different subsamples. A failure to account for this might significantly underestimate the overall measurement uncertainty. The data from ref [189] allow for the back-calculation of the RSD associated with sample

preparation, yielding values of 5% for ^{13}C and 8% for ^{31}P. These values were significantly higher than the RSD values associated with actual NMR measurement, which are 3% and 5%, respectively. These values highlight the significance of sampling and sample preparation as a major source of uncertainty. The elevated RSD in ^{31}P NMR may be attributed to the additional derivatisation step required, which is unnecessary for ^{13}C NMR. These values were higher than the RSD, which was attributed to the NMR measurement.

(2) Carbohydrate impurities: The lignin samples contain carbohydrate impurities such as cellulose and hemicellulose. The signals of these compounds overlap with signals originating from lignin in the aliphatic region in the NMR spectrum of lignin samples and can lead to an overestimation of results.

(3) Chemical alteration in the production of lignins: In the pulping process, lignin often changes its chemical composition and degrades aliphatic bonds and aromatic rings in a few cases. These changes must be addressed explicitly in uncertainty assessment frameworks, as leaving them out can lead to significant quantification errors.

The literature survey results are presented in Table 1 of Article I.

4.1.3 Accuracy and Trends in the Quantification of Lignin Analysis

In the structural analysis of lignin using NMR, some specific structural fragments yield higher measurement accuracy in their quantification than others due to their relative abundance and distinctive spectral data. The important functional groups, such as the methoxy group, hydroxyl group, and aromatic hydrogens, along with the quantification of S and G units and their ratio (S/G), are generally determined with high reliability. The accuracy is good because these features produce strong, well-distinct NMR signals, making them easy to quantify. In contrast, linkages such as β–β, β–5, and β–1 exhibit lower signal intensity and significant spectral overlap, leading to increased integration uncertainty and reduced quantification reliability. Different NMR methods influence accuracy; for example, for hydroxyl-group quantification in lignin ^{13}C NMR has been reported to provide higher accuracy than ^{31}P NMR [8]. In ^{31}P NMR, the selection and stability of internal standards are vital for ensuring the reliability and accuracy of results [8]. The most commonly used standards are cyclohexanol, endo-*N*-hydroxy-5-norbornene-2,3-dicarboximide, trioxane, and *N*-hydroxy-1,8-naphthalimide. An unsuitable standard has lower chemical stability or overlapping chemical shifts, which can compromise spectral resolution and quantification. For example, benzoic acid is generally avoided in lignin studies because its chemical shift overlaps with the resonance of carboxylic acid (COOH) groups in lignin, leading to inaccurate peak assignments and distorted quantitative data [8]. While early studies often overlooked detailed accuracy assessments, more recent research,

particularly the work of Balakshin and Capanema, has systematically addressed these issues, highlighting the advancement of qNMR techniques in lignin analysis [8,56,188]. Recent publications demonstrate reduced standard deviation and bias, which is reflected in reduced RSD and improved reproducibility compared to articles published in 1980–2000.

The accuracy of lignin quantification using qNMR methods is affected by several issues. Firstly, variations in industrial extraction and treatment approaches of lignin might change its chemical composition. As identified earlier, this uncertainty source becomes particularly significant with lignins that have undergone extensive treatment during processing. In such cases, defining the measurand can become problematic, as the nature of the sample may have partially or fully changed during processing. For partly decomposed or processed lignins, the question arises: what exactly is being measured? Is it the ratio of structural units in the original, unaltered lignin, or is it the ratio in the partially decomposed lignin, which has undergone chemical transformations and/or loss of functional groups? This distinction is crucial, as it directly impacts the interpretation of the measurement and its relevance to the intended analysis. Secondly, several studies report replicate measurements but often provide insufficient information about experimental conditions, raising the question of what exactly the meaning of the reported RSD or other precision estimates is. Finally, bias is inconsistently reported in the literature, often described as an "error", and frequently not taken into account. There is often no consideration of whether the reference models used truly reflect the complex structure of lignin, leading to potentially inaccurate bias estimates.

Additionally, most reports do not differentiate between within-day and long-term bias. Within-day bias refers to systematic errors observed within a single day of measurements, which may be random errors over a long time period (i.e. on different days, the magnitude and direction of bias may be different), while long-term bias persists across extended periods. This lack of differentiation affects the accuracy of lignin analysis by failing to address systematic errors optimally.

Based on the analysis of the literature sources, three main approaches are proposed in article I that can advance the field of lignin qNMR analysis. First, the measurand must be clearly defined: whether it reflects bulk lignin or a specific sample, and whether it refers to treated or untreated lignin, as this affects the uncertainty involved. Second, when reporting qNMR results, essential details should be included: number of replicate measurements, timing and within-day or over a long period of timing of measurements, repetition of sample preparation steps, and if comparison with reference values, it is important to assess bias accurately. Lastly, there is a need for reliable reference values.

At the time of this research, the COMAR database does not list any certified reference materials. which would be closely related to lignin. Although certified lignin reference materials are lacking, studies show consistent results across certain lignin types like Alcell and Indulin [188], suggesting that these materials could be formalised and distributed as reference materials for certification, e.g.

via an interlaboratory comparison. This way, these lignins could become standardised reference materials, providing a strong base for future lignin quantification efforts. This approach could help reduce variability between laboratories and offer a pathway to creating a widely accepted set of certified lignin reference materials, which can be used in further research work. In addition, future research may focus on creating a range of reference materials representing various types of lignin, treated under various conditions, from different technologies to support a broader range of analyses and applications. Such initiatives would significantly enhance the reproducibility and standardisation of qNMR results in lignin studies, advancing both fundamental research and industrial applications of lignin.

4.2 Sampling Uncertainty in qNMR

Sampling uncertainty is crucial to overall measurement uncertainty, especially in quantitative analysis of complex solid materials like lignin, which are inhomogeneous to some degree. However, as became apparent in the previous part of this thesis, sampling uncertainty has been largely neglected or inadequately addressed in most previous studies involving qNMR [I].

In this study, a comprehensive investigation into sampling and subsampling variability was explicitly conducted for commercial lignin. Sampling uncertainty is not limited to the qNMR technique. It is inherent to any other quantitative technique, arising before the measurement starts. Thus, essentially any quantitative technique could be used to investigate sampling uncertainty. However, for several reasons, qNMR is a very suitable technique for this purpose. It provides non-destructive, reproducible and accurate measurement results without the need for reference standards. By evaluating the contributions of sampling and measurement-related variability, this research aimed to elucidate the significance of sampling uncertainty in the quantitative analysis of lignin and provide two different calculation approaches for its assessment.

4.2.1 Evaluation of Sampling Uncertainty Using qNMR Analysis

Sampling uncertainty arises from the variability introduced while selecting the samples and subsampling from bulk samples, without accounting for errors arising from sample preparation or measurement procedures. In qNMR spectroscopy, this type of uncertainty shows up as signal intensity fluctuations. To ensure accurate analysis, it is crucial to distinguish between variability due to sampling and other sources of variability.

In order to ensure that as large a share as possible of the variability in the signals was due to the variability in sampling, the variability due to NMR measurement needed to be minimal. In order to ensure this, only particular signals and spectral ranges were selected (as shown above in Figure 2) for analysis to assess the effect of sample preparation on the variability of integrals, where the variability caused by NMR measurement and integration would have as low

effect as possible. Because of this, the following criteria for the selection of suitable signals were established: the signals should (1) be well separated and not overlap, (2) be sufficiently intense to provide reliable data without being excessively strong, and (3) enable satisfactory baseline correction. Because of these peak selection criteria, many peaks were omitted from the analysis. The selection process aimed to minimise errors caused by poor baseline correction or weak signals and to enhance the accurate evaluation of sampling-related uncertainties.

4.2.1.1 Data Analysis to Evaluate Sampling Uncertainty

The primary objective of the data analysis was to dissect the overall variability of relative peak intensities into two distinct components: variability arising from measurement and variability attributed to sampling. This data analysis was performed separately for the ten intensity ratios described in Section 3.3.1, and the ratios are presented in Table 1. Two analytical approaches were employed for this purpose. The first approach was the traditional Analysis of Variance (ANOVA) approach, comprehensively described in reference [190]. The second approach was a simplified approach, breaking the total variability down into two distinct parts: variability due to sampling (RSD_{Sampling}) and RSD_{Meas} [II]. The relationship between these components is described by the following Eq. (8):

$$RSD_{\text{Total}} = \sqrt{RSD_{\text{Sampling}}^2 + RSD_{\text{Meas}}^2} \tag{8}$$

From this Eq. (8), the RSD_{Sampling} can be expressed as follows:

$$RSD_{\text{Sampling}} = \sqrt{RSD_{\text{Total}}^2 - RSD_{\text{Meas}}^2} \tag{9}$$

Both RSD_{Total} and RSD_{Meas} are directly available from the experiment. The total variability (RSD_{Total}), calculated as the standard deviation of results obtained from all samples drawn from the bulk material, encompasses both sampling-related variability and measurement-related variability. In contrast, the variability determined from replicate measurements of the same sample (RSD_{Meas}) reflects only the variability introduced by the measurement process itself.

Both methods yielded consistent results, confirming the robustness of the analysis. The calculated pooled RSD values (averages from the two data analysis approaches) are presented in Table 1. Full details, data of the individual approaches and calculation files are available in the Appendix of Article II.

Table 1. Overall Relative Standard Deviations of Signal Ratios (RSD_{Total}), RSD due to measurement (RSD_{Meas}), and RSD due to sampling ($RSD_{Sampling}$), the values represent averages from the two data analysis approaches.

Signal Integrals Used for Calculating the Ratios against Signal at 8.40–8.65 ppm (Formate Salt Integral-2)	***RSD*$_{Total}$**	***RSD*$_{Meas}$**	***RSD*$_{Sampling}$**
		Individual RSD Values	
Aldehyde Integral-1 (9.18 to 9.30 ppm)	3.5%	2.7%	2.3%
Aromatic Region Integral-3 (5.80 to 8.00 ppm)	4.8%	3.4%	3.4%
O–CH/O–CH_2 Integral-4 (4.13 to 5.10 ppm)	7.4%	6.3%	3.9%
Integral-7 (1.77 to 1.79 ppm)	3.7%	3.1%	2.0%
Integral-8 (1.56 to 1.60 ppm)	3.5%	2.7%	2.2%
Integral-9 (1.40 to 1.45 ppm)	4.5%	4.0%	2.1%
Integral-10 (1.26 to 1.32 ppm)	4.5%	4.1%	1.7%
Integral-11 (1.19 to 1.23 ppm)	5.7%	5.5%	1.6%
Integral-12 (1.12 to 1.15ppm)	6.7%	6.4%	1.9%
Integral-13 (1.03 to 1.08 ppm)	3.3%	2.8%	1.8%
Integral-14 (0.76 to 0.79 ppm)	5.4%	5.0%	1.9%
		Pooled RSD Values	
	5.0%	4.4%	2.4%

The RSD values for individual signal intensity ratios, as presented in Table 1, ranged from 3.3% to 7.4% for RSD_{Total}, 2.7% to 6.4% for RSD_{Meas}, and 1.6% to 3.9% for $RSD_{Sampling}$. According to this data, measurement-related variability usually surpassed sampling variability, which is $RSD_{Sampling}$. However, despite the observed variability, no evident pattern or outliers were identified, suggesting that statistical fluctuations cause the differences.

The pooled RSD values under the used experimental conditions (Table 1) indicate that the RSD related to NMR measurements (including peak integration) and sampling differ approximately by two times. Thus, although not the dominant uncertainty source under our conditions, sampling uncertainty contributes significantly to overall measurement uncertainty, as shown by this result. Unlike the common practice up to now [I], it should always be considered.

Minor variations in peak shape and chemical shift were observed in replicate NMR measurements, but these issues were resolved by the increasing number of scans, which enabled a precise assessment of sampling uncertainty. Future studies could benefit from exploring sampling variability in lignin derived from different production technologies and other natural materials. It is expected that raw industrial samples have a higher level of inhomogeneity and, consequently, more significant sampling uncertainty is expected, compared to the relatively homogeneous, commercially sourced fine lignin powder used in this research.

4.3 The "Sigmoid Curve" Approach of Water Content Analysis

4.3.1 Sigmoid Curve Modelling

A model termed "sigmoid curve" was applied to describe temperature-dependent water release and to identify the optimal oven temperature in vap-C-KFT. Water content in lignin reference samples was measured using a vap-C-KFT equipped with a sampling oven. A key parameter of this method is the oven temperature. Using different oven temperatures leads to different water content results. In vap-C-KFT, the oven temperature influences the amount of water released from lignin samples. As explained in 2.1.4, low oven temperatures may result in incomplete water release, while excessively high temperatures can lead to the release of an excess amount of water due to sample decomposition. A typical example of such decomposition process is presented by the elimination reaction in Section 2.1.4. Optimisation of the oven temperature for accurate determination of water content in lignin using the sigmoid curve approach was represented by Eq. (10).

$$C = C_0 - a_1 e^{-b_1 T} + a_2 e^{b_2 T} \tag{10}$$

where C represents the concentration of water found from the vap-C-KFT measurement, T is the oven temperature, a_1 is the offset of the lower curve (see Figure 4), a_2 is the offset of the higher curve, b_1 determines the shape of the lower curve, and b_2 determines the shape of the higher curve. The lower curve (Figure 4) represented by the red line corresponds to insufficient water release due to low oven temperatures, whereas the higher curve represented by the green line corresponds to the higher water release due to the decomposition of samples. The constant term (C_0) represents the "plateau", indicating the best estimate of the actual water content of the sample where a balance is achieved between in-complete water release and water generated from partial decomposition of the material. The C_0 value provides an estimation of the non-chemically bound water content within the samples. The oven temperature that results in this equilibrium is considered the optimal temperature for conducting vap-C-KFT of the material, ensuring unbiased moisture determination.

The optimal analysis temperature T_{opt} is defined as the temperature where the negative bias from incomplete release is compensated by the positive bias from decomposition, i.e., where $C = C_0$. Equating C and C_0 in Eq. (10) and rearranging yields:

$$T_{opt} = \frac{ln\,(a_1) - ln\,(a_2)}{b_1 + b_2} \tag{11}$$

Water content in different lignins was measured at oven temperatures ranging from 50 °C to 250 °C to investigate the effect of oven temperature. The obtained water content values were plotted against the corresponding oven temperatures,

and the experimental data were fitted using the model described in Figure 4. To achieve the best fit of Eq. (10) to the experimental data, the constants C_0, a_1, a_2, b_1, and b_2 were systematically adjusted. The value of C_0, representing the plateau in the curve, was interpreted as the actual water content of the sample.

Figure 4 shows an example of the graph used to determine the optimal oven temperature, which in this case is 130 °C. The sigmoid graphs of all the main types of lignin–KL (471003 & 370959), Lignova Fibenol, and DAL results are published in article IV. In all four studied lignin types, the model equation fits the experimental data points at a satisfactory level.

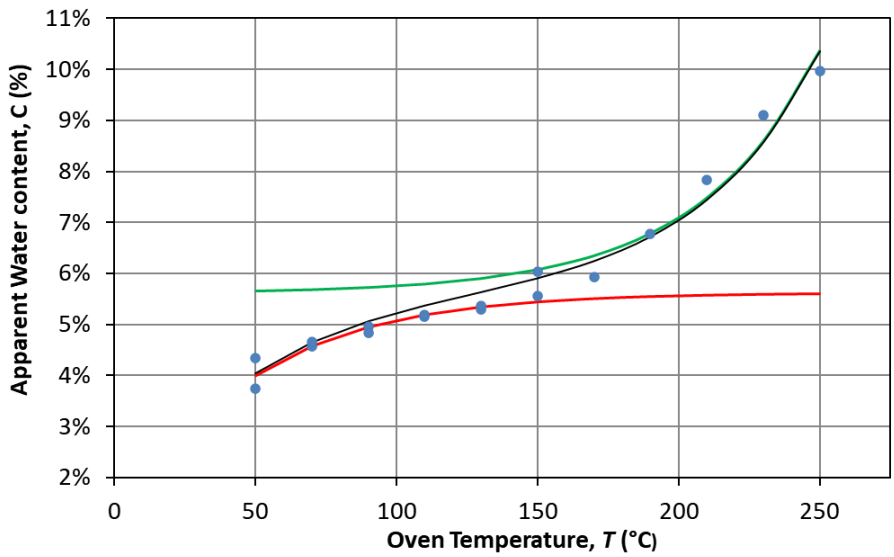

Figure 4. Representative water vap-C-KFT water content measurement results for KL (471003) across varying oven temperatures. The red line indicates insufficient water release, the green line signifies sample decomposition, and the black line represents the overall model described by Eq. (10).

Based on these graphs, oven temperatures were selected for the different types of lignin using the vap-C-KFT method. Table 2 gives an overview of the oven temperatures and vap-C-KFT results obtained for four lignin reference samples.

4.3.2 Optimisation of Temperatures for Lignin Materials and Measurement Uncertainty

Table 2 presents for every lignin type the determined optimal analysis temperature (°C), the corresponding water content in different lignin types (%), and the combined standard uncertainty of water content. The optimal temperature for Fibenol Lignova was determined to be 114 °C; however, a round temperature 110 °C was used for the vap-C-KFT measurements. Likewise, for KL (471003), the

optimal temperature was 129 °C and 130 °C was used during analysis. In the case of KL (370959), the sigmoid-curve model initially indicated an apparent optimal temperature of 130 °C. However, the data points for this type of lignin do not fit the model very well, and after further investigation, another optimal temperature estimate was found to be 164 °C. Because the sigmoid curve for KL (370959) did not fit well all experimental data points and because the temperature 164 °C is very different from the temperature 130 °C found for the other type of KL, as well as very different from the temperature used for any other lignin, the temperature was not further adjusted, and the same analytical temperature used for KL (471003) was retained for determining the water content in KL (370959). The suitability of this decision is demonstrated in section 4.4.2.3. The combined standard uncertainty (see next subsection) for all lignin samples was 0.2–0.3 %, which is suitably low. Table 3 presents the optimal parameters found for the different lignin sample types.

Table 2. Different studied lignin materials, the optimal vap-C-KFT temperatures, water contents C_{water} (% by mass) and combined standard uncertainties.

Material	$T_{optimal}$ **(°C)**	C_{water} **(%)**	$u_c(C_{water})$ **(%)**
Lignova lignin	114	3.2	0.2
Kraft lignin (471003)	129	5.6	0.3
Kraft lignin (370959)	130/164	3.4	0.3
Dealkaline lignin	130	11.5	0.3

Table 3. Summary of fitted parameters for sigmoid graphs in different lignin samples.

Plant-derived Samples **Parameters**	**Lignova Fibenol**	**Kraft lignin (471003)**	**Kraft lignin (370959)**	**Dealkaline lignin**
Plateau, C_0:	3.17%	5.61%	3.35%	11.52%
Lower offset, a_1:	0.0129	0.0490	0.0202	0.0454
Lower shape, b_1:	0.0259	0.0221	0.0170	0.0350
Higher offset, a_2:	2.36×10^{-5}	1.41×10^{-4}	2.03×10^{-6}	2.87×10^{-6}
Higher shape, b_2:	0.0295	0.0233	0.0390	0.0395
Optimal temperature (°C):	114	129	164	130

4.3.3 Uncertainty Evaluation and Suitability of the Sigmoid Curve Approach

The water content at the optimal analysis temperature, $C(T_{opt})$, is described by using the following mathematical model:

$$C(T_{opt}) = C_0 + \delta C_{sampl} + \delta C_{model} \quad (12)$$

where C_0 corresponds to the plateau value of the sigmoid curve model, (δC_{sampl}) denotes the possible correction arising from the variability between measurement results of subsamples analysed at the same temperatures, and (δC_{model}) represents the possible correction of the mismatch between model values and experimental values. The values of both of these corrections (δC_{sampl}) and (δC_{model}) are estimated as zero, but their uncertainties differ from zero.

The principal sources of uncertainty include the following: sampling uncertainty (difference in water content between individual subsamples), modelling uncertainty (mismatch between the experimental data points and the model) and a systematic uncertainty component accounting for deviations of the Karl Fischer titrator response from the reference water content of α-D-lactose (5.00% by mass). Other potential uncertainty sources, such as blank correction and temperature measurement accuracy, were considered less significant and are at least partly encompassed within these three primary uncertainty components.

Sampling uncertainty, $u(\delta C_{sampl})$, is inherently random in nature, and its effect can be estimated for each material as explained in Section 4.2.1.1. Modelling uncertainty, $u(\delta C_{model})$ was estimated as the RMS deviation of the mean experimental values at the same temperatures from the model curve. Clearly, the data points closest to the optimal temperature contribute the most to the result. Therefore, the five data points closest to the optimal temperature were used for evaluating this uncertainty contribution. The uncertainty component $u(C_0)$ was determined by calculating the relative deviation from the reference value of 5.00% for α-D-lactose and applying this relative difference to the water content of the material under investigation. The combined standard uncertainty (u_c) was subsequently calculated as follows:

$$u_c = \sqrt{u(\delta C_{sampl})^2 + u(\delta C_{model})^2 + u(C_0)^2} \quad (13)$$

The estimated combined standard uncertainties for the various studied lignins are summarised in Table 2. Water content uncertainties for different lignin samples range from 0.2% to 0.3%. These values facilitate an assessment of the method's suitability across the different lignin types.

4.4 Evaluation of Moisture and Water Content in Lignin

The aim of this part of the thesis was to assess whether water and moisture content in lignin can be accurately measured using ATR-FTIR combined with PLS modelling, and if possible, create a proof-of-principle ATR-FTIR method for water and moisture content of lignin.

To achieve this, a set of lignin reference samples with known moisture or water content was required for calibration. The water and moisture content reference values were determined using three different established techniques. The water content was determined using vap-C-KFT, whereas the moisture content was determined by gravimetric analysis combined with oven-drying (7 h and 48 h) and freeze-drying. Then, using these reference values, four PLS-R models were developed for ATR-FTIR data, and the performance of the models was evaluated using an independent test set of samples.

4.4.1 Water and Moisture Content Analysis of the Samples

The water content of the lignin samples was determined using vap-C-KFT under the optimised measurement parameters described in Section 4.3.2 and is presented in Table 4.

Table 4. Overview of the water content measurement results in lignin samples with vap-C-KFT.

No.	Sample Name	Temperature used for vap-C-KFT (°C)	Water content (% by mass)
Calibration samples (training set samples)			
1	Fibenol Lignova 1 Sample-2	110	0.57
2	Fibenol Lignova 1 Sample-1	110	1.30
3	Kraft lignin (370959) Sample-1	130	1.00
4	Dealkaline lignin Sample-4	130	1.39
5	Fibenol Lignova 2	110	2.21
6	Kraft lignin (471003) Sample-1	130	2.38
7	Fibenol Lignova 6	110	1.90
8	Fibenol Lignova 1	110	2.86
9	Dealkaline lignin Sample-1	130	3.18
10	Kraft lignin (370959)	130	2.94
11	Fibenol Lignova 1 Sample-4	110	4.03
12	Fibenol Lignova 3	110	3.78
13	Fibenol Lignova 1 Sample-9	110	4.39
14	Dealkaline lignin Sample-3	130	5.16
15	Kraft lignin (471003)	130	5.35
16	Kraft lignin (370959) Sample-3	130	5.60
17	Kraft lignin (471003) Sample-3	130	5.33
18	Kraft lignin (370959) Sample-5	130	6.46
19	Fibenol Lignova 1 Sample-3	110	7.00

No.	Sample Name	Temperature used for vap-C-KFT (°C)	Water content (% by mass)
20	Fibenol Lignova 1 Sample-7	110	7.47
21	Fibenol Lignova 1 Sample-8	110	7.56
22	Fibenol Lignova 1 Sample-5	110	8.68
23	Dealkaline lignin Sample-5	130	10.17
24	Fibenol Lignova 1 Sample-6	110	9.69
25	Kraft lignin (370959) Sample-4	130	10.32
26	Kraft lignin (471003) Sample-5	130	10.19
27	Dealkaline lignin (TCI)	130	11.10
28	Kraft lignin (471003) Sample-2	130	1.10
29	Fibenol Lignova 4	110	2.70
30	Fibenol Lignova 5	110	3.02
Test set samples			
31	Dealkaline lignin Sample-2	130	4.13
32	Fibenol Lignova 7	110	3.90
33	Fibenol Lignova 1 Sample-10	110	5.99
34	Kraft lignin (471003) Sample-4	130	6.95
35	Kraft lignin (370959) Sample-2	130	9.04

Gravimetric analysis was used to determine the moisture content of the lignin reference samples. In this study, the drying process with gravimetric analysis involved oven-drying and freeze-drying. The moisture content of lignin samples was calculated as a percentage of moisture content using Eq. (7).

The precision of the methods was calculated by pooled standard deviation of replicate results obtained over different periods ranging from weeks to months. For vap-C-KFT, results collected over 3–6 weeks were used, whereas for the oven-drying and freeze-drying methods, results obtained within 2–3 months. Precision was presented as mass % of moisture or water. The pooled standard deviation was 0.08% vap-C-KFT, 0.13 % for freeze-drying, 0.25% for oven-drying (48 h), and 0.30% for oven-drying (7 h).

The moisture contents of the reference samples are presented in Table 5.

Table 5. Overview of the moisture content results in lignin samples with the Gravimetric analysis methods (all values in mass percent).

No.	Sample Name	Freeze-drying	Oven-drying (48 h)	Oven-drying (7 h)
Calibration samples (training set samples)				
1	Fibenol Lignova 1 Sample-2	0.24	0.74	0.66
2	Fibenol Lignova 1 Sample-1	1.07	1.69	1.66
3	Kraft lignin (370959) Sample-1	0.58	1.76	1.67
4	Dealkaline lignin Sample-4	0.53	1.78	1.21
5	Fibenol Lignova 2	2.19	2.21	2.34
6	Kraft lignin (471003) Sample-1	1.01	3.12	2.68
7	Fibenol Lignova 6	1.84	3.43	2.33
8	Fibenol Lignova 1	2.86	3.43	3.52
9	Dealkaline lignin Sample-1	2.58	3.87	3.23
10	Kraft lignin (370959)	3.08	3.87	3.72
11	Fibenol Lignova 1 Sample-4	4.16	4.60	4.50
12	Fibenol Lignova 3	4.02	4.81	4.36
13	Fibenol Lignova 1 Sample-9	4.56	5.14	4.89
14	Dealkaline lignin Sample-3	4.98	5.92	5.52
15	Kraft lignin (471003)	4.86	6.26	5.98
16	Kraft lignin (370959) Sample-3	5.61	6.64	6.44
17	Kraft lignin (471003) Sample-3	3.32	6.84	6.41
18	Kraft lignin (370959) Sample-5	6.90	7.47	7.43
19	Fibenol Lignova 1 Sample-3	7.36	7.76	7.68
20	Fibenol Lignova 1 Sample-7	7.87	8.07	7.96
21	Fibenol Lignova 1 Sample-8	7.99	8.28	8.17
22	Fibenol Lignova 1 Sample-5	9.18	9.58	9.27
23	Dealkaline lignin Sample-5	10.01	10.61	10.38
24	Fibenol Lignova 1 Sample-6	10.55	10.90	10.73
25	Kraft lignin (370959) Sample-4	10.93	11.54	11.40
26	Kraft lignin (471003) Sample-5	8.81	11.81	10.85
27	Lignin Dealkaline (TCI)	11.23	12.03	11.69
28	Kraft lignin (471003) Sample-2	-	-	-
29	Fibenol Lignova 4	-	-	-
30	Fibenol Lignova 5	-	-	-
Test set samples				
31	Dealkaline lignin Sample-2	3.68	4.60	4.24
32	Fibenol Lignova 7	4.27	5.58	4.69
33	Fibenol Lignova 1 Sample-10	6.28	6.66	6.47
34	Kraft lignin (471003) Sample-4	6.40	7.96	7.54
35	Kraft lignin (370959) Sample-2	10.28	10.32	10.20

4.4.2 ATR-FTIR Combined with the Partial Least Squares Regression Method

4.4.2.1 Infrared Spectra of Lignin Samples

In FTIR spectra, water is characterised by absorption bands in the 3600–3200 cm^{-1} region, corresponding to the O–H stretching vibration, and in the 1655–1640 cm^{-1} region, attributed to the H–O–H bending vibration [13,150,167,191]. A broad and intense peak in the 3600–3200 cm^{-1} region is typically observed and varies depending on the moisture content due to the hydrogen-bonded O–H stretch. The absorption ranges of water largely overlap with the absorption ranges of hydroxylic groups in lignin. Moreover, the main functional groups in lignin, such as hydroxyl, methoxy, carbonyl, and carboxyl, can influence water absorption. These functional groups can interact with water molecules by forming hydrogen bonds, affecting the intensity and position of the water absorption bands and thereby influencing the overall FTIR spectrum of lignin.

Figure 5 represents the ATR-FTIR spectra of lignin samples that belong to the calibration model. Different colours were used for lignins produced by different technological processes. The spectra presented for the dataset show differences between the lignin samples caused by different water contents and compositional differences resulting from the different origins and technological processes. These variations can be attributed to factors such as different botanical origins, different extraction processes, impurities introduced during pulping, and chemical modification. The lignin samples that were included in the model contained water in the range of 0.24–11.23%. The variation in the range of water strongly influences the IR spectra of different lignins. The technological processes used to extract, treat, or modify lignin also strongly impact the IR spectrum. For example, lignins were extracted from different wood types using various extraction processes, temperatures and treatment conditions, leading to structural diversity and differences in functional group composition and their interaction with water molecules. Contaminants introduced during the extraction process, such as residual acids, bases or any other chemical, may be attributed to spectral differences.

The spectral variations caused by the inherent structural differences in lignin complicate determining water using IR spectra, as it becomes challenging to distinguish between spectral changes caused by water content versus those resulting from the inherent variability in lignin structure due to processing methods. Due to this overlap and structural variability, univariate calibration approaches are insufficient for accurate quantification of water in lignin. By extracting latent variables that maximise the covariance between spectral data and the reference water or moisture content values, PLS-R enables robust calibration even in the presence of extensive spectral overlapping and where spectral variability is influenced by the concentration of the analyte and also by other sources of variability.

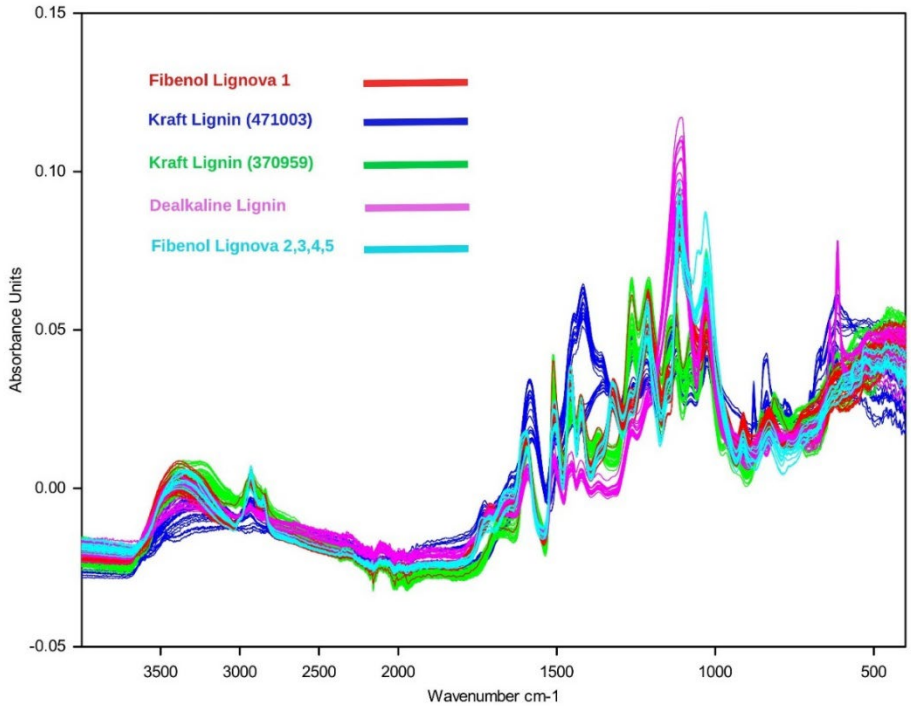

Figure 5. ATR-FTIR spectra of all the training set samples.

4.4.2.2 Developing and Optimising Calibration Models

The PLS-R calibration method was developed using reference values from the vap-C-KFT method and from gravimetric analysis to determine water and moisture content independently. Four different PLS models were developed: using the vap-C-KFT reference values for water, and the other three for moisture determination.

The set of samples was divided into a training set and a test set. The test set, explicitly used for validating the model's predictive performance, consisted of five samples. To select these samples, all 35 lignin samples were first ranked in ascending order. Samples with very low or high moisture content, i.e. below 1.8% and above 10.2%, were avoided due to the danger that the test-set samples will be outside the calibration ranges. This reduced the pool of possible test set samples to 22 suitable candidates. From this list, every fourth sample was selected to form the test set and to ensure an even distribution across the mid-range of moisture/water values. These samples are indicated in Table 4 and Table 5 and were used to assess the model's accuracy in predicting water and moisture content.

The same division between calibration and test sets was applied consistently across all four measurement methods. These five test set samples were utilised to validate all four water/moisture content determination ATR-FTIR methods to

ensure uniformity and comparability in model evaluation. The training set for the PLS model used in vap-C-KFT water content determination consisted of 30 samples. The training set comprised only 27 samples for the other three measurands due to the limited amount available of samples numbered 28 to 30, which were used exclusively for vap-C-KFT measurements. While the number of calibration samples is relatively small, it is considered adequate for this proof-of-principle study.

The PLS methods were optimised to achieve the lowest root mean square error of cross-validation (RMSECV) by systematically varying key parameters, including the spectral range (within 3997–350 cm^{-1}), preprocessing techniques within the calibration regions and the number of principal components used in the model. The optimal parameters were determined through the optimisation process in the Opus Quant software. This optimisation process involved selecting the spectral ranges that best correlate with the water content in the sample. The software uses statistical techniques to identify which spectral bands provide the most relevant information for the calibration model. The model's efficiency was evaluated by the squared coefficient of correlation (R^2) and RMSECV. Different spectral ranges were used in the development of the models. The vap-C-KFT method demonstrated the lowest RMSECV of 0.53% with a high R^2 value of 0.973, utilising the spectral ranges of 3997–3267, 2538–2172, 1810–1442, and 1080–350 cm^{-1}. The freeze-drying method, which employed spectral ranges of 3997–1442 and 1080–350 cm^{-1}, achieved an R^2 value of 0.973 with an RMSECV of 0.57%. Two separate calibration models were created for the air-drying oven method for reference values of 7 h and 48 h. The oven-drying for 7 hours utilised spectral regions of 3997–3267, 2538–2172, 1810–1442, and 1080–350 cm^{-1} resulting in an R^2 of 0.974 and RMSECV of 0.53%, whereas for 48 hours employed spectral ranges from 3997–3267, 2905–2536, and 1810–1442 cm^{-1}, resulting in an R^2 of 0.964 and an RMSECV of 0.66%.

Table 6. Statistical parameters of PLS models were developed using moisture/water content data and FTIR spectral data of lignin samples. [a]

Component	Spectral range (cm^{-1})	Rank	R^2	RMSECV (%)
vap-C-KFT	3997–3267 / 2538–2172 / 1810–1442 / 1080–350	10	0.973	0.53
Freeze-drying	3997–1442 / 1080–350	9	0.973	0.57
Air oven-drying (7 h)	3997–3267 / 2538–2172 / 1810–1442 / 1080–350	10	0.974	0.53
Air oven-drying (48 h)	3997–3267 / 2905–2536 / 1810–1442	9	0.964	0.66

[a] R^2 is squared coefficient of correlation; RMSECV is root mean square error of cross-validation; Rank is the number of latent variables used.

4.4.2.3 External Validation of the Calibration Model

The five test set samples cover a water content range of 3.68% to 10.28%, as well as the main production technologies involved in the dataset, making the test set representative of the used lignin types and moisture variation. The test set samples used to validate the calibration model exhibit variations in their components and structures, resulting in differences in the corresponding ATR-FTIR spectra of these lignins, as presented in Figure 6.

The validation results summarised in Table 7. The obtained root mean square errors of prediction (RMSEP) range between 0.33% to 1.00%, which are considered satisfactory for a fast, uncomplicated analysis method at the "proof of principle" level. The results reported in Reference [13] demonstrated high prediction accuracy using micro-FTIR combined with PLS-R, calibrated against a DVS method under controlled conditions and, most importantly, using only one type of lignin, with RMSEP 0.12–0.17% and R^2 99.9%. In contrast, the present work achieved satisfactory predictive performance (RMSEP 0.33–1.00%) across a range of lignin samples from different production processes under ambient (room temperature) conditions, highlighting robustness and its relevance to routine analytical practice.

The RMSEP values obtained for the ATR-FTIR with PLS-R calibration combined with uncertainties of reference values (u_c approximately 0.3% by mass, Table 2) can be used to estimate the combined standard uncertainty of the method leading to u_c values 0.8%, 0.8%, 1.0% and 0.4% for C-KFT, Freeze-drying, Air oven-drying 7 h and Air oven-drying 48 h methods, respectively. This interpretation is based on an experimental approach used to obtain the reference values employed for model calibration and validation. Measurement data were obtained from replicate measurements of independently taken subsamples for all four reference methods, ensuring that the RMSEP incorporates all sampling-related uncertainty. The small differences from reference values obtained for KL (370959) demonstrate that employing 130 °C oven temperatures for vap-C-KFT measurements was an appropriate choice. The selected temperature yields reliable reference values, which enable accurate PLS-R model predictions.

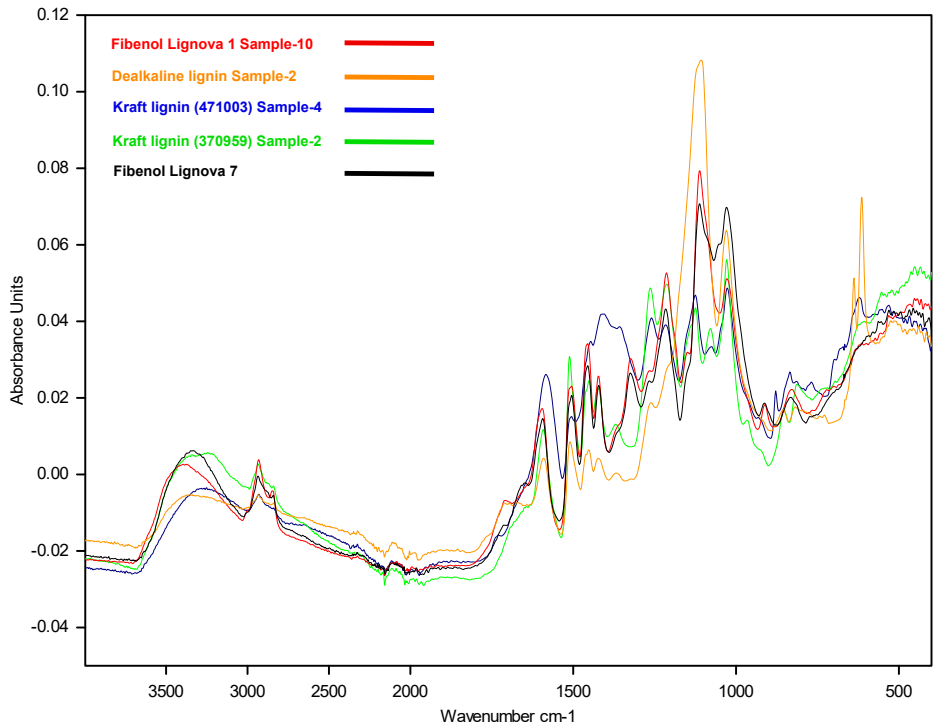

Figure 6. Representative ATR-FTIR spectra of test set lignin samples.

Table 7. External Test Set Validation of the PLS-R Method (all values in mass percent).

Samples	Reference values				Predicted values				Differences			
	C-KFT	**Freeze-drying**	**Air oven-drying 7 h**	**Air oven-drying 48 h**	**C-KFT**	**Freeze-drying**	**Air oven-drying 7 h**	**Air oven-drying 48 h**	**C-KFT**	**Freeze-drying**	**Air oven-drying 7 h**	**Air oven-drying 48 h**
Dealkaline lignin Sample-2	4.13	3.68	4.60	4.24	4.71	4.42	4.66	4.75	0.58	0.74	0.06	0.51
Fibenol Lignova 7	3.90	4.27	5.58	4.69	2.79	3.72	7.61	4.61	-1.11	-0.55	2.03	-0.08
Fibenol Lignova 1 Sample-10	5.99	6.28	6.66	6.47	6.66	6.93	7.20	7.00	0.67	0.65	0.54	0.53
Kraft lignin (471003) Sample-4	6.95	6.40	7.96	7.54	6.32	5.46	7.33	7.53	-0.63	-0.94	-0.63	-0.01
Kraft lignin (370959) Sample-2	9.04	10.28	10.32	10.20	9.17	9.73	9.84	10.13	0.13	-0.55	-0.48	-0.07
Root mean square errors of prediction (RMSEP)									0.70	0.70	1.00	0.33

SUMMARY

This thesis is dedicated to enhancing the reliability of quantitative lignin analysis, explicitly focusing on compositional characterisation by the qNMR approach and on the assessment of water and moisture content in lignin. During this work, methods based on ATR-FTIR spectroscopy combined with PLS-R calibration models were developed to determine the water and moisture content of lignin.

The first part of this thesis addresses the accuracy of qNMR methods used for quantitative lignin analysis. A critical analysis of reported qNMR studies revealed significant inconsistencies in the reporting of precision, bias, and accuracy. Different measurands and reporting formats are often used without clearly defining the type of accuracy or the source of the reported error. Measurement uncertainty that would account for all relevant sources is rarely assessed, and the contribution of sampling-related variability is often overlooked. These shortcomings make it difficult to compare and interpret quantitative data.

Based on this analysis, a study was carried out to assess sampling-related uncertainty in lignin analysis. Although lignin is often considered relatively homogeneous, it is a solid natural material, and subsamples taken from the same bulk material may differ in composition. The results demonstrated that variability between samples constitutes a significant part of the total variability in qNMR measurements. The relative standard deviation (RSD) due to sampling-related variability was 2.4%, while other factors, such as baseline shifts and signal overlap, contributed 4.4%. The RSD accounting for all sources of variability was 5.0%.

The second part of the thesis focuses on determining the water and moisture content of lignin. Accurate determination of water and moisture content is challenging due to the chemical complexity, heterogeneity, and highly branched structure of lignin, as well as the presence of water in different forms.

To determine water and moisture content, a series of calibration samples was prepared from lignins originating from different plant species and industrial extraction processes. vap-C-KFT was applied to determine the water content of the calibration samples, and a modelling approach based on sigmoid-shaped temperature–water release curves was developed to identify optimal temperatures for evaporating water from the sample. This approach enables the selection of a temperature at which chemically unbound water is released while avoiding significant additional water formation due to thermal degradation. At lower temperatures, vap-C-KFT leads to incomplete water release, whereas at higher temperatures, additional water may form due to lignin degradation. Gravimetric methods–oven drying and lyophilisation were used to determine the moisture content of the calibration samples.

The resulting calibration samples were used to develop a rapid and non-destructive “proof of principle” method for determining water and moisture content using ATR-FTIR spectroscopy combined with partial least squares regression models. The resulting method has good predictive ability across a wide

range of lignin types, requires only a small sample amount, and involves minimal sample preparation.

In conclusion, this thesis demonstrates that in quantitative analysis, clearly defining the measurand and providing sufficient information on precision and trueness are essential. Sampling uncertainty was shown to be a significant, previously underestimated factor in the total measurement uncertainty in lignin analysis. A simple and rapid ATR-FTIR method, combined with chemometric analysis, was developed for the determination of water and moisture content in lignin.

REFERENCES

[1] V.K. Thakur, M.K. Thakur, Recent advances in green hydrogels from lignin: a review, Int. J. Biol. Macromol. 72 (2015) 834–847. https://doi.org/10.1016/j.ijbiomac.2014.09.044.

[2] P. Jadhav, P. Bhuyar, I.I. Misnon, M.H.A. Rahim, R. Roslan, Advancement of lignin into bioactive compounds through selective organic synthesis methods, Int. J. Biol. Macromol. 276 (2024) 134061. https://doi.org/10.1016/j.ijbiomac.2024.134061.

[3] Y. Tobimatsu, F. Chen, J. Nakashima, L.L. Escamilla-Trevino, L. Jackson, R.A. Dixon, J. Ralph, Coexistence but Independent Biosynthesis of Catechyl and Guaiacyl/Syringyl Lignin Polymers in Seed Coats, The Plant Cell 25 (2013) 2587–2600. https://doi.org/10.1105/tpc.113.113142.

[4] D.D.S. Argyropoulos, C. Crestini, C. Dahlstrand, E. Furusjö, C. Gioia, K. Jedvert, G. Henriksson, C. Hulteberg, M. Lawoko, C. Pierrou, J.S.M. Samec, E. Subbotina, H. Wallmo, M. Wimby, Kraft Lignin: A Valuable, Sustainable Resource, Opportunities and Challenges, ChemSusChem 16 (2023) e202300492. https://doi.org/10.1002/cssc.202300492.

[5] A. Lisý, A. Ház, R. Nadányi, M. Jablonský, I. Šurina, About Hydrophobicity of Lignin: A Review of Selected Chemical Methods for Lignin Valorisation in Biopolymer Production, Energies 15 (2022) 6213. https://doi.org/10.3390/en15176213.

[6] M. Ayyachamy, F.E. Cliffe, J.M. Coyne, J. Collier, M.G. Tuohy, Lignin: untapped biopolymers in biomass conversion technologies, Biomass Convers. Biorefin. 3 (2013) 255–269. https://doi.org/10.1007/s13399-013-0084-4.

[7] S.W.A. Shah, Q. Xu, M.W. Ullah, Zahoor, S. Sethupathy, G.M. Morales, J. Sun, D. Zhu, Lignin-based additive materials: A review of current status, challenges, and future perspectives, Additive Manufacturing 74 (2023) 103711. https://doi.org/10.1016/j.addma.2023.103711.

[8] M. Balakshin, E. Capanema, On the Quantification of Lignin Hydroxyl Groups With ^{31}P and ^{13}C NMR Spectroscopy, J. Wood Chem. Technol. 35 (2015) 220–237. https://doi.org/10.1080/02773813.2014.928328.

[9] H. Wang, Y. Pu, A. Ragauskas, B. Yang, From lignin to valuable products–strategies, challenges, and prospects, Bioresour. Technol. 271 (2019) 449–461. https://doi.org/10.1016/j.biortech.2018.09.072.

[10] R. Shorey, A. Salaghi, P. Fatehi, T.H. Mekonnen, Valorization of lignin for advanced material applications: a review, RSC Sustainability 2 (2024) 804–831. https://doi.org/10.1039/D3SU00401E.

[11] O. Musl, S. Galler, G. Wurzer, M. Bacher, I. Sulaeva, I. Sumerskii, A.K. Mahler, T. Rosenau, A. Potthast, High-Resolution Profiling of the Functional Heterogeneity of Technical Lignins, Biomacromolecules 23 (2022) 1413–1422. https://doi.org/10.1021/acs.biomac.1c01630.

[12] L. Wang, G. Li, X. Chen, Y. Yang, R.K. Liew, H.M. Abo-Dief, S.S. Lam, R. Sellami, W. Peng, H. Li, Extraction strategies for lignin, cellulose, and hemicellulose to obtain valuable products from biomass, Adv Compos Hybrid Mater 7 (2024) 219. https://doi.org/10.1007/s42114-024-01009-y.

[13] T. Xiao, H. Yuan, Q. Ma, X. Guo, Y. Wu, An approach for in situ qualitative and quantitative analysis of moisture adsorption in nanogram-scaled lignin by using micro-FTIR spectroscopy and partial least squares regression, Int. J. Biol. Macromol. 132 (2019) 1106–1111. https://doi.org/10.1016/j.ijbiomac.2019.04.043.

[14] X. Guo, H. Yuan, T. Xiao, Y. Wu, Application of micro-FTIR spectroscopy to study molecular association of adsorbed water with lignin, Int. J. Biol. Macromol. 131 (2019) 1038–1043. https://doi.org/10.1016/j.ijbiomac.2019.03.193.
[15] O. Faix, D.S. Argyropoulos, D. Robert, V. Neirinck, Determination of Hydroxyl Groups in Lignins Evaluation of ^{1}H-, ^{13}C-, ^{31}P-NMR, FTIR and Wet Chemical Methods, Holzforschung 48 (1994) 387–394. https://doi.org/10.1515/hfsg.1994.48.5.387.
[16] J.-L. Wen, S.-L. Sun, B.-L. Xue, R.-C. Sun, Recent Advances in Characterization of Lignin Polymer by Solution-State Nuclear Magnetic Resonance (NMR) Methodology, Materials 6 (2013) 359–391. https://doi.org/10.3390/ma6010359.
[17] X. Meng, C. Crestini, H. Ben, N. Hao, Y. Pu, A.J. Ragauskas, D.S. Argyropoulos, Determination of hydroxyl groups in biorefinery resources via quantitative 31P NMR spectroscopy, Nat. Protoc. 14 (2019) 2627–2647. https://doi.org/10.1038/s41596-019-0191-1.
[18] G. Gellerstedt, D. Robert, V.D. Parker, M. Oivanen, L. Eberson, Quantitative 13C NMR Analysis of Kraft Lignins., Acta Chem. Scand. 41b (1987) 541–546. https://doi.org/10.3891/acta.chem.scand.41b-0541.
[19] L. Zhang, G. Gellerstedt, Quantitative 2D HSQC NMR determination of polymer structures by selecting suitable internal standard references, Magn. Reson. Chem. 45 (2007) 37–45. https://doi.org/10.1002/mrc.1914.
[20] D.R. Letourneau, B.P. Marzullo, A. Alexandridou, M.P. Barrow, P.B. O'Connor, D.A. Volmer, Characterizing lignins from various sources and treatment processes after optimized sample preparation techniques and analysis via ESI-HRMS and custom mass defect software tools, Anal. Bioanal.Chem. 415 (2023) 6663–6675. https://doi.org/10.1007/s00216-023-04942-x.
[21] B.M. Upton, A.M. Kasko, Strategies for the Conversion of Lignin to High-Value Polymeric Materials: Review and Perspective, Chem. Rev. 116 (2016) 2275–2306. https://doi.org/10.1021/acs.chemrev.5b00345.
[22] N. Smyk, J. Sjöström, G. Henriksson, O. Sevastyanova, UV–vis spectroscopy as a rapid method for evaluation of total phenolic hydroxyl structures in lignin, Nordic Pulp & Paper Research Journal 39 (2024) 731–746. https://doi.org/10.1515/npprj-2023-0095.
[23] O. Faix, Fourier Transform Infrared Spectroscopy, in: S.Y. Lin, C.W. Dence (Eds.), Methods in Lignin Chemistry, Springer Berlin Heidelberg, Berlin, Heidelberg, 1992: pp. 83–109. https://doi.org/10.1007/978-3-642-74065-7_7.
[24] G. Van Erven, R. De Visser, P. De Waard, W.J.H. Van Berkel, M.A. Kabel, Uniformly^{13} C Labeled Lignin Internal Standards for Quantitative Pyrolysis−GC−MS Analysis of Grass and Wood, ACS Sustainable Chem. Eng. 7 (2019) 20070–20076. https://doi.org/10.1021/acssuschemeng.9b05926.
[25] B.-U. Batjargal, M. Kang, Y. Cho, S. Park, S.-W. Hwang, H.W. Kwak, I.-G. Choi, H. Yeo, Near-infrared spectroscopy for moisture content prediction in soil-mixed woody biomass, Sci Rep 16 (2026) 6096. https://doi.org/10.1038/s41598-026-36901-8.
[26] G.E. Acquah, B.K. Via, O.O. Fasina, L.G. Eckhardt, Rapid Quantitative Analysis of Forest Biomass Using Fourier Transform Infrared Spectroscopy and Partial Least Squares Regression, J. Anal. Methods Chem. 2016 (2016) 1–10. https://doi.org/10.1155/2016/1839598.
[27] S. Heikkinen, M.M. Toikka, P.T. Karhunen, I.A. Kilpeläinen, Quantitative 2D HSQC (Q-HSQC) via Suppression of *J* -Dependence of Polarization Transfer in

NMR Spectroscopy: Application to Wood Lignin, J. Am. Chem. Soc. 125 (2003) 4362–4367. https://doi.org/10.1021/ja029035k.
[28] M. Zawadzki, A. Ragauskas, N-Hydroxy Compounds as New Internal Standards for the ^{31}P-NMR Determination of Lignin Hydroxy Functional Groups, Holzforschung 55 (2001) 283–285. https://doi.org/10.1515/HF.2001.047.
[29] C.-L. Chen, D. Robert, Characterization of lignin by ^{1}H and ^{13}C NMR spectroscopy, in: Methods in Enzymology, Elsevier, 1988: pp. 137–174. https://doi.org/10.1016/0076-6879(88)61017-2.
[30] M.H. Ramsey, S.L. Ellison, P. Rostron, Measurement uncertainty arising from sampling: A guide to methods and approaches, Eurachem/EUROLAB/CITAC/ Nordtest/AMC Guide Second Edition (2019).
[31] M. DelSesto, People–plant interactions and the ecological self, Plants People Planet 2 (2020) 201–211. https://doi.org/10.1002/ppp3.10087.
[32] M. Zhou, J. Xu, J. Jiang, B.K. Sharma, A Review of Microwave Assisted Liquefaction of Lignin in Hydrogen Donor Solvents: Effect of Solvents and Catalysts, Energies 11 (2018) 2877. https://doi.org/10.3390/en11112877.
[33] L. Fan, Y. Zhang, S. Liu, N. Zhou, P. Chen, Y. Cheng, M. Addy, Q. Lu, M.M. Omar, Y. Liu, Y. Wang, L. Dai, E. Anderson, P. Peng, H. Lei, R. Ruan, Bio-oil from fast pyrolysis of lignin: Effects of process and upgrading parameters, Bioresour. Technol. 241 (2017) 1118–1126. https://doi.org/10.1016/j.biortech.2017.05.129.
[34] A. Kazachenko, F. Akman, N. Vasilieva, Y. Malyar, O. Fetisova, M. Lutoshkin, Y. Berezhnaya, A. Miroshnikova, N. Issaoui, Z. Xiang, Sulfation of Wheat Straw Soda Lignin with Sulfamic Acid over Solid Catalysts, Polymers 14 (2022) 3000. https://doi.org/10.3390/polym14153000.
[35] Z. Xu, P. Lei, R. Zhai, Z. Wen, M. Jin, Recent advances in lignin valorization with bacterial cultures: microorganisms, metabolic pathways, and bio-products, Biotechnol. Biofuels 12 (2019) 32. https://doi.org/10.1186/s13068-019-1376-0.
[36] D. Delmer, R.A. Dixon, K. Keegstra, D. Mohnen, The plant cell wall—dynamic, strong, and adaptable—is a natural shapeshifter, The Plant Cell 36 (2024) 1257–1311. https://doi.org/10.1093/plcell/koad325.
[37] J.D. Gargulak, S.E. Lebo, T.J. McNally, Lignin, in: Kirk-Othmer (Ed.), Kirk-Othmer Encyclopedia of Chemical Technology, 1st ed., Wiley, 2015: pp. 1–26. https://doi.org/10.1002/0471238961.12090714120914.a01.pub3.
[38] P. Azadi, O.R. Inderwildi, R. Farnood, D.A. King, Liquid fuels, hydrogen and chemicals from lignin: A critical review, Renew. Sust. Energ. 21 (2013) 506–523. https://doi.org/https://doi.org/10.1016/j.rser.2012.12.022.
[39] R. Vanholme, B. De Meester, J. Ralph, W. Boerjan, Lignin biosynthesis and its integration into metabolism, Curr. Opin. Biotechnol. 56 (2019) 230–239. https://doi.org/10.1016/j.copbio.2019.02.018.
[40] R. Gaspar, M.C.D.S. Muguet, P. Fardim, Advanced Fractionation of Kraft Lignin by Aqueous Hydrotropic Solutions, Molecules 28 (2023) 687. https://doi.org/10.3390/molecules28020687.
[41] W. Schutyser, T. Renders, S. Van Den Bosch, S.-F. Koelewijn, G.T. Beckham, B.F. Sels, Chemicals from lignin: an interplay of lignocellulose fractionation, depolymerisation, and upgrading, Chem. Soc. Rev. 47 (2018) 852–908. https://doi.org/10.1039/C7CS00566K.
[42] F. Fink, F. Emmerling, J. Falkenhagen, Identification and Classification of Technical Lignins by means of Principle Component Analysis and k-Nearest Neighbor Algorithm, Chem. Methods 1 (2021) 354–361.

https://doi.org/10.1002/cmtd.202100028.
[43] V. Georgs, H. Piili, J. Gustafsson, C. Xu, A critical review on lignin structure, chemistry, and modification towards utilisation in additive manufacturing of lignin-based composites, Ind. Crops Prod. 233 (2025) 121416. https://doi.org/10.1016/j.indcrop.2025.121416.
[44] L. Yan, A.J. Huertas-Alonso, H. Liu, L. Dai, C. Si, M.H. Sipponen, Lignin polymerization: towards high-performance materials, Chem. Soc. Rev. 54 (2025) 6634–6651. https://doi.org/10.1039/D4CS01044B.
[45] M. Yildirim, A brief review of the structure and extraction methods of lignin, Sustain. Chem. Environ. 13 (2026) 100311. https://doi.org/10.1016/j.scenv.2025.100311.
[46] Y. Lu, Y.-C. Lu, H.-Q. Hu, F.-J. Xie, X.-Y. Wei, X. Fan, Structural Characterization of Lignin and Its Degradation Products with Spectroscopic Methods, J. Spectrosc. 2017 (2017) 1–15. https://doi.org/10.1155/2017/8951658.
[47] Z. Wan, H. Zhang, Y. Guo, H. Li, Advances in Catalytic Depolymerization of Lignin, ChemistrySelect 7 (2022) e202202582. https://doi.org/10.1002/slct.202202582.
[48] N.D. Patil, N.R. Tanguy, N. Yan, Lignin Interunit Linkages and Model Compounds, in: Lignin in Polymer Composites, Elsevier, 2016: pp. 27–47. https://doi.org/10.1016/B978-0-323-35565-0.00003-5.
[49] S.H. Ghaffar, M. Fan, Structural analysis for lignin characteristics in biomass straw, Biomass Bioenergy 57 (2013) 264–279. https://doi.org/10.1016/j.biombioe.2013.07.015.
[50] C. Lapierre, B. Monties, C. Rolando, L.D. Chirale, Thioacidolysis of Lignin: Comparison with Acidolysis, J. Wood Chem. Technol. 5 (1985) 277–292. https://doi.org/10.1080/02773818508085193.
[51] M. Yamamura, T. Hattori, S. Suzuki, D. Shibata, T. Umezawa, Microscale thioacidolysis method for the rapid analysis of β-O-4 substructures in lignin, Plant Biotechnol. 29 (2012) 419–423. https://doi.org/10.5511/plantbiotechnology.12.0627a.
[52] K. Freudenberg, W. Lautsch, K. Engler, Die Bildung von Vanillin aus Fichtenlignin, Ber. Dtsch. Chem. Ges. A/B 73 (1940) 167–171. https://doi.org/10.1002/cber.19400730302.
[53] F. Lu, J. Ralph, Derivatization Followed by Reductive Cleavage (DFRC Method), a New Method for Lignin Analysis: Protocol for Analysis of DFRC Monomers, J. Agric. Food Chem. 45 (1997) 2590–2592. https://doi.org/10.1021/jf970258h.
[54] A. Skulcova, V. Majova, M. Kohutova, M. Grosik, J. Sima, M. Jablonsky, UV/Vis Spectrometry as a Quantification Tool for Lignin Solubilized in Deep Eutectic Solvents, BioResources 12 (2017) 6713–6722. https://doi.org/10.15376/biores.12.3.6713-6722.
[55] S.G. Kostryukov, H.B. Matyakubov, Yu.Yu. Masterova, A.Sh. Kozlov, M.K. Pryanichnikova, A.A. Pynenkov, N.A. Khluchina, Determination of Lignin, Cellulose, and Hemicellulose in Plant Materials by FTIR Spectroscopy, J. Anal. Chem. 78 (2023) 718–727. https://doi.org/10.1134/S1061934823040093.
[56] M.Yu. Balakshin, E.A. Capanema, R.B. Santos, H. Chang, H. Jameel, Structural analysis of hardwood native lignins by quantitative ^{13}C NMR spectroscopy, Holzforschung 70 (2016) 95–108. https://doi.org/10.1515/hf-2014-0328.
[57] E.S. Esakkimuthu, N. Marlin, M.-C. Brochier-Salon, G. Mortha, Study of the Reactivity of Lignin Model Compounds to Fluorobenzylation Using ^{13}C and ^{19}F

NMR: Application to Lignin Phenolic Hydroxyl Group Quantification by ^{19}F NMR, Molecules 25 (2020) 3211. https://doi.org/10.3390/molecules25143211.
[58] E.A. Capanema, M.Y. Balakshin, C.-L. Chen, J.S. Gratzl, H. Gracz, Structural Analysis of Residual and Technical Lignins by ^{1}H–^{13}C Correlation 2D NMR-Spectroscopy, Holzforschung 55 (2001) 302–308. https://doi.org/10.1515/HF.2001.050.
[59] S.D. Mansfield, H. Kim, F. Lu, J. Ralph, Whole plant cell wall characterization using solution-state 2D NMR, Nat Protoc 7 (2012) 1579–1589. https://doi.org/10.1038/nprot.2012.064.
[60] Y. Gong, X. Chen, W. Wu, Application of Fourier Transform Infrared (FTIR) spectroscopy in sample preparation: Material characterization and mechanism investigation, Adv. Sample Prep. 11 (2024) 100122. https://doi.org/10.1016/j.sampre.2024.100122.
[61] J. Reyes-Rivera, T. Terrazas, Lignin Analysis by HPLC and FTIR, in: M. De Lucas, J.P. Etchhells (Eds.), Xylem, Springer New York, New York, NY, 2017: pp. 193–211. https://doi.org/10.1007/978-1-4939-6722-3_14.
[62] W. Boerjan, J. Ralph, M. Baucher, Lignin Biosynthesis, Annu. Rev. Plant Biol. 54 (2003) 519–546. https://doi.org/10.1146/annurev.arplant.54.031902.134938.
[63] V.B. Agbor, N. Cicek, R. Sparling, A. Berlin, D.B. Levin, Biomass pretreatment: Fundamentals toward application, Biotechnol. Adv. 29 (2011) 675–685. https://doi.org/10.1016/j.biotechadv.2011.05.005.
[64] N.L. Radhika, S. Sachdeva, M. Kumar, Lignin depolymerization and biotrans-formation to industrially important chemicals/biofuels, Fuel 312 (2022) 122935. https://doi.org/10.1016/j.fuel.2021.122935.
[65] F. Roberto Paz Cedeno, B. Belon De Siqueira, E. Gabriel Solorzano Chavez, I. Ulises Miranda Roldán, L. Moreira Ropelato, J. Paul Martínez Galán, F. Masarin, Recovery of cellulose and lignin from Eucalyptus by-product and assessment of cellulose enzymatic hydrolysis, Renewable Energy 193 (2022) 807–820. https://doi.org/10.1016/j.renene.2022.05.027.
[66] X. Lu, X. Gu, A review on lignin pyrolysis: pyrolytic behavior, mechanism, and relevant upgrading for improving process efficiency, Biotechnol. Biofuels Bioprod. 15 (2022) 106. https://doi.org/10.1186/s13068-022-02203-0.
[67] H. Gremlich, Infrared and Raman Spectroscopy, in: Wiley-VCH (Ed.), Ullmann's Encyclopedia of Industrial Chemistry, 1st ed., Wiley, 2000. https://doi.org/10.1002/14356007.b05_429.
[68] J. Zakzeski, P.C.A. Bruijnincx, A.L. Jongerius, B.M. Weckhuysen, The Catalytic Valorization of Lignin for the Production of Renewable Chemicals, Chem. Rev. 110 (2010) 3552–3599. https://doi.org/10.1021/cr900354u.
[69] P. Figueiredo, K. Lintinen, J.T. Hirvonen, M.A. Kostiainen, H.A. Santos, Properties and chemical modifications of lignin: Towards lignin-based nanomaterials for bio-medical applications, Prog. Mater Sci. 93 (2018) 233–269. https://doi.org/10.1016/j.pmatsci.2017.12.001.
[70] A. Bacchus, P. Fatehi, Drying temperature effect on the characteristics of catio-nically polymerized kraft lignin, Int. J. Biol. Macromol. 280 (2024) 135935. https://doi.org/10.1016/j.ijbiomac.2024.135935.
[71] J.-Y. Kim, H. Hwang, S. Oh, Y.-S. Kim, U.-J. Kim, J.W. Choi, Investigation of structural modification and thermal characteristics of lignin after heat treatment, Int. J. Biol. Macromol. 66 (2014) 57–65. https://doi.org/10.1016/j.ijbiomac.2014.02.013.

[72] Y. Shao, K. Sun, Q. Li, L. Zhang, T. Wei, G. Gao, S. Zhang, Y. Wang, Q. Liu, X. Hu, Dealkaline lignin–The waste from the pulp and paper industry as acid catalyst in biorefinery, Bioresour. Technol. Rep. 7 (2019) 100218. https://doi.org/10.1016/j.biteb.2019.100218.
[73] TCI EUROPE N.V., Lignin 8061-51-6, TCI Chemicals (n.d.). https://www.tcichemicals.com/EE/en/p/L0045 (accessed March 3, 2026).
[74] P.S. Jiju, A.K. Patel, N.S. Shruthy, S. Shalu, C.-D. Dong, R.R. Singhania, Sustainability through lignin valorization: recent innovations and applications driving industrial transformation, Bioresour. Bioprocess. 12 (2025) 88. https://doi.org/10.1186/s40643-025-00929-x.
[75] D.C. Monagas, Lignovations' new ingredient based on Fibenol's LIGNOVA, LignoGuard, is safe for use in cosmetic products, World Bio Market Insights (2023). https://worldbiomarketinsights.com/lignovations-new-ingredient-based-on-fibenols-lignova-lignoguard-is-safe-for-use-in-cosmetic-products/ (accessed March 23, 2026).
[76] Fibenol, Biomaterials and Bioproducts done right | Fibenol, (n.d.). https://fibenol.com/products (accessed February 26, 2026).
[77] Fibenol, Environmental Product Declaration: LIGNOVA^{TM} Crude, Fibenol, 2023.
[78] R.E. Lumpkin, Rapid Pretreatment, US10844413B2, 2020. https://patents.google.com/patent/US10844413B2.
[79] nova-Institute, Lignovations' functional ingredient LignoGuard® based on Fibenol LIGNOVA^{TM} lignin confirmed safe for use in cosmetic products, Renewable Carbon News (2023). https://renewable-carbon.eu/news/lignovations-functional-ingredient-lignoguard-based-on-fibenol-lignova-lignin-confirmed-safe-for-use-in-cosmetic-products/ (accessed May 2, 2026).
[80] M. Erfani Jazi, G. Narayanan, F. Aghabozorgi, B. Farajidizaji, A. Aghaei, M.A. Kamyabi, C.M. Navarathna, T.E. Mlsna, Structure, chemistry and physicochemistry of lignin for material functionalization, SN Appl. Sci. 1 (2019) 1094. https://doi.org/10.1007/s42452-019-1126-8.
[81] T.T. Nge, Y. Tobimatsu, M. Yamamura, S. Takahashi, E. Takata, T. Umezawa, T. Yamada, Effect of Heat Treatment on the Chemical Structure and Thermal Properties of Softwood-Derived Glycol Lignin, Molecules 25 (2020) 1167. https://doi.org/10.3390/molecules25051167.
[82] H. Yang, R. Yan, H. Chen, D.H. Lee, C. Zheng, Characteristics of hemicellulose, cellulose and lignin pyrolysis, Fuel 86 (2007) 1781–1788. https://doi.org/10.1016/j.fuel.2006.12.013.
[83] M. Brebu, C. Vasile, Thermal Degradation of Lignin – A Review, Cellulose Chem. Technol. 44 (2010) 353–363.
[84] C. Cui, H. Sadeghifar, S. Sen, D.S. Argyropoulos, Toward Thermoplastic Lignin Polymers; Part II: Thermal & Polymer Characteristics of Kraft Lignin & Derivatives, BioResources 8 (2013) 864–886. https://doi.org/10.15376/biores.8.1.864-886.
[85] S. Sen, S. Patil, D.S. Argyropoulos, Thermal properties of lignin in copolymers, blends, and composites: a review, Green Chem. 17 (2015) 4862–4887. https://doi.org/10.1039/C5GC01066G.
[86] ISO, Lignins — Determination of dry matter content — Oven-drying and freeze-drying methods, (2024). https://www.iso.org/standard/82215.html.
[87] M. Funaoka, T. Kako, I. Abe, Condensation of lignin during heating of wood, Wood Sci.Technol. 24 (1990) 277–288. https://doi.org/10.1007/BF01153560.

[88] A. Mazar, M. Paleologou, Comparison of the effects of three drying methods on lignin properties, Int. J. Biol. Macromol. 258 (2024) 128974. https://doi.org/10.1016/j.ijbiomac.2023.128974.
[89] B. Prieur, M. Meub, M. Wittemann, R. Klein, S. Bellayer, G. Fontaine, S. Bourbigot, Phosphorylation of lignin: characterization and investigation of the thermal decomposition, RSC Adv. 7 (2017) 16866–16877. https://doi.org/10.1039/C7RA00295E.
[90] R. Samuelsson, C. Nilsson, J. Burvall, Sampling and GC-MS as a method for analysis of volatile organic compounds (VOC) emitted during oven drying of biomass materials, Biomass Bioenergy 30 (2006) 923–928. https://doi.org/10.1016/j.biombioe.2006.06.003.
[91] R. Samuelsson, J. Burvall, R. Jirjis, Comparison of different methods for the determination of moisture content in biomass, Biomass Bioenergy 30 (2006) 929–934. https://doi.org/10.1016/j.biombioe.2006.06.004.
[92] International Organization for Standardization, Solid biofuels — Determination of moisture content — Part 1: Reference method, (2022).
[93] D. Zhu, B. Yang, H. Wang, Mohd. Shahnawaz, Editorial: Lignin valorization: Recent trends and future perspective, Front. Bioeng. Biotechnol. 11 (2023) 1190128. https://doi.org/10.3389/fbioe.2023.1190128.
[94] W. Zhang, X. Qiu, C. Wang, L. Zhong, F. Fu, J. Zhu, Z. Zhang, Y. Qin, D. Yang, C.C. Xu, Lignin derived carbon materials: current status and future trends, Carbon Res. 1 (2022) 14. https://doi.org/10.1007/s44246-022-00009-1.
[95] V.K. Ponnusamy, D.D. Nguyen, J. Dharmaraja, S. Shobana, J.R. Banu, R.G. Saratale, S.W. Chang, G. Kumar, A review on lignin structure, pretreatments, fermentation reactions and biorefinery potential, Bioresour. Technol. 271 (2019) 462–472. https://doi.org/10.1016/j.biortech.2018.09.070.
[96] H. Qiang, J. Wang, H. Liu, Y. Zhu, From vanillin to biobased aromatic polymers, Polym. Chem. 14 (2023) 4255–4274. https://doi.org/10.1039/D3PY00767G.
[97] D. Ji, Y. Wang, J. Peng, D. Yuan, Z. Li, D. Ji, H. Wu, Recent Advances in Depolymerization and High-Value Utilization of Lignin: A Review, Ind. Eng. Chem. Res. 63 (2024) 19916–19935. https://doi.org/10.1021/acs.iecr.4c02617.
[98] H. Dong, M. Li, Y. Jin, Y. Wu, C. Huang, J. Yang, Preparation of Graphene-Like Porous Carbons With Enhanced Thermal Conductivities From Lignin Nanoparticles by Combining Hydrothermal Carbonization and Pyrolysis, Front. Energy Res. 8 (2020) 148. https://doi.org/10.3389/fenrg.2020.00148.
[99] J. Liu, W. Qu, Y. Xie, B. Zhu, T. Wang, X. Bai, X. Wang, Thermal conductivity and annealing effect on structure of lignin-based microscale carbon fibers, Carbon 121 (2017) 35–47. https://doi.org/10.1016/j.carbon.2017.05.066.
[100] K. Nakajima, M. Hara, Amorphous Carbon with SO_3 H Groups as a Solid Brønsted Acid Catalyst, ACS Catal. 2 (2012) 1296–1304. https://doi.org/10.1021/cs300103k.
[101] K. Shimizu, A. Satsuma, Toward a rational control of solid acid catalysis for green synthesis and biomass conversion, Energy Environ. Sci. 4 (2011) 3140. https://doi.org/10.1039/c1ee01458g.
[102] F. Su, Y. Guo, Advancements in solid acid catalysts for biodiesel production, Green Chem. 16 (2014) 2934–2957. https://doi.org/10.1039/C3GC42333F.
[103] Y. Huang, Y. Duan, S. Qiu, M. Wang, C. Ju, H. Cao, Y. Fang, T. Tan, Lignin-first biorefinery: a reusable catalyst for lignin depolymerization and application of

lignin oil to jet fuel aromatics and polyurethane feedstock, Sustainable Energy Fuels 2 (2018) 637–647. https://doi.org/10.1039/C7SE00535K.
[104] J. Ralph, K. Lundquist, G. Brunow, F. Lu, H. Kim, P.F. Schatz, J.M. Marita, R.D. Hatfield, S.A. Ralph, J.H. Christensen, W. Boerjan, Lignins: Natural polymers from oxidative coupling of 4-hydroxyphenyl- propanoids, Phytochem. Rev. 3 (2004) 29–60. https://doi.org/10.1023/B:PHYT.0000047809.65444.a4.
[105] R. Vanholme, B. Demedts, K. Morreel, J. Ralph, W. Boerjan, Lignin Biosynthesis and Structure, Plant Physiol. 153 (2010) 895–905. https://doi.org/10.1104/pp.110.155119.
[106] L. Zhang, G. Gellerstedt, NMR observation of a new lignin structure, a spiro-dienone, Chem. Commun. (2001) 2744–2745. https://doi.org/10.1039/b108285j.
[107] T.-Q. Yuan, S.-N. Sun, F. Xu, R.-C. Sun, Characterization of Lignin Structures and Lignin–Carbohydrate Complex (LCC) Linkages by Quantitative ^{13}C and 2D HSQC NMR Spectroscopy, J. Agric. Food Chem. 59 (2011) 10604–10614.
[108] M. Talebi Amiri, S. Bertella, Y.M. Questell-Santiago, J.S. Luterbacher, Establishing lignin structure-upgradeability relationships using quantitative ^{1}H– ^{13}C heteronuclear single quantum coherence nuclear magnetic resonance (HSQC-NMR) spectroscopy, Chem. Sci. 10 (2019) 8135–8142. https://doi.org/10.1039/C9SC02088H.
[109] Z. Xia, L.G. Akim, D.S. Argyropoulos, Quantitative ^{13}C NMR Analysis of Lignins with Internal Standards, J. Agric. Food Chem. 49 (2001) 3573–3578. https://doi.org/10.1021/jf010333v.
[110] M. Sette, R. Wechselberger, C. Crestini, Elucidation of Lignin Structure by Quantitative 2D NMR, Chem. Eur. J. 17 (2011) 9529–9535. https://doi.org/10.1002/chem.201003045.
[111] D. Robert, Carbon-13 Nuclear Magnetic Resonance Spectrometry, in: S.Y. Lin, C.W. Dence (Eds.), Methods in Lignin Chemistry, Springer Berlin Heidelberg, Berlin, Heidelberg, 1992: pp. 250–273. https://doi.org/10.1007/978-3-642-74065-7_18.
[112] L.L. Landucci, Quantitative ^{13}C NMR Characterization of Lignin 1. A Methodology for High Precision, Holzforschung 39 (1985) 355–360. https://doi.org/10.1515/hfsg.1985.39.6.355.
[113] J. Gracia-Vitoria, M. Rubens, E. Feghali, P. Adriaensens, K. Vanbroekhoven, R. Vendamme, Low-field benchtop versus high-field NMR for routine ^{31}P analysis of lignin, a comparative study, Ind. Crops Prod. 176 (2022) 114405. https://doi.org/10.1016/j.indcrop.2021.114405.
[114] J. Ralph, L.L. Landucci, NMR of Lignins, in: Lignin and Lignans; Advances in Chemistry, Taylor & Francis, Boca Raton, 2010: pp. 137–234.
[115] K. Lundquist, K. Stern, Analysis of lignins by ^{1}H NMR spectroscopy, Nordic Pulp & Paper Research Journal 4 (1989) 210–213. https://doi.org/10.3183/npprj-1989-04-03-p210-213.
[116] M. Karlsson, J. Romson, T. Elder, Å. Emmer, M. Lawoko, Lignin Structure and Reactivity in the Organosolv Process Studied by NMR Spectroscopy, Mass Spectrometry, and Density Functional Theory, Biomacromolecules 24 (2023) 2314–2326. https://doi.org/10.1021/acs.biomac.3c00186.
[117] Y. Pu, S. Cao, A.J. Ragauskas, Application of quantitative ^{31}P NMR in biomass lignin and biofuel precursors characterization, Energy Environ. Sci. 4 (2011) 3154. https://doi.org/10.1039/c1ee01201k.

[118] L.B. Krivdin, NMR studies of lignin and lignin-derived products: recent advances and perspectives, RUSS CHEM REV 94 (2025) RCR5159. https://doi.org/10.59761/RCR5159.
[119] J.F. Araneda, I.W. Burton, M. Paleologou, S.D. Riegel, M.C. Leclerc, Analysis of lignins using ^{31}P benchtop NMR spectroscopy: quantitative assessment of substructures and comparison to high-field NMR, Can. J. Chem. 100 (2022) 799–808. https://doi.org/10.1139/cjc-2022-0041.
[120] International Organization for Standardization, ISO/IEC Guide 98-3:2008 — Uncertainty of measurement – Part 3: Guide to the expression of uncertainty in measurement (GUM:1995), (2008). https://www.iso.org/standard/50461.html.
[121] Evaluation of measurement data – Guide to the expression of uncertainty in measurement, (2008). https://doi.org/10.59161/JCGM100-2008E.
[122] M.G. Ntunka, S.T. Vallabh, Advances in Integrated Lignin Valorization Pathways for Sustainable Biorefineries, Molecules 31 (2026) 380. https://doi.org/10.3390/molecules31020380.
[123] M.H. Ramsey, Sampling as a source of measurement uncertainty: techniques for quantification and comparison with analytical sources, J. Anal. At. Spectrom. 13 (1998) 97–104. https://doi.org/10.1039/a706815h.
[124] A. Menditto, M. Patriarca, B. Magnusson, Understanding the meaning of accuracy, trueness and precision, Accredit. Qual. Assur. 12 (2007) 45–47. https://doi.org/10.1007/s00769-006-0191-z.
[125] METTLER TOLEDO, Moisture and Water Content Analysis in Food, METTLER TOLEDO (n.d.). https://www.mt.com/my/en/home/applications/laboratory/food-and-beverages/moisture-water.html (accessed March 24, 2026).
[126] M. Schubnell, C.D. Caro, K. Raphael, Moisture content, water content, loss on drying, Part 1: What exactly is meant and how are these quantities determined?, METTLER TOLEDO, Nänikon, Switzerland, 2021. https://www.mt.com/dam/non-indexed/po/ana/ta-applications/UC511.pdf.
[127] Petro Industry, An Introduction to Water Quantification, Petro Online (n.d.). https://www.petro-online.com/news/analytical-instrumentation/11/breaking-news/an-introduction-to-water-quantification/49324 (accessed March 24, 2026).
[128] A. Sella, Karl Fischer's titrator, Chemistry World (2012). https://www.chemistryworld.com/opinion/karl-fischers-titrator/5695.article (accessed March 24, 2026).
[129] C.M. Beck, Classical analysis. A look at the past, present, and future, Anal. Chem. 66 (1994) 224A-239A. https://doi.org/10.1021/ac00076a001.
[130] R.L. Bradley, Moisture and Total Solids Analysis, in: S.S. Nielsen (Ed.), Food Analysis, Springer US, Boston, MA, 2010: pp. 85–104. https://doi.org/10.1007/978-1-4419-1478-1_6.
[131] R.S. Kirk, R. Sawyer, H. Egan, D. Pearson, Pearson's composition and analysis of foods, 9th Edition, Longman Scientific & Technical, Essex, UK, Harlow, 1991.
[132] Y. Roggo, P. Chalus, L. Maurer, C. Lema-Martinez, A. Edmond, N. Jent, A review of near infrared spectroscopy and chemometrics in pharmaceutical technologies, J. Pharm. Biomed. Anal. 44 (2007) 683–700. https://doi.org/10.1016/j.jpba.2007.03.023.
[133] D. Duncan, Headspace Moisture Analysis for Determination of Residual Moisture Content in Lyophilized Pharmaceutical Products, 40 (2016) 28–31.

[134] K. Fischer, Neues Verfahren zur maßanalytischen Bestimmung des Wassergehaltes von Flüssigkeiten und festen Körpern, Angewandte Chemie 48 (1935) 394–396. https://doi.org/10.1002/ange.19350482605.
[135] C. Gillet, W. Splawski, F. Aguirre, B. Hassoune-Rhabbour, T. Tchalla, V. Nassiet, Use of Karl Fischer titration for the localized measurement of water content in FRP composite aircraft parts removed from service, J. Compos. Mater. 57 (2023) 1495–1510. https://doi.org/10.1177/00219983231158860.
[136] D. Olszewska-Pastuszak, Z. Suchorab, K. Tabiś, K. Pluta, Application of Karl Fischer titration method to determine moisture content of building materials, Measurement 256 (2025) 118363. https://doi.org/10.1016/j.measurement.2025.118363.
[137] P. Rivera-Quintero, G.S. Patience, N.A. Patience, D.C. Boffito, X. Banquy, D. Schieppati, Experimental methods in chemical engineering: Karl Fischer titration, Can. J. Chem. Eng. 102 (2024) 2980–2997. https://doi.org/10.1002/cjce.25295.
[138] Coulometric Karl Fischer titrators, (n.d.). https://www.metrohm.com/en/products/karl-fischer-titration/kf-coulometers.html (accessed April 10, 2025).
[139] M. Margreth, R. Schlink, A. Steinbach, Water Determination By Karl Fischer Titration, in: S.C. Gad (Ed.), Pharmaceutical Sciences Encyclopedia, 1st ed., Wiley, 2010: pp. 1–34. https://doi.org/10.1002/9780470571224.pse415.
[140] R. Aro, M.W. Ben Ayoub, I. Leito, É. Georgin, Moisture in Solids: Comparison Between Evolved Water Vapor and Vaporization Coulometric Karl Fischer Methods, Int. J. Thermophys. 41 (2020) 113. https://doi.org/10.1007/s10765-020-02697-6.
[141] Mettler-Toledo AG, Introduction to Karl Fischer Titration, Mettler-Toledo AG, Schwerzenbach, Switzerland, 2012.
[142] International Organization for Standardization (ISO), Natural gas — Determination of water by the Karl Fischer method — Part 3: Coulometric procedure ISO 10101-3:2022, (2022).
[143] E. Scholz, Karl Fischer Titration, Springer Berlin Heidelberg, Berlin, Heidelberg, 1984. https://doi.org/10.1007/978-3-642-69989-4.
[144] Metrohm AG, Coulometric Water Content Determination According to Karl Fischer, Metrohm International Headquarters, Herisau, Switzerland, 2020. https://www.metrohm.com/content/dam/metrohm/shared/documents/application-bulletins/AB-137_6.pdf (accessed April 15, 2026).
[145] S. Inagaki, T. Asakai, M. Numata, N. Hanari, K. Ishikawa, K. Kitanaka, M. Hagiwara, S. Kotaki, Certification of water content in NMIJ CRM 4222-a, water standard solution 0.1 mg g^{-1}, by coulometric and volumetric Karl Fischer titration, Anal. Methods 6 (2014) 2785–2790. https://doi.org/10.1039/C3AY42314J.
[146] Oven method for sample preparation in Karl Fischer titration, (n.d.). https://www.metrohm.com/en/discover/blog/20-21/oven-method-for-sample-preparation-in-karl-fischer-titration.html (accessed March 18, 2026).
[147] Edinburgh Instruments, (n.d.). https://www.edinst.com/resource/what-is-ftir-spectroscopy/ (accessed April 11, 2025).
[148] Attenuated total reflectance (ATR) | Anton Paar Wiki, Anton Paar (n.d.). https://wiki.anton-paar.com/en/attenuated-total-reflectance-atr/ (accessed April 11, 2025).
[149] A.H. Harker, Principles of materials characterization and metrology: by Kannan M. Krishnan, Oxford, UK, Oxford University Press, 2021, 20 + 849 pp., ISBN

978–0–19–883025–2 (hbk), ISBN 978–0–19–883026–9 (pbk). Scope: textbook. Level: undergraduate, early postgraduate., Contemporary Physics 62 (2021) 242–242. https://doi.org/10.1080/00107514.2022.2081723.
[150] B.H. Stuart, Infrared Spectroscopy: Fundamentals and Applications, 1st ed., Wiley, 2004. https://doi.org/10.1002/0470011149.
[151] P.R. Griffiths, J.A. De Haseth, Fourier Transform Infrared Spectrometry, 1st ed., Wiley, 2007. https://doi.org/10.1002/047010631X.
[152] J. Greener, B. Abbasi, E. Kumacheva, Attenuated total reflection Fourier transform infrared spectroscopy for on-chip monitoring of solute concentrations, Lab Chip 10 (2010) 1561. https://doi.org/10.1039/c001889a.
[153] Measurlabs, ATR-FTIR Analysis | Attenuated Total Reflectance | Measurlabs, (n.d.). https://measurlabs.com/methods/atr-ftir-analysis/ (accessed March 24, 2026).
[154] R. Md Salim, J. Asik, M.S. Sarjadi, Chemical functional groups of extractives, cellulose and lignin extracted from native Leucaena leucocephala bark, Wood Sci. Technol. 55 (2021) 295–313. https://doi.org/10.1007/s00226-020-01258-2.
[155] M.P. Tucker, Q.A. Nguyen, F.P. Eddy, K.L. Kadam, L.M. Gedvilas, J.D. Webb, Fourier Transform Infrared Quantitative Analysis of Sugars and Lignin in Pretreated Softwood Solid Residues, ABAB 91–93 (2001) 51–62. https://doi.org/10.1385/ABAB:91-93:1-9:51.
[156] J.S. Lupoi, S. Singh, R. Parthasarathi, B.A. Simmons, R.J. Henry, Recent innovations in analytical methods for the qualitative and quantitative assessment of lignin, Renewable Sustainable Energy Rev. 49 (2015) 871–906. https://doi.org/10.1016/j.rser.2015.04.091.
[157] H. Chen, C. Ferrari, M. Angiuli, J. Yao, C. Raspi, E. Bramanti, Qualitative and quantitative analysis of wood samples by Fourier transform infrared spectroscopy and multivariate analysis, Carbohydr. Polym. 82 (2010) 772–778. https://doi.org/10.1016/j.carbpol.2010.05.052.
[158] S. Pasieczna-Patkowska, M. Cichy, J. Flieger, Application of Fourier Transform Infrared (FTIR) Spectroscopy in Characterization of Green Synthesized Nanoparticles, Molecules 30 (2025) 684. https://doi.org/10.3390/molecules30030684.
[159] M. Fan, D. Dai, B. Huang, Fourier Transform Infrared Spectroscopy for Natural Fibres, in: S. Salih (Ed.), Fourier Transform – Materials Analysis, InTech, 2012. https://doi.org/10.5772/35482.
[160] D.L. Pavia, G.M. Lampman, G.S. Kriz, J. Vyvyan, Introduction to spectroscopy, 5th edition, 2015.
[161] L. He, W. Hu, Y. Wei, Lignocellulose Determination and Categorization Analysis for Biofuel Pellets Based on FT-IR Spectra, Spectroscopy (2022) 14–22. https://doi.org/10.56530/spectroscopy.hg8068b2.
[162] F. Xu, J. Yu, T. Tesso, F. Dowell, D. Wang, Qualitative and quantitative analysis of lignocellulosic biomass using infrared techniques: A mini-review, Appl. Energy 104 (2013) 801–809. https://doi.org/10.1016/j.apenergy.2012.12.019.
[163] N.-E. El Mansouri, J. Salvadó, Analytical methods for determining functional groups in various technical lignins, Ind. Crops Prod. 26 (2007) 116–124. https://doi.org/10.1016/j.indcrop.2007.02.006.
[164] O. Faix, Classification of Lignins from Different Botanical Origins by FT-IR Spectroscopy, Holzforschung 45 (1991) 21–28. https://doi.org/10.1515/hfsg.1991.45.s1.21.

[165] X. Guo, Y. Qing, Y. Wu, Q. Wu, Molecular association of adsorbed water with lignocellulosic materials examined by micro-FTIR spectroscopy, Int. J. Biol. Macromol. 83 (2016) 117–125. https://doi.org/10.1016/j.ijbiomac.2015.11.047.
[166] M. Consumi, G. Leone, G. Tamasi, A. Magnani, Water content quantification by FTIR in carboxymethyl cellulose food additive, Food Addit. Contam. Part A 38 (2021) 1629–1635. https://doi.org/10.1080/19440049.2021.1948619.
[167] A. Célino, O. Gonçalves, F. Jacquemin, S. Fréour, Qualitative and quantitative assessment of water sorption in natural fibres using ATR-FTIR spectroscopy, Carbohydr. Polym. 101 (2014) 163–170. https://doi.org/10.1016/j.carbpol.2013.09.023.
[168] S.F. Sim, A.L. Jeffrey Kimura, Partial Least Squares (PLS) Integrated Fourier Transform Infrared (FTIR) Approach for Prediction of Moisture in Transformer Oil and Lubricating Oil, J. Spectro. 2019 (2019) 1–10. https://doi.org/10.1155/2019/5916506.
[169] R.G. Brereton, Chemometrics: Multivariate Statistical Analysis of Analytical Chemical and Biomolecular Data, in: K. Roy (Ed.), Chemometrics and Cheminformatics in Aquatic Toxicology, 1st ed., Wiley, 2021: pp. 45–60. https://doi.org/10.1002/9781119681397.ch3.
[170] S. Wold, Chemometrics; what do we mean with it, and what do we want from it?, Chemometrics and Intelligent Laboratory Systems 30 (1995) 109–115. https://doi.org/10.1016/0169-7439(95)00042-9.
[171] R.G. Brereton, Chemometrics: Data Analysis for the Laboratory and Chemical Plant, 1st ed., Wiley, 2003. https://doi.org/10.1002/0470863242.
[172] B. Salisu, S. Anua, W. Rosli, N. Mazlan, An improved Fourier-Transform Infrared Spectroscopy combined with partial least squares regression for rapid quantification of total aflatoxins in commercial chicken feeds and food grains, J. Adv. Vet. Anim. Res. 9 (2022) 546. https://doi.org/10.5455/javar.2022.i624.
[173] N. Sousa, M.J. Moreira, C. Saraiva, J.M.M.M. De Almeida, Applying Fourier Transform Mid Infrared Spectroscopy to Detect the Adulteration of Salmo salar with Oncorhynchus mykiss, Foods 7 (2018) 55. https://doi.org/10.3390/foods7040055.
[174] M. Taylor, A.M.A. Elhissi, Predicting the physical properties of tablets from ATR-FTIR spectra using partial least squares regression, Pharm. Dev. Technol. 16 (2011) 110–117. https://doi.org/10.3109/10837450903499374.
[175] C. Zhou, W. Jiang, Q. Cheng, B.K. Via, Multivariate Calibration and Model Integrity for Wood Chemistry Using Fourier Transform Infrared Spectroscopy, J. Anal. Methods Chem. 2015 (2015) 1–9. https://doi.org/10.1155/2015/429846.
[176] F. Heen Blindheim, J. Ruwoldt, Quantifying the Abundance of Alkane Moieties in Lignins with FTIR Spectroscopy and PLS Regression; Estimating Grafting Degree of Esterification, ChemSusChem 18 (2025) e202400938. https://doi.org/10.1002/cssc.202400938.
[177] C.S. Lancefield, S. Constant, P. de Peinder, P.C.A. Bruijnincx, Linkage Abundance and Molecular Weight Characteristics of Technical Lignins by Attenuated Total Reflection-FTIR Spectroscopy Combined with Multivariate Analysis, ChemSusChem 12 (2019) 1139–1146. https://doi.org/10.1002/cssc.201802809.
[178] S. Mukherjee, J.A. Martinez-Gonzalez, A.A. Gowen, Feasibility of attenuated total reflection-fourier transform infrared (ATR-FTIR) chemical imaging and partial least squares regression (PLSR) to predict protein adhesion on polymeric surfaces, Analyst 144 (2019) 1535–1545. https://doi.org/10.1039/C8AN01768A.

[179] G. Zhou, G. Taylor, A. Polle, FTIR-ATR-based prediction and modelling of lignin and energy contents reveals independent intra-specific variation of these traits in bioenergy poplars, Plant Methods 7 (2011) 9. https://doi.org/10.1186/1746-4811-7-9.
[180] L.A. Riddell, P. De Peinder, V. Polizzi, K. Vanbroekhoven, F. Meirer, P.C.A. Bruijnincx, Predicting Molecular Weight Characteristics of Reductively Depolymerized Lignins by ATR-FTIR and Chemometrics, ACS Sustainable Chem. Eng. 12 (2024) 8968–8977. https://doi.org/10.1021/acssuschemeng.4c03100.
[181] J. Rodrigues, O. Faix, H. Pereira, Determination of Lignin Content of *Eucalyptus globulus* Wood Using FTIR Spectroscopy, Holzforschung 52 (1998) 46–50. https://doi.org/10.1515/hfsg.1998.52.1.46.
[182] R. Javier-Astete, J. Melo, J. Jimenez-Davalos, G. Zolla, Classification of Amazonian fast-growing tree species and wood chemical determination by FTIR and multivariate analysis (PLS-DA, PLS), Sci. Rep. 13 (2023) 7827. https://doi.org/10.1038/s41598-023-35107-6.
[183] C. Pasquini, Near infrared spectroscopy: A mature analytical technique with new perspectives – A review, Anal. Chim. Acta 1026 (2018) 8–36. https://doi.org/10.1016/j.aca.2018.04.004.
[184] X. Guo, L. Liu, J. Wu, J. Fan, Y. Wu, Qualitatively and quantitatively characterizing water adsorption of a cellulose nanofiber film using micro-FTIR spectroscopy, RSC Adv. 8 (2018) 4214–4220. https://doi.org/10.1039/C7RA09894D.
[185] I. Leito, I. Helm, L. Jalukse, Using MOOCs for teaching analytical chemistry: experience at University of Tartu, Anal. Bioanal.Chem. 407 (2015) 1277–1281. https://doi.org/10.1007/s00216-014-8399-y.
[186] D.B. Rorabacher, Statistical treatment for rejection of deviant values: critical values of Dixon's "Q" parameter and related subrange ratios at the 95% confidence level, Anal. Chem. 63 (1991) 139–146. https://doi.org/10.1021/ac00002a010.
[187] J.N. Miller, J.C. Miller, Statistics and chemometrics for analytical chemistry, 6th ed, Pearson Education Limited, Harlow, 2010.
[188] M.Yu. Balakshin, E.A. Capanema, Comprehensive structural analysis of biorefinery lignins with a quantitative ^{13}C NMR approach, RSC Adv. 5 (2015) 87187–87199. https://doi.org/10.1039/C5RA16649G.
[189] P.M. Froass, A.J. Ragauskas, J. Jiang, Nuclear Magnetic Resonance Studies. 4. Analysis of Residual Lignin after Kraft Pulping, Ind. Eng. Chem. Res. 37 (1998) 3388–3394. https://doi.org/10.1021/ie970812c.
[190] A.M.H. Van Der Veen, J. Pauwels, Uncertainty calculations in the certification of reference materials. 1. Principles of analysis of variance, Accredit. Qual. Assur. 5 (2000) 464–469. https://doi.org/10.1007/s007690000237.
[191] V.I. Tsaryuk, A.V. Frantsesson, Infrared study of the water contained in cellulose, Polym. Sci. U.S.S.R. 33 (1991) 260–267. https://doi.org/10.1016/0032-3950(91)90189-W.

SUMMARY IN ESTONIAN

Proovivõtu ning vee- ja niiskusesisalduse määramise metroloogilised aspektid ligniini näitel

Käesolev doktoritöö on pühendatud ligniini kvantitatiivse analüüsi usaldusväärsuse parandamisele, keskendudes eelkõige proovivõtu määramatuse hindamisele qNMR-meetodi abil ning vee- ja niiskusesisalduse määramisele. Töö käigus töötati välja ATR-FTIR spektroskoopial ja PLS kalibreerimismudelitel põhinevad meetodid ligniini vee- ja niiskusesisalduse määramiseks.

Viimastel aastatel vaadeldakse ligniini üha enam kui potentsiaalselt olulist taastuvat toorainet biotehnoloogia ja materjaliteaduse rakendustes. Seetõttu on usaldusväärsed analüüsitulemused vajalikud nii teadus- kui ka tööstusrakenduste jaoks.

Doktoritöö esimene osa käsitleb qNMR-meetodite täpsust kvantitatiivses ligniini analüüsis. Avaldatud qNMR-uuringute kriitiline hindamine näitas märkimisväärseid vastuolusid täpsuse ja selle erinevate komponentide esitamisel. Sageli kasutatakse erinevaid mõõdetavaid suurusi ja tulemuste esitamise vorme ilma selgelt määratlemata, millise täpsuse tüübi või millise veaallika alusel tulemusi esitatakse. Mõõtemääramatust, mis võtaks arvesse kõiki olulisi allikaid, hinnatakse harva ning proovivõtuga seotud varieeruvuse panus jäetakse sageli tähelepanuta. Need puudujäägid raskendavad kvantitatiivsete andmete võrdlemist ja tõlgendamist.

Selle analüüsi tulemuste põhjal viidi läbi uuring proovivõtust tuleneva määramatuse hindamiseks ligniini analüüsis, kasutades qNMR-spektroskoopiat. Kuigi ligniini peetakse sageli suhteliselt homogeenseks materjaliks, on tegemist loodusliku tahke ainega ning samast lähtematerjalist võetud alamproovid võivad koostise poolest erineda. Tulemused näitasid, et proovidevaheline varieeruvus moodustab märkimisväärse osa qNMR-mõõtmiste koguvarieeruvusest. Töös pakuti välja kaks praktilist meetodit proovivõtust tuleneva määramatuse hindamiseks kordusmõõtmiste andmete põhjal. Proovivõtust tingitud varieeruvuse suhteline standardhälve (RSD) oli 2,4%, samas kui muud tegurid, nagu baastaseme nihked ja signaalide kattumine, andsid panuse 4,4%. Kõiki varieeruvuse allikaid arvesse võttev RSD oli 5,0%.

Doktoritöö teine põhiosa keskendub vee- ja niiskusesisalduse määramisele ligniinis. Vee- ja niiskuse täpne määramine on ligniini puhul keeruline ligniini keemilise keerukuse, heterogeensuse ja tugevalt hargnenud struktuuri tõttu, samuti vee esinemise tõttu erinevates vormides.

Niiskuse- ja veesisalduse määramiseks valmistati kalibreerimisproovide seeria ligniinidest, mis pärinesid erinevatest taimeliikidest ja erinevatest tööstuslikest eraldamisprotsessidest. Kalibreerimisproovide veesisalduse määramiseks rakendati aurufaasilist kulonomeetrilist Karl Fischeri tiitrimist (vap-C-KFT) ning töötati välja modelleerimisviis, mis põhineb sigmoidaalse kujuga temperatuuri–vee eraldumise kõveratel, et määrata optimaalsed vee proovist välja aurustamise temperatuurid. See lähenemine võimaldab valida temperatuuri, mille juures eraldub

keemiliselt sidumata vesi, vältides samal ajal olulist vee lisandumist termilise lagunemise tagajärjel. Madalamatel temperatuuridel annab vap-C-KFT allahinnatud tulemused vee mittetäieliku eraldumise tõttu, samas kui kõrgematel temperatuuridel võib ligniini lagunemise tõttu tekkida täiendav vesi. Kalibreerimisproovide niiskusesisalduse määramiseks kasutati gravimeetrilisi meetodeid: ahjukuivatamist ja lüofiliseerimist.

Saadud kalibreerimisproove kasutati kiire ja mittedestruktiivse vee- ja niiskusesisalduse määramise meetodi esmasel tasemel väljatöötamiseks, kasutades ATR-FTIR-spektroskoopiat koos osalisel vähimruutude regressioonil põhinevate kalibreerimismudelitega. Saadud meetodil on hea ennustusvõime laia valiku ligniinitüüpide puhul, piisab väikesest proovikogusest ja minimaalsest proovi-ettevalmistusest.

Kokkuvõttes näitab käesolev doktoritöö, et kvantitatiivses analüüsis on mõõdetava suuruse selge määratlemine ning piisava info esitamine täpsuse ja õigsuse kohta hädavajalik. Proovivõtust tulenev määramatus osutus oluliseks ja seni alahinnatud teguriks ligniini analüüsi kogumääramatuses. Loodi ATR-FTIR põhine kiire ja lihtne ligniinis vee- ja niiskusesisalduse määramise meetod.

ACKNOWLEDGEMENTS

I sincerely thank Estonia, the beautiful city of Tartu, the University of Tartu, and the Institute of Chemistry for providing me with the opportunity to study and grow in such an inspiring and supportive academic environment. Pursuing my education in this wonderful place has been a privilege, and I am deeply grateful for the knowledge and experiences I have gained here.

I express my deepest gratitude to my mentor, Prof. Ivo Leito, as well as Assoc. Prof. Koit Herodes and Dr. Lauri Toom, for their continuous guidance and encouragement throughout my studies in Estonia. Their patience, motivation, enthusiasm, and profound knowledge have been invaluable and have significantly contributed to the quality of this work. I am also sincerely thankful to my colleagues at the Chair of Analytical Chemistry and my co-authors, especially Dr. Martin Vilbaste and Andres Siiman, for their support and guidance in helping me develop practical knowledge and research skills. I am also grateful to Mr. Gert Preegel (Fibenol) and Dr. Siim Salmar for providing lignin samples essential for this research.

I extend my heartfelt thanks to my beloved parents, Mrs. Seema Pawade and Mr. Shivaji Pawade, my siblings and cousins – Shashikant, Sudhir, Shital, Dnyaneshwar, and Swapnali – and all my family members, whose unwavering belief in me and constant support have been my greatest strength throughout this journey. Their unconditional love has inspired and sustained me at every step. A special note of gratitude goes to my wife, Ms. Deepika Pawade (Shinde), whose unwavering support during challenging times gave me immense strength and resilience.

I am genuinely grateful for the encouragement and cherished companionship of my friends from India: Aakansha Negi, Akash, Shashikant. I also gratefully acknowledge the continued support during my doctoral studies by Dr. Pratik Shinde, Dr. Ajai Pathak, Dr. Sandip Kadam, Dr. Gajanan Raut, and Dr. Durga Prasad, whose guidance has meant a great deal to me over the years. I would also like to thank to Akshith, Katyayaniji, Sanu, Surbhi, Deepika, Arpan, and Rohish, for their constant motivation, friendship, and presence throughout this journey. I want to thank all my colleagues, especially Jan-Michael and Ernesto, for making PhD life more exciting and bearable.

Finally, I sincerely thank the Estonian Ministry of Education and Research (Centre of Excellence TK210), the ASTRA project PER ASPERA Graduate School of Functional Materials and Technologies and the Estonian Research Council (PRG690 and PRG2557) for their support of this work.

PUBLICATIONS

CURRICULUM VITAE

Name: Shrikant Shivaji Pawade
Date of birth: April 2, 1994, Pune, Maharashtra, India
Citizenship: Indian
Contact: Institute of Chemistry, University of Tartu, Ravila 14a, Tartu, 50411, Estonia
E-mail: shrikant.shivaji.pawade@ut.ee, shrisp4@gmail.com

Education:

2020–….	University of Tartu, Institute of Chemistry, PhD student in Chemistry
2015–2017	Fergusson College, Pune (India), Savitribai Phule Pune, University, Master of Science: Chemistry with specialisation in Organic Chemistry
2012–2015	Modern College, Pune, Savitribai Phule Pune University, India. Bachelor of Science: Chemistry

Professional employment:

2017–2020	Aurigene Discovery technologies Ltd., Bangalore, India. Designation: Research Associate.

Research grants and scholarships

- Research supported by Estonian Research Council (PRG690 and PRG2557).
- The experiments were carried out using the instrumentation at the Estonian Centre of Analytical Chemistry (TT4, www.akki.ee).
- Doctoral scholarship from University of Tartu.

Scientific publications:

I. **S. S. Pawade**, L. Toom, K. Herodes, and I. Leito, "Accuracy of Quantitative NMR Analysis: A Case Study of Lignin," *Journal of Chemical Metrology* 17, no. 1 (January/June 2023): 114–127, https://doi.org/10.25135/jcm.88.2304.2753

II. **S. S. Pawade**, L. Toom, K. Herodes, and I. Leito, "Evaluating Sampling Uncertainty in the Quantitative ^{1}H Nuclear Magnetic Resonance Analysis of Lignin." *BioResources* 20, no. 1 (January 27, 2025): 2234–42. https://doi.org/10.15376/biores.20.1.2234-2242

III. **S. S. Pawade**, M. Vilbaste, A. Siiman, L. Toom, K. Herodes, I. Leito, A quantitative approach to determine water and moisture content of different types of lignin using attenuated total reflectance Fourier transform infrared spectroscopy combined with partial least squares regression, Biofuels, Bio-products & Biorefining 20 (2026) 919–930. https://doi.org/10.1002/bbb.70124

IV. M. Vilbaste, **S. S. Pawade**, I. Leito, Optimisation of temperature for accurate water content determination in plant-derived materials using vaporisation–coulometric Karl Fischer titration, *Journal of Chemical Metrology* (2025) 114–127. https://doi.org/10.25135/jcm.126.2511.3730

ELULOOKIRJELDUS

Nimi: Shrikant Shivaji Pawade
Sünniaeg: 2. aprill 1994, Pune, Maharashtra, India
Kodakondsus: India
Kontakt: Tartu Ülikool, Keemia Instituut Ravila 14a, Tartu 50411, Eesti
E-post: shrikant.shivaji.pawade@ut.ee/ shrisp4@gmail.com

Haridus

2020–....	Tartu Ülikool, Keemia Instituut keemia doktorant
2015–2017	Fergusson College, Pune, India, Savitribai Phule Pune Ülikool, Magistrikraad keemias (MSc), spetsialiseerumine orgaanilisele keemiale
2012–2015	Modern College, Pune, India, Savitribai Phule Pune Ülikool, Bakalaureusekraad keemias (BSc)

Töökogemus

2017–2020	Aurigene Discovery Technologies Ltd., Bangalore, India ametikoht: Research Associate

Teadusgrandid ja stipendiumid

- Uurimistööd on toetanud Eesti Teadusagentuuri projekt PRG690 ja PRG2557.
- Katsed viidi läbi Eesti Analüütilise Keemia Tippkeskuse (TT4, www.akki.ee) aparatuuril.
- Tartu Ülikooli doktorandistipendium.

Teaduspublikatsioonid

I. **S. S. Pawade**, L. Toom, K. Herodes, and I. Leito, "Accuracy of Quantitative NMR Analysis: A Case Study of Lignin," *Journal of Chemical Metrology* 17, no. 1 (January/June 2023): 114–127, https://doi.org/10.25135/jcm.88.2304.2753

II. **S. S. Pawade**, L. Toom, K. Herodes, and I. Leito, "Evaluating Sampling Uncertainty in the Quantitative ^{1}H Nuclear Magnetic Resonance Analysis of Lignin." *BioResources* 20, no. 1 (January 27, 2025): 2234–42. https://doi.org/10.15376/biores.20.1.2234-2242

III. **S. S. Pawade**, M. Vilbaste, A. Siiman, L. Toom, K. Herodes, I. Leito, A quantitative approach to determine water and moisture content of different types of lignin using attenuated total reflectance Fourier transform infrared spectroscopy combined with partial least squares regression, Biofuels, Bioproducts & Biorefining 20 (2026) 919–930. https://doi.org/10.1002/bbb.70124

IV. M. Vilbaste, **S. S. Pawade**, I. Leito, Optimisation of temperature for accurate water content determination in plant-derived materials using vaporisation–coulometric Karl Fischer titration, *Journal of Chemical Metrology* (2025) 114–127. https://doi.org/10.25135/jcm.126.2511.3730

DISSERTATIONES CHIMICAE UNIVERSITATIS TARTUENSIS

1. **Toomas Tamm.** Quantum-chemical simulation of solvent effects. Tartu, 1993, 110 p.
2. **Peeter Burk.** Theoretical study of gas-phase acid-base equilibria. Tartu, 1994, 96 p.
3. **Victor Lobanov.** Quantitative structure-property relationships in large descriptor spaces. Tartu, 1995, 135 p.
4. **Vahur Mäemets.** The ^{17}O and ^{1}H nuclear magnetic resonance study of H_2O in individual solvents and its charged clusters in aqueous solutions of electrolytes. Tartu, 1997, 140 p.
5. **Andrus Metsala.** Microcanonical rate constant in nonequilibrium distribution of vibrational energy and in restricted intramolecular vibrational energy redistribution on the basis of slater's theory of unimolecular reactions. Tartu, 1997, 150 p.
6. **Uko Maran.** Quantum-mechanical study of potential energy surfaces in different environments. Tartu, 1997, 137 p.
7. **Alar Jänes.** Adsorption of organic compounds on antimony, bismuth and cadmium electrodes. Tartu, 1998, 219 p.
8. **Kaido Tammeveski.** Oxygen electroreduction on thin platinum films and the electrochemical detection of superoxide anion. Tartu, 1998, 139 p.
9. **Ivo Leito.** Studies of Brønsted acid-base equilibria in water and non-aqueous media. Tartu, 1998, 101 p.
10. **Jaan Leis.** Conformational dynamics and equilibria in amides. Tartu, 1998, 131 p.
11. **Toonika Rinken.** The modelling of amperometric biosensors based on oxidoreductases. Tartu, 2000, 108 p.
12. **Dmitri Panov.** Partially solvated Grignard reagents. Tartu, 2000, 64 p.
13. **Kaja Orupõld.** Treatment and analysis of phenolic wastewater with microorganisms. Tartu, 2000, 123 p.
14. **Jüri Ivask.** Ion Chromatographic determination of major anions and cations in polar ice core. Tartu, 2000, 85 p.
15. **Lauri Vares.** Stereoselective Synthesis of Tetrahydrofuran and Tetrahydropyran Derivatives by Use of Asymmetric Horner-Wadsworth-Emmons and Ring Closure Reactions. Tartu, 2000, 184 p.
16. **Martin Lepiku.** Kinetic aspects of dopamine D_2 receptor interactions with specific ligands. Tartu, 2000, 81 p.
17. **Katrin Sak.** Some aspects of ligand specificity of P2Y receptors. Tartu, 2000, 106 p.
18. **Vello Pällin.** The role of solvation in the formation of iotsitch complexes. Tartu, 2001, 95 p.
19. **Katrin Kollist.** Interactions between polycyclic aromatic compounds and humic substances. Tartu, 2001, 93 p.

20. **Ivar Koppel.** Quantum chemical study of acidity of strong and superstrong Brønsted acids. Tartu, 2001, 104 p.
21. **Viljar Pihl.** The study of the substituent and solvent effects on the acidity of OH and CH acids. Tartu, 2001, 132 p.
22. **Natalia Palm.** Specification of the minimum, sufficient and significant set of descriptors for general description of solvent effects. Tartu, 2001, 134 p.
23. **Sulev Sild.** QSPR/QSAR approaches for complex molecular systems. Tartu, 2001, 134 p.
24. **Ruslan Petrukhin.** Industrial applications of the quantitative structure-property relationships. Tartu, 2001, 162 p.
25. **Boris V. Rogovoy.** Synthesis of (benzotriazolyl)carboximidamides and their application in relations with *N*- and *S*-nucleophyles. Tartu, 2002, 84 p.
26. **Koit Herodes.** Solvent effects on UV-vis absorption spectra of some solvatochromic substances in binary solvent mixtures: the preferential solvation model. Tartu, 2002, 102 p.
27. **Anti Perkson.** Synthesis and characterisation of nanostructured carbon. Tartu, 2002, 152 p.
28. **Ivari Kaljurand.** Self-consistent acidity scales of neutral and cationic Brønsted acids in acetonitrile and tetrahydrofuran. Tartu, 2003, 108 p.
29. **Karmen Lust.** Adsorption of anions on bismuth single crystal electrodes. Tartu, 2003, 128 p.
30. **Mare Piirsalu.** Substituent, temperature and solvent effects on the alkaline hydrolysis of substituted phenyl and alkyl esters of benzoic acid. Tartu, 2003, 156 p.
31. **Meeri Sassian.** Reactions of partially solvated Grignard reagents. Tartu, 2003, 78 p.
32. **Tarmo Tamm.** Quantum chemical modelling of polypyrrole. Tartu, 2003. 100 p.
33. **Erik Teinemaa.** The environmental fate of the particulate matter and organic pollutants from an oil shale power plant. Tartu, 2003. 102 p.
34. **Jaana Tammiku-Taul.** Quantum chemical study of the properties of Grignard reagents. Tartu, 2003. 120 p.
35. **Andre Lomaka.** Biomedical applications of predictive computational chemistry. Tartu, 2003. 132 p.
36. **Kostyantyn Kirichenko.** Benzotriazole – Mediated Carbon–Carbon Bond Formation. Tartu, 2003. 132 p.
37. **Gunnar Nurk.** Adsorption kinetics of some organic compounds on bismuth single crystal electrodes. Tartu, 2003, 170 p.
38. **Mati Arulepp.** Electrochemical characteristics of porous carbon materials and electrical double layer capacitors. Tartu, 2003, 196 p.
39. **Dan Cornel Fara.** QSPR modeling of complexation and distribution of organic compounds. Tartu, 2004, 126 p.
40. **Riina Mahlapuu.** Signalling of galanin and amyloid precursor protein through adenylate cyclase. Tartu, 2004, 124 p.

41. **Mihkel Kerikmäe.** Some luminescent materials for dosimetric applications and physical research. Tartu, 2004, 143 p.
42. **Jaanus Kruusma.** Determination of some important trace metal ions in human blood. Tartu, 2004, 115 p.
43. **Urmas Johanson.** Investigations of the electrochemical properties of polypyrrole modified electrodes. Tartu, 2004, 91 p.
44. **Kaido Sillar.** Computational study of the acid sites in zeolite ZSM-5. Tartu, 2004, 80 p.
45. **Aldo Oras.** Kinetic aspects of dATPαS interaction with $P2Y_1$ receptor. Tartu, 2004, 75 p.
46. **Erik Mölder.** Measurement of the oxygen mass transfer through the air-water interface. Tartu, 2005, 73 p.
47. **Thomas Thomberg.** The kinetics of electroreduction of peroxodisulfate anion on cadmium (0001) single crystal electrode. Tartu, 2005, 95 p.
48. **Olavi Loog.** Aspects of condensations of carbonyl compounds and their imine analogues. Tartu, 2005, 83 p.
49. **Siim Salmar.** Effect of ultrasound on ester hydrolysis in aqueous ethanol. Tartu, 2006, 73 p.
50. **Ain Uustare.** Modulation of signal transduction of heptahelical receptors by other receptors and G proteins. Tartu, 2006, 121 p.
51. **Sergei Yurchenko.** Determination of some carcinogenic contaminants in food. Tartu, 2006, 143 p.
52. **Kaido Tämm.** QSPR modeling of some properties of organic compounds. Tartu, 2006, 67 p.
53. **Olga Tšubrik.** New methods in the synthesis of multisubstituted hydrazines. Tartu. 2006, 183 p.
54. **Lilli Sooväli.** Spectrophotometric measurements and their uncertainty in chemical analysis and dissociation constant measurements. Tartu, 2006, 125 p.
55. **Eve Koort.** Uncertainty estimation of potentiometrically measured ph and pK_a values. Tartu, 2006, 139 p.
56. **Sergei Kopanchuk.** Regulation of ligand binding to melanocortin receptor subtypes. Tartu, 2006, 119 p.
57. **Silvar Kallip.** Surface structure of some bismuth and antimony single crystal electrodes. Tartu, 2006, 107 p.
58. **Kristjan Saal.** Surface silanization and its application in biomolecule coupling. Tartu, 2006, 77 p.
59. **Tanel Tätte.** High viscosity $Sn(OBu)_4$ oligomeric concentrates and their applications in technology. Tartu, 2006, 91 p.
60. **Dimitar Atanasov Dobchev**. Robust QSAR methods for the prediction of properties from molecular structure. Tartu, 2006, 118 p.
61. **Hannes Hagu**. Impact of ultrasound on hydrophobic interactions in solutions. Tartu, 2007, 81 p.
62. **Rutha Jäger.** Electroreduction of peroxodisulfate anion on bismuth electrodes. Tartu, 2007, 142 p.

63. **Kaido Viht.** Immobilizable bisubstrate-analogue inhibitors of basophilic protein kinases: development and application in biosensors. Tartu, 2007, 88 p.
64. **Eva-Ingrid Rõõm.** Acid-base equilibria in nonpolar media. Tartu, 2007, 156 p.
65. **Sven Tamp.** DFT study of the cesium cation containing complexes relevant to the cesium cation binding by the humic acids. Tartu, 2007, 102 p.
66. **Jaak Nerut.** Electroreduction of hexacyanoferrate(III) anion on Cadmium (0001) single crystal electrode. Tartu, 2007, 180 p.
67. **Lauri Jalukse.** Measurement uncertainty estimation in amperometric dissolved oxygen concentration measurement. Tartu, 2007, 112 p.
68. **Aime Lust.** Charge state of dopants and ordered clusters formation in CaF_2:Mn and CaF_2:Eu luminophors. Tartu, 2007, 100 p.
69. **Iiris Kahn**. Quantitative Structure-Activity Relationships of environmentally relevant properties. Tartu, 2007, 98 p.
70. **Mari Reinik.** Nitrates, nitrites, N-nitrosamines and polycyclic aromatic hydrocarbons in food: analytical methods, occurrence and dietary intake. Tartu, 2007, 172 p.
71. **Heili Kasuk.** Thermodynamic parameters and adsorption kinetics of organic compounds forming the compact adsorption layer at Bi single crystal electrodes. Tartu, 2007, 212 p.
72. **Erki Enkvist.** Synthesis of adenosine-peptide conjugates for biological applications. Tartu, 2007, 114 p.
73. **Svetoslav Hristov Slavov**. Biomedical applications of the QSAR approach. Tartu, 2007, 146 p.
74. **Eneli Härk.** Electroreduction of complex cations on electrochemically polished Bi(*hkl*) single crystal electrodes. Tartu, 2008, 158 p.
75. **Priit Möller.** Electrochemical characteristics of some cathodes for medium temperature solid oxide fuel cells, synthesized by solid state reaction technique. Tartu, 2008, 90 p.
76. **Signe Viggor.** Impact of biochemical parameters of genetically different pseudomonads at the degradation of phenolic compounds. Tartu, 2008, 122 p.
77. **Ave Sarapuu.** Electrochemical reduction of oxygen on quinone-modified carbon electrodes and on thin films of platinum and gold. Tartu, 2008, 134 p.
78. **Agnes Kütt.** Studies of acid-base equilibria in non-aqueous media. Tartu, 2008, 198 p.
79. **Rouvim Kadis.** Evaluation of measurement uncertainty in analytical chemistry: related concepts and some points of misinterpretation. Tartu, 2008, 118 p.
80. **Valter Reedo.** Elaboration of IVB group metal oxide structures and their possible applications. Tartu, 2008, 98 p.
81. **Aleksei Kuznetsov.** Allosteric effects in reactions catalyzed by the cAMP-dependent protein kinase catalytic subunit. Tartu, 2009, 133 p.

82. **Aleksei Bredihhin.** Use of mono- and polyanions in the synthesis of multisubstituted hydrazine derivatives. Tartu, 2009, 105 p.
83. **Anu Ploom.** Quantitative structure-reactivity analysis in organosilicon chemistry. Tartu, 2009, 99 p.
84. **Argo Vonk.** Determination of adenosine A_{2A}- and dopamine D_1 receptor-specific modulation of adenylate cyclase activity in rat striatum. Tartu, 2009, 129 p.
85. **Indrek Kivi.** Synthesis and electrochemical characterization of porous cathode materials for intermediate temperature solid oxide fuel cells. Tartu, 2009, 177 p.
86. **Jaanus Eskusson.** Synthesis and characterisation of diamond-like carbon thin films prepared by pulsed laser deposition method. Tartu, 2009, 117 p.
87. **Marko Lätt.** Carbide derived microporous carbon and electrical double layer capacitors. Tartu, 2009, 107 p.
88. **Vladimir Stepanov.** Slow conformational changes in dopamine transporter interaction with its ligands. Tartu, 2009, 103 p.
89. **Aleksander Trummal.** Computational Study of Structural and Solvent Effects on Acidities of Some Brønsted Acids. Tartu, 2009, 103 p.
90. **Eerold Vellemäe.** Applications of mischmetal in organic synthesis. Tartu, 2009, 93 p.
91. **Sven Parkel.** Ligand binding to 5-HT_{1A} receptors and its regulation by Mg^{2+} and Mn^{2+}. Tartu, 2010, 99 p.
92. **Signe Vahur.** Expanding the possibilities of ATR-FT-IR spectroscopy in determination of inorganic pigments. Tartu, 2010, 184 p.
93. **Tavo Romann**. Preparation and surface modification of bismuth thin film, porous, and microelectrodes. Tartu, 2010, 155 p.
94. **Nadežda Aleksejeva.** Electrocatalytic reduction of oxygen on carbon nanotube-based nanocomposite materials. Tartu, 2010, 147 p.
95. **Marko Kullapere.** Electrochemical properties of glassy carbon, nickel and gold electrodes modified with aryl groups. Tartu, 2010, 233 p.
96. **Liis Siinor.** Adsorption kinetics of ions at Bi single crystal planes from aqueous electrolyte solutions and room-temperature ionic liquids. Tartu, 2010, 101 p.
97. **Angela Vaasa.** Development of fluorescence-based kinetic and binding assays for characterization of protein kinases and their inhibitors. Tartu 2010, 101 p.
98. **Indrek Tulp.** Multivariate analysis of chemical and biological properties. Tartu 2010, 105 p.
99. **Aare Selberg.** Evaluation of environmental quality in Northern Estonia by the analysis of leachate. Tartu 2010, 117 p.
100. **Darja Lavõgina.** Development of protein kinase inhibitors based on adenosine analogue-oligoarginine conjugates. Tartu 2010, 248 p.
101. **Laura Herm.** Biochemistry of dopamine D_2 receptors and its association with motivated behaviour. Tartu 2010, 156 p.

102. **Terje Raudsepp.** Influence of dopant anions on the electrochemical properties of polypyrrole films. Tartu 2010, 112 p.
103. **Margus Marandi.** Electroformation of Polypyrrole Films: *In-situ* AFM and STM Study. Tartu 2011, 116 p.
104. **Kairi Kivirand.** Diamine oxidase-based biosensors: construction and working principles. Tartu, 2011, 140 p.
105. **Anneli Kruve.** Matrix effects in liquid-chromatography electrospray mass-spectrometry. Tartu, 2011, 156 p.
106. **Gary Urb.** Assessment of environmental impact of oil shale fly ash from PF and CFB combustion. Tartu, 2011, 108 p.
107. **Nikita Oskolkov.** A novel strategy for peptide-mediated cellular delivery and induction of endosomal escape. Tartu, 2011, 106 p.
108. **Dana Martin.** The QSPR/QSAR approach for the prediction of properties of fullerene derivatives. Tartu, 2011, 98 p.
109. **Säde Viirlaid.** Novel glutathione analogues and their antioxidant activity. Tartu, 2011, 106 p.
110. **Ülis Sõukand.** Simultaneous adsorption of Cd^{2+}, Ni^{2+}, and Pb^{2+} on peat. Tartu, 2011, 124 p.
111. **Lauri Lipping.** The acidity of strong and superstrong Brønsted acids, an outreach for the "limits of growth": a quantum chemical study. Tartu, 2011, 124 p.
112. **Heisi Kurig.** Electrical double-layer capacitors based on ionic liquids as electrolytes. Tartu, 2011, 146 p.
113. **Marje Kasari.** Bisubstrate luminescent probes, optical sensors and affinity adsorbents for measurement of active protein kinases in biological samples. Tartu, 2012, 126 p.
114. **Kalev Takkis.** Virtual screening of chemical databases for bioactive molecules. Tartu, 2012, 122 p.
115. **Ksenija Kisseljova**. Synthesis of aza-β^3-amino acid containing peptides and kinetic study of their phosphorylation by protein kinase A. Tartu, 2012, 104 p.
116. **Riin Rebane.** Advanced method development strategy for derivatization LC/ESI/MS. Tartu, 2012, 184 p.
117. **Vladislav Ivaništšev.** Double layer structure and adsorption kinetics of ions at metal electrodes in room temperature ionic liquids. Tartu, 2012, 128 p.
118. **Irja Helm.** High accuracy gravimetric Winkler method for determination of dissolved oxygen. Tartu, 2012, 139 p.
119. **Karin Kipper.** Fluoroalcohols as Components of LC-ESI-MS Eluents: Usage and Applications. Tartu, 2012, 164 p.
120. **Arno Ratas.** Energy storage and transfer in dosimetric luminescent materials. Tartu, 2012, 163 p.
121. **Reet Reinart-Okugbeni**. Assay systems for characterisation of subtype-selective binding and functional activity of ligands on dopamine receptors. Tartu, 2012, 159 p.

122. **Lauri Sikk.** Computational study of the Sonogashira cross-coupling reaction. Tartu, 2012, 81 p.
123. **Karita Raudkivi.** Neurochemical studies on inter-individual differences in affect-related behaviour of the laboratory rat. Tartu, 2012, 161 p.
124. **Indrek Saar.** Design of GalR2 subtype specific ligands: their role in depression-like behavior and feeding regulation. Tartu, 2013, 126 p.
125. **Ann Laheäär.** Electrochemical characterization of alkali metal salt based non-aqueous electrolytes for supercapacitors. Tartu, 2013, 127 p.
126. **Kerli Tõnurist.** Influence of electrospun separator materials properties on electrochemical performance of electrical double-layer capacitors. Tartu, 2013, 147 p.
127. **Kaija Põhako-Esko.** Novel organic and inorganic ionogels: preparation and characterization. Tartu, 2013, 124 p.
128. **Ivar Kruusenberg.** Electroreduction of oxygen on carbon nanomaterial-based catalysts. Tartu, 2013, 191 p.
129. **Sander Piiskop.** Kinetic effects of ultrasound in aqueous acetonitrile solutions. Tartu, 2013, 95 p.
130. **Ilona Faustova**. Regulatory role of L-type pyruvate kinase N-terminal domain. Tartu, 2013, 109 p.
131. **Kadi Tamm.** Synthesis and characterization of the micro-mesoporous anode materials and testing of the medium temperature solid oxide fuel cell single cells. Tartu, 2013, 138 p.
132. **Iva Bozhidarova Stoyanova-Slavova.** Validation of QSAR/QSPR for regulatory purposes. Tartu, 2013, 109 p.
133. **Vitali Grozovski**. Adsorption of organic molecules at single crystal electrodes studied by *in situ* STM method. Tartu, 2014, 146 p.
134. **Santa Veikšina**. Development of assay systems for characterisation of ligand binding properties to melanocortin 4 receptors. Tartu, 2014, 151 p.
135. **Jüri Liiv.** PVDF (polyvinylidene difluoride) as material for active element of twisting-ball displays. Tartu, 2014, 111 p.
136. **Kersti Vaarmets.** Electrochemical and physical characterization of pristine and activated molybdenum carbide-derived carbon electrodes for the oxygen electroreduction reaction. Tartu, 2014, 131 p.
137. **Lauri Tõntson**. Regulation of G-protein subtypes by receptors, guanine nucleotides and Mn^{2+}. Tartu, 2014, 105 p.
138. **Aiko Adamson.** Properties of amine-boranes and phosphorus analogues in the gas phase. Tartu, 2014, 78 p.
139. **Elo Kibena**. Electrochemical grafting of glassy carbon, gold, highly oriented pyrolytic graphite and chemical vapour deposition-grown graphene electrodes by diazonium reduction method. Tartu, 2014, 184 p.
140. **Teemu Näykki.** Novel Tools for Water Quality Monitoring – From Field to Laboratory. Tartu, 2014, 202 p.
141. **Karl Kaupmees.** Acidity and basicity in non-aqueous media: importance of solvent properties and purity. Tartu, 2014, 128 p.

142. **Oleg Lebedev**. Hydrazine polyanions: different strategies in the synthesis of heterocycles. Tartu, 2015, 118 p.
143. **Geven Piir.** Environmental risk assessment of chemicals using QSAR methods. Tartu, 2015, 123 p.
144. **Olga Mazina.** Development and application of the biosensor assay for measurements of cyclic adenosine monophosphate in studies of G protein-coupled receptor signalinga. Tartu, 2015, 116 p.
145. **Sandip Ashokrao Kadam.** Anion receptors: synthesis and accurate binding measurements. Tartu, 2015, 116 p.
146. **Indrek Tallo.** Synthesis and characterization of new micro-mesoporous carbide derived carbon materials for high energy and power density electrical double layer capacitors. Tartu, 2015, 148 p.
147. **Heiki Erikson.** Electrochemical reduction of oxygen on nanostructured palladium and gold catalysts. Tartu, 2015, 204 p.
148. **Erik Anderson.** *In situ* Scanning Tunnelling Microscopy studies of the interfacial structure between Bi(111) electrode and a room temperature ionic liquid. Tartu, 2015, 118 p.
149. **Girinath G. Pillai.** Computational Modelling of Diverse Chemical, Biochemical and Biomedical Properties. Tartu, 2015, 140 p.
150. **Piret Pikma.** Interfacial structure and adsorption of organic compounds at Cd(0001) and Sb(111) electrodes from ionic liquid and aqueous electrolytes: an *in situ* STM study. Tartu, 2015, 126 p.
151. **Ganesh babu Manoharan.** Combining chemical and genetic approaches for photoluminescence assays of protein kinases. Tartu, 2016, 126 p.
152. **Carolin Siimenson**. Electrochemical characterization of halide ion adsorption from liquid mixtures at Bi(111) and pyrolytic graphite electrode surface. Tartu, 2016, 110 p.
153. **Asko Laaniste.** Comparison and optimisation of novel mass spectrometry ionisation sources. Tartu, 2016, 156 p.
154. **Hanno Evard.** Estimating limit of detection for mass spectrometric analysis methods. Tartu, 2016, 224 p.
155. **Kadri Ligi.** Characterization and application of protein kinase-responsive organic probes with triplet-singlet energy transfer. Tartu, 2016, 122 p.
156. **Margarita Kagan.** Biosensing penicillins' residues in milk flows. Tartu, 2016, 130 p.
157. **Marie Kriisa.** Development of protein kinase-responsive photoluminescent probes and cellular regulators of protein phosphorylation. Tartu, 2016, 106 p.
158. **Mihkel Vestli.** Ultrasonic spray pyrolysis deposited electrolyte layers for intermediate temperature solid oxide fuel cells. Tartu, 2016, 156 p.
159. **Silver Sepp**. Influence of porosity of the carbide-derived carbon on the properties of the composite electrocatalysts and characteristics of polymer electrolyte fuel cells. Tartu, 2016, 137 p.
160. **Kristjan Haav**. Quantitative relative equilibrium constant measurements in supramolecular chemistry. Tartu, 2017, 158 p.

161. **Anu Teearu**. Development of MALDI-FT-ICR-MS methodology for the analysis of resinous materials. Tartu, 2017, 205 p.
162. **Taavi Ivan**. Bifunctional inhibitors and photoluminescent probes for studies on protein complexes. Tartu, 2017, 140 p.
163. **Maarja-Liisa Oldekop**. Characterization of amino acid derivatization reagents for LC-MS analysis. Tartu, 2017, 147 p.
164. **Kristel Jukk**. Electrochemical reduction of oxygen on platinum- and palladium-based nanocatalysts. Tartu, 2017, 250 p.
165. **Siim Kukk**. Kinetic aspects of interaction between dopamine transporter and *N*-substituted nortropane derivatives. Tartu, 2017, 107 p.
166. **Birgit Viira**. Design and modelling in early drug development in targeting HIV-1 reverse transcriptase and Malaria. Tartu, 2017, 172 p.
167. **Rait Kivi**. Allostery in cAMP dependent protein kinase catalytic subunit. Tartu, 2017, 115 p.
168. **Agnes Heering**. Experimental realization and applications of the unified acidity scale. Tartu, 2017, 123 p.
169. **Delia Juronen**. Biosensing system for the rapid multiplex detection of mastitis-causing pathogens in milk. Tartu, 2018, 85 p.
170. **Hedi Rahnel.** ARC-inhibitors: from reliable biochemical assays to regulators of physiology of cells. Tartu, 2018, 176 p.
171. **Anton Ruzanov.** Computational investigation of the electrical double layer at metal–aqueous solution and metal–ionic liquid interfaces. Tartu, 2018, 129 p.
172. **Katrin Kestav.** Crystal Structure-Guided Development of Bisubstrate-Analogue Inhibitors of Mitotic Protein Kinase Haspin. Tartu, 2018, 166 p.
173. **Mihkel Ilisson.** Synthesis of novel heterocyclic hydrazine derivatives and their conjugates. Tartu, 2018, 101 p.
174. **Anni Allikalt.** Development of assay systems for studying ligand binding to dopamine receptors. Tartu, 2018, 160 p.
175. **Ove Oll.** Electrical double layer structure and energy storage characteristics of ionic liquid based capacitors. Tartu, 2018, 187 p.
176. **Rasmus Palm.** Carbon materials for energy storage applications. Tartu, 2018, 114 p.
177. **Jörgen Metsik.** Preparation and stability of poly(3,4-ethylenedioxythiophene) thin films for transparent electrode applications. Tartu, 2018, 111 p.
178. **Sofja Tšepelevitš.** Experimental studies and modeling of solute-solvent interactions. Tartu, 2018, 109 p.
179. **Märt Lõkov.** Basicity of some nitrogen, phosphorus and carbon bases in acetonitrile. Tartu, 2018, 104 p.
180. **Anton Mastitski**. Preparation of α-aza-amino acid precursors and related compounds by novel methods of reductive one-pot alkylation and direct alkylation. Tartu, 2018, 155 p.
181. **Jürgen Vahter**. Development of bisubstrate inhibitors for protein kinase CK2. Tartu, 2019, 186 p.

182. **Piia Liigand.** Expanding and improving methodology and applications of ionization efficiency measurements. Tartu, 2019, 189 p.
183. **Sigrid Selberg.** Synthesis and properties of lipophilic phosphazene-based indicator molecules. Tartu, 2019, 74 p.
184. **Jaanus Liigand.** Standard substance free quantification for LC/ESI/MS analysis based on the predicted ionization efficiencies. Tartu, 2019, 254 p.
185. **Marek Mooste.** Surface and electrochemical characterisation of aryl film and nanocomposite material modified carbon and metal-based electrodes. Tartu, 2019, 304 p.
186. **Mare Oja.** Experimental investigation and modelling of pH profiles for effective membrane permeability of drug substances. Tartu, 2019, 306 p.
187. **Sajid Hussain.** Electrochemical reduction of oxygen on supported Pt catalysts. Tartu, 2019, 220 p.
188. **Ronald Väli.** Glucose-derived hard carbon electrode materials for sodium-ion batteries. Tartu, 2019, 180 p.
189. **Ester Tee.** Analysis and development of selective synthesis methods of hierarchical micro- and mesoporous carbons. Tartu, 2019, 210 p.
190. **Martin Maide.** Influence of the microstructure and chemical composition of the fuel electrode on the electrochemical performance of reversible solid oxide fuel cell. Tartu, 2020, 144 p.
191. **Edith Viirlaid.** Biosensing Pesticides in Water Samples. Tartu, 2020, 102 p.
192. **Maike Käärik.** Nanoporous carbon: the controlled nanostructure, and structure-property relationships. Tartu, 2020, 162 p.
193. **Artur Gornischeff.** Study of ionization efficiencies for derivatized compounds in LC/ESI/MS and their application for targeted analysis. Tartu, 2020, 124 p.
194. **Reet Link.** Ligand binding, allosteric modulation and constitutive activity of melanocortin-4 receptors. Tartu, 2020, 108 p.
195. **Pilleriin Peets.** Development of instrumental methods for the analysis of textile fibres and dyes. Tartu, 2020, 150 p.
196. **Larisa Ivanova.** Design of active compounds against neurodegenerative diseases. Tartu, 2020, 152 p.
197. **Meelis Härmas.** Impact of activated carbon microstructure and porosity on electrochemical performance of electrical double-layer capacitors. Tartu, 2020, 122 p.
198. **Ruta Hecht.** Novel Eluent Additives for LC-MS Based Bioanalytical Methods. Tartu, 2020, 202 p.
199. **Max Hecht.** Advances in the Development of a Point-of-Care Mass Spectrometer Test. Tartu, 2020, 168 p.
200. **Ida Rahu.** Bromine formation in inorganic bromide/nitrate mixtures and its application for oxidative aromatic bromination. Tartu, 2020, 116 p.
201. **Sander Ratso**. Electrocatalysis of oxygen reduction on non-precious metal catalysts. Tartu, 2020, 371 p.
202. **Astrid Darnell.** Computational design of anion receptors and evaluation of host-guest binding. Tartu, 2021, 150 p.

203. **Ove Korjus.** The development of ceramic fuel electrode for solid oxide cells. Tartu, 2021, 150 p.
204. **Merit Oss.** Ionization efficiency in electrospray ionization source and its relations to compounds' physico-chemical properties. Tartu, 2021, 124 p.
205. **Madis Lüsi**. Electroreduction of oxygen on nanostructured palladium catalysts. Tartu, 2021, 180 p.
206. **Eliise Tammekivi.** Derivatization and quantitative gas-chromatographic analysis of oils. Tartu, 2021, 122 p.
207. **Simona Selberg.** Development of Small-Molecule Regulators of Epi-transcriptomic Processes. Tartu, 2021, 122 p.
208. **Olivier Etebe Nonga.** Inhibitors and photoluminescent probes for in vitro studies on protein kinases PKA and PIM. Tartu, 2021, 189 p.
209. **Riinu Härmas.** The structure and H2 diffusion in porous carbide-derived carbon particles. Tartu, 2022, 123 p.
210. **Maarja Paalo.** Synthesis and characterization of novel carbon electrodes for high power density electrochemical capacitors. Tartu, 2022, 144 p.
211. **Jinfeng Zhao.** Electrochemical characteristics of Bi(hkl) and micro-meso-porous carbon electrodes in ionic liquid based electrolytes. Tartu, 2022, 134 p.
212. **Alar Heinsaar.** Investigation of oxygen electrode materials for high-temperature solid oxide cells in natural conditions. Tartu, 2022, 120 p.
213. **Jaana Lilloja.** Transition metal and nitrogen doped nanocarbon cathode catalysts for anion exchange membrane fuel cells. Tartu, 2022, 202 p.
214. **Maris-Johanna Tahk.** Novel fluorescence-based methods for illuminating transmembrane signal transduction by G-protein coupled receptors. Tartu, 2022, 200 p.
215. **Eerik Jõgi.** Development and Applications of E. coli Immunosensor. Tartu, 2022, 103 p.
216. **Alo Rüütel.** Design principles of synthetic molecular receptors for anion-selective electrodes. Tartu, 2022, 109 p.
217. **Tanel Sõrmus.** Development of stimuli-responsive and covalent bisubstrate inhibitors of protein kinases. Tartu, 2022, 148 p.
218. **Oleg Artemchuk.** Autotrophic nitrogen removal processes for nutrient removal from sidestream and mainstream wastewater. Tartu, 2022, 115 p.
219. **Andre Leesment.** Quantitative studies of Brønsted acidity in biphasic systems and gas-phase. Tartu, 2023, 83 p.
220. **Meeli Arujõe-Sado.** Structural effects in aza-peptide bond formation reaction. Tartu, 2023, 83 p.
221. **Jonas Mart Linge.** Electrochemical reduction of oxygen on silver-based catalysts. Tartu, 2023, 269 p.
222. **Tõnis Laasfeld.** Integrating Image Analysis and Quantitative Modeling for a Holistic View of GPCR Ligand Binding Dynamics. Tartu, 2023, 226 p.
223. **Ernesto de Jesus Zapata Flores.** Derivatization Reagents used in negative mode electrospray LC-MS. Tartu, 2023, 107 p.

224. **Patrick Teppor.** Obtaining platinum-free oxygen reduction catalysts through biomass valorization: a case study of peat. Tartu, 2023, 161 p.
225. **Peeter Valk.** Methanol Oxidation on Platinum-Rare-Earth Metal Oxide Activated Catalysts. Tartu, 2023, 162 p.
226. **Shidong Chen.** Unravelling prehistoric plant exploitation in eastern Baltic: organic residue analysis of plant-based materials by multi-method approach. Tartu, 2023, 245 p.
227. **Yogesh Kumar.** M-N_4 macrocycle-based catalysts for electrocatalysis of oxygen reduction and oxygen evolution. Tartu, 2023, 224 p.
228. **Kerli Martin.** Recognition of carboxylates by synthetic receptors – from structure-affinity studies to solid-contact anion-selective electrode prototyping. Tartu, 2024, 130 p.
229. **Huy Quí Vinh Nguyen.** Development of Carbon Supported Pt–CeO_2 Catalysts for Proton Exchange Membrane Fuel Cells. Tartu, 2024, 198 p.
230. **Heigo Ers**. Adsorption and Structuring Processes at Single Crystal Electrode – Ionic Liquid Interface – Insights from Simulations and *in situ* Studies. Tartu, 2024, 137 p.
231. **Ritums Cepitis.** Modelling Structural and Geometrical Effects in Carbon Dioxide and Oxygen Electrocatalysis. Tartu, 2024, 99 p.
232. **Kaarel Kisand.** Resorcinol-derived carbon-based catalysts for polymer electrolyte fuel cell cathodes. Tartu, 2024, 205 p.
233. **Akmal Kosimov**. Template-assisted Mechanosynthesis (TAMS) for the production of bifunctional transition metal-based catalysts. Tartu, 2024, 123 p.
234. **Larissa Silva Macieli.** Derivatization-targeted LC-MS analysis of compounds containing amino group. Tartu, 2024, 157 p.
235. **Silvester Jürjo.** Separation of rare earth elements from Estonian phosphorite ore using liquid extraction followed by electrochemical reduction. Tartu, 2024, 99 p.
236. **Jan-Michael C. Cayme.** Organic-inorganic interactions in experimental and archaeological ceramics. Tartu, 2025, 156 p.
237. **Miriam Koppel.** The diffusion of H2 adsorbed in carbide-derived carbons: a quasi-elastic neutron scattering study. Tartu, 2025, 138 p.
238. **Kenneth Tuul.** Evaluating lithium-ion pouch cells and hydrogen storage materials under extreme conditions using advanced techniques. Tartu, 2025, 188 p.
239. **Marta-Lisette Pikma.** Exploring the basicity of phosphanes and related compounds. Tartu, 2025, 100 p.
240. **Indrek Saar.** Development of novel on-site chemical analysis tests – from alternative materials and technologies to functional prototypes. Tartu, 2025, 214 p.
241. **Gulnara Yusibova.** TAL MOF-Derived M-N-C Electrocatalysts for Oxygen Reduction and Evolution Reactions. Tartu, 2025, 120 p.

242. **Karl Marti Toots.** Cheminformatics Approaches for Analyzing and Modeling the Gas-Ionic Liquid Distribution of Organic Solutes. Tartu, 2025, 249 p.
243. **Freddy Kukk.** Electrochemical Characterization of Structurally and Chemically Modified Solid Oxide Cells Operated in Electrolysis Mode. Tartu, 2026, 142 p.